New polynuclear copper complexes active in oxidation reactions

Elena Salvadeo

▶ **To cite this version:**

Elena Salvadeo. New polynuclear copper complexes active in oxidation reactions. Inorganic chemistry. Université Grenoble Alpes, 2017. English. NNT : 2017GREAV068 . tel-01715264

HAL Id: tel-01715264
https://theses.hal.science/tel-01715264

Submitted on 22 Feb 2018

HAL is a multi-disciplinary open access archive for the deposit and dissemination of scientific research documents, whether they are published or not. The documents may come from teaching and research institutions in France or abroad, or from public or private research centers.

L'archive ouverte pluridisciplinaire **HAL**, est destinée au dépôt et à la diffusion de documents scientifiques de niveau recherche, publiés ou non, émanant des établissements d'enseignement et de recherche français ou étrangers, des laboratoires publics ou privés.

Communauté
UNIVERSITÉ Grenoble Alpes

THÈSE

Pour obtenir le grade de

DOCTEUR DE LA COMMUNAUTE UNIVERSITE GRENOBLE ALPES

Spécialité : Chimie inorganique et Bio inorganique

Arrêté ministériel : 25 mai 2016

Présentée par

Elena SALVADEO

Thèse dirigée par **Jean-Marc LATOUR, Directeur de recherche, CEA Grenoble**, et
codirigée par **Lionel DUBOIS, Directeur de recherche, CEA Grenoble**

préparée au sein du **Laboratoire de Chimie et Biologie des Métaux**
dans **l'École Doctorale Chimie et Sciences du Vivant**

Nouveaux complexes polynucléaires de cuivre actifs en oxydation

Thèse soutenue publiquement le **27 novembre 2017**,
devant le jury composé de :

Madame Catherine BELLE
Directrice de Recherche, CNRS, Présidente du jury
Madame Marine DESAGE-EL MURR
Professeure, Université de Strasbourg, Rapporteure
Madame Jalila SIMAAN
Directrice de Recherche, CNRS, Rapporteure
Monsieur Christophe BUCHER
Directeur de Recherche, CNRS, Examinateur
Monsieur Jean-Marc LATOUR
Directeur de recherche, CEA-Grenoble, Directeur de thèse
Monsieur Lionel DUBOIS
Directeur de Recherche, CEA Grenoble, Codirecteur de thèse

À la fin de cette belle expérience de thèse je voudrais exprimer ma gratitude vers toutes les personnes avec lesquelles j'ai pu travailler et qui ont été proches de moi pendant ces trois années.

Tout d'abord, je tiens à remercier les membres du jury qui ont accepté d'évaluer mon travail de thèse et avec lesquelles j'ai pu avoir des discussions intéressantes et enrichissantes pendant ma soutenance.

Je remercie l'Université Grenoble Alpes, l'Institut BIG et le Laboratoire Chimie et Biologie des Métaux pour m'avoir accueillie dans leurs structures, en me donnant tous les moyens pour travailler pendant mon doctorat. En particulier je remercie les équipes PMB et CAMPE au sein de lesquelles j'ai effectué tous mes travaux.

Un gros merci à Jean-Marc et Lionel pour m'avoir guidé pendant ces trois années. Grâce à vous et à votre expérience j'ai pu apprendre beaucoup et, pourquoi pas, devenir aussi une personne plus adulte. Vos conseils ont été précieux et je vais toujours les rappeler.

Je veux ensuite remercier toutes les personnes de l'équipe PMB de laquelle j'ai fait partie pendant trois années ; à partir de Geneviève, disponible à nous écouter et conseiller, et Patrick, avec son aide insubstituable et son bonheur qui rend plus agréable la vie au labo aussi quand rien ne veut pas marcher à la paillasse. Je remercie aussi Olivier, Ricardo, Martin et Amélie pour tous les échanges (scientifiques et pas scientifiques) qu'on a eu pendant trois années.
Je remercie aussi l'équipe RICC/CAMPE pour m'avoir accueillie et avec laquelle j'ai eu aussi la possibilité de travailler. En particulier je veux remercier Serge Gambarelli, Colette Lebrun, Jacques Pécaut et Pascale Maldivi qui avec leur expertise m'ont beaucoup aidé à mieux comprendre les systèmes sur lesquels j'ai travaillé.

Un gros merci à tous les doctorants post-doctorants et stagiaires avec lesquels j'ai travaillé pendant trois années et qui ont contribué à la bonne ambiance du labo. Avant du tout merci à Cristina, qui m'accueillie en première dans son bureau, en m'apprenant les bases du français et en m'aidant à m'intégrer au labo. Je vais toujours rappeler ta gentillesse. Merci à Guillaume, avec lequel j'ai passé quasiment toutes les trois années de thèse, et Friaume et Jordan, qui sont arrivés pendant les années. Merci pour votre bonheur et toutes les bonnes (et longues) discussions, les moments partagés au labo et aussi toutes les rigolades qui aident quand on est un peu de mauvaise humeur.
Un gros merci à Harish. Ton amitié est importante et précieuse pour moi et je vais toujours rappeler tous les bons moments passés ensemble au labo et dehors, à discuter autour d'un verre.
Merci aussi à Johan et Seydou, pour leur bonheur et pour avoir amené au premier étage la tradition du café pendant l'après-midi, comme moment de détente et d'échange des idées.
Merci à tous les autres que ma mémoire en ce moment oublie pour tous ce qu'ils ont apporté pendant ces années.

Ensuite je veux remercier tous mes amis. Ceux que je connais depuis longtemps, certains restés en Italie, les autres un peu partout en Europe et dans le monde. Merci à vous, pour être restés proches de moi, même quand on est séparés par des kilomètres et parfois des décalages horaires l'amitié ne connaît pas de frontière. Merci aussi à tous les amis que j'ai connus sur Grenoble, j'ai des beaux souvenirs avec vous et j'espère de garder les contacts avec vous aussi une fois que je vais partir d'ici. Merci en particulier à Clara, avec laquelle j'ai habité pour trois ans, partageant les moments de vie de doctorants en France.

Et finalement merci à ma famille. Ce que je suis comme personne est surtout grâce à vous, à votre éducation et à votre soutien. Merci pour tout.

Table of contents

Chapter 1: General Introduction

In this introductive chapter, a theoretical background of the work will be presented. A first recall to the chemistry of molecular oxygen will be described, followed by examples of its reactivity in enzymatic and bioinspired systems, with a focus on both oxidation and oxygenation reactions. A correlation between this latter class of reactions and nitrene transfer will be then presented through the concept of isolobal analogy. The work presented in the following chapters will be then introduced.

a. Electronic structure of molecular oxygen. Thermodynamic and kinetic aspects of oxygen reduction reaction

Molecular oxygen is a paramagnetic molecule with a triplet fundamental state. Its electronic configuration can be easily described through the molecular orbital theory, as shown in Figure 1b. O_2 has an electron pair in a σ orbital, two electron pairs in bonding Π orbitals and two unpaired electrons in antibonding Π^* orbitals, $\sigma^2\Pi_x^2\Pi_y^2\Pi_x^{*1}\Pi_y^{*1}$ configuration contributing a double bond O=O. The structure of the oxygen molecule with low energy empty orbitals gives the possibility of hosting further electrons and, in this way, allowing it to react with molecules capable of donating it one or more electrons. The complete reduction of molecular oxygen to water consists in a four-electron process which can be divided in four one-electron processes, shown in Figure 1c-d-e-f. Adding one and two electrons in these Π^* orbitals generates successively the superoxide $O_2^{\bullet-}$ radical anion (Figure 1c) and the peroxide dianion O_2^{2-} (Figure 1d), a strong base which exists as two protonated forms, the hydroperoxide anion HO_2^- and hydrogen peroxide H_2O_2. The addition of these two electrons fills the Π^* orbitals, leading to a decrease of the bond order, and the existence of a single O-O bond. The addition of a further electron in the last available antibonding orbital σ^* causes the cleavage of the O-O bond, with the formation of an oxide dianion O^{2-} and an oxyl radical anion $O^{\bullet-}$, as shown in Figure 1e. Both species exist mostly as their protonated forms, the hydroxide anion HO^- and the very reactive hydroxyl radical $HO^{\bullet}$. Addition of the fourth electron leads to the further reduction of the oxyl radical with the formation of a second oxide (or a hydroxide) (Figure 1f).

This formal description of stepwise reduction of dioxygen highlights one crucial point: the cleavage of the O-O bond intervenes after addition of the third electron. This reaction generates the very oxidizing oxyl radical anion $O^{\bullet-}$ which must be reduced to an oxide O^{2-}

before causing any deleterious effect. This may be the reason why Nature chose to elaborate enzymes with a trinuclear active site to perform O_2 reduction such as multicopper oxidases, which all harbor the needed fourth electron in another metal center[1]. Handling the oxyl radical anion is crucial and enzymes achieved it through binding to iron or copper ions to master it. An analogous process is achieved by the so-called oxygenase enzymes which are able to activate dioxygen reductively and transfer oxygen activated species to several substrates. These enzymes possess active sites with redox flexible metals such as iron and copper. In the following paragraphs, these natural systems will be described, allowing the delineation of the main issues of these processes. In addition, the most important functional models devised so far will be presented.

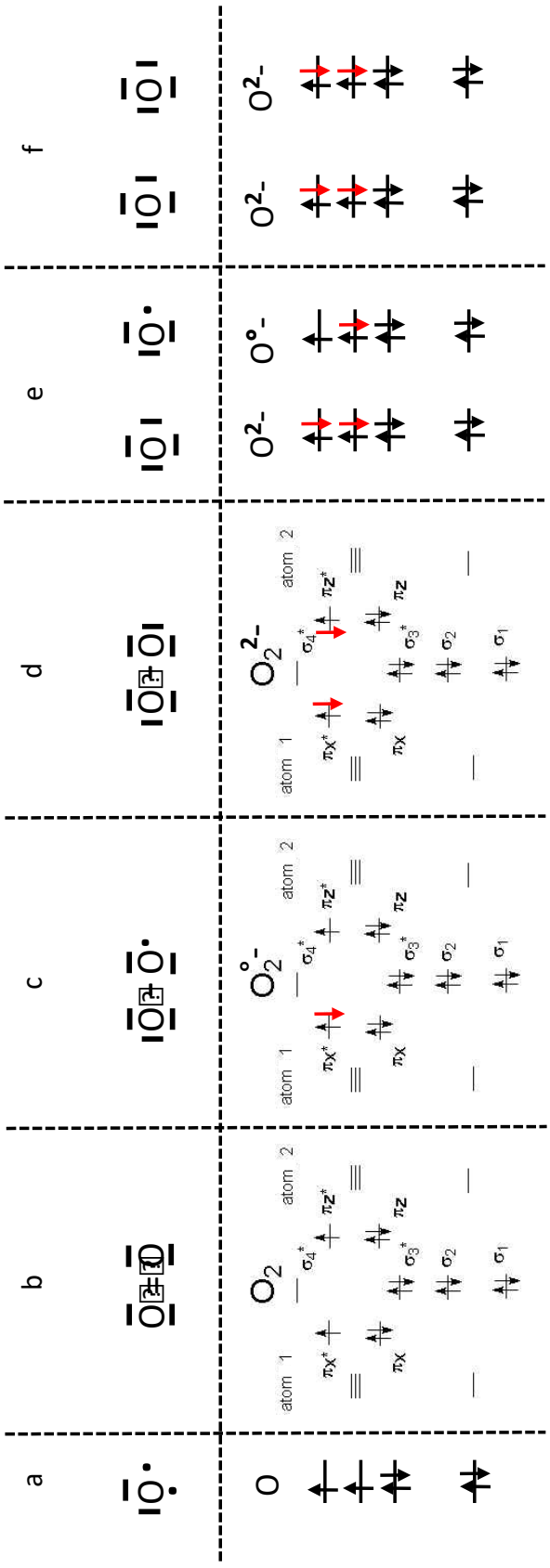

Figure 1: *Electronic structure of O_2 and its reduction products. a) oxygen atom; b) dioxygen molecule; c) superoxide anion; d) peroxide dianion; e) oxide dianion + oxyl radical anion; f) two oxide dianions.*

Looking at the thermodynamic aspects of the oxygen reduction reaction it is possible to observe that the overall process is exothermic, as shown in the Frost diagram (Figure 2). Nevertheless, the first step of the reaction, which leads to the formation of superoxide species, is endothermic, while the direct two-electron and four-electron processes are exothermic.

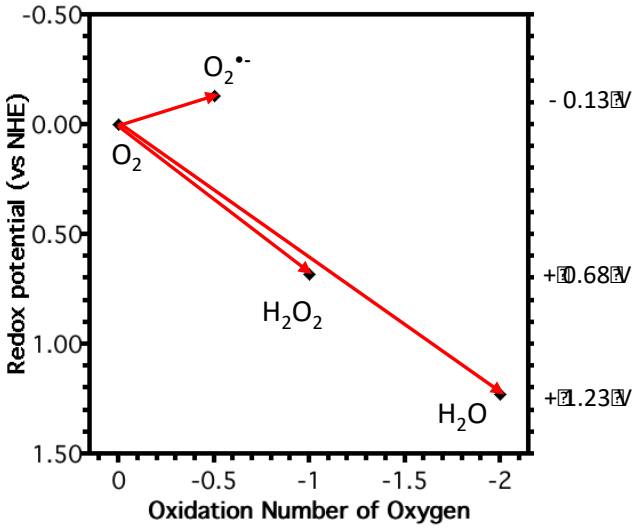

Figure 2: *Frost diagram with redox potential indicated at pH= 0.*

In spite of its quite strong oxidizing power, molecular oxygen exhibits a weak reactivity. Molecular oxygen has a triplet electronic ground state whereas the majority of organic compounds are singlets. Selection rules forbid reactions with variation of the spin state, leading to kinetic unreactivity of dioxygen. This lack of reactivity has a capital importance for living beings because otherwise the majority of the organic molecules would be oxidized in an irreversible way and destroyed; as a consequence, life as we know it could not be possible.

b. The oxygen reduction reaction and the production of energy: from the synthesis of ATP in the cells to the fuel cells technology

As described above, four-electron reduction of molecular oxygen releases an important amount of energy, which can be used for promoting other endergonic reactions. An efficient example, given by Nature, is represented by cytochrome c oxidase present in mitochondria. It couples the exergonic chemistry of the four-electron reduction of O_2 to endergonic proton translocation across the mitochondrial and bacterial membranes.[2] The generated proton

motive force associated to the H^+ gradient is then used as a driving force for ATP synthesis and cellular energy production. The overall reaction catalyzed by cytochrome c oxidases is summarized in the following equation where the two sides of the membrane are indicated by N (negative) and P (positive):

$$O_2 + 4e^- (P) + 8H^+ (N) \longrightarrow 2H_2O + 4H^+ (P)$$

Moreover, all the system is highly efficient and during the catalysis there is no release of partially reduced oxygen species such as $HO^{\bullet}$, which could be very harmful for the cellular environment. The X-ray structure of the enzyme has been extensively studied by Yoshikawa and co-workers [3,4]. It contains several metal sites which can be grouped in the following way:

- A $heme_{a3}$-Cu_B center (Figure 3a and 3b) which is the active site for O_2 reduction. It consists in a pentacoordinated high-spin heme with an axial histidine and a copper bound by three histidines.
- A hexacoordinated low-spin $heme_a$ and Cu_A center for electron storage (Figure 3a). Focusing on the Cu_A center, this is a binuclear copper species with the two metals doubly bridged by two cysteinates and switching between two redox states Cu^ICu^I and Cu^ICu^{II}, with a delocalization of the mixed valence state $Cu^{1.5}Cu^{1.5}$. It accepts one electron at once from reduced cytochrome c and passes it to $heme_a$, which is then capable to transfer the electron to the active site for the reduction of oxygen $heme_{a3}$-Cu_B. The oxidized enzyme is able to store four electrons in the fully reduced state as $heme_{a3}$-Fe^{II}-Cu^I_B, $heme_a$-Fe^{II} and $(Cu^ICu^I)_A$. It is then able to transfer four electrons to molecular oxygen.

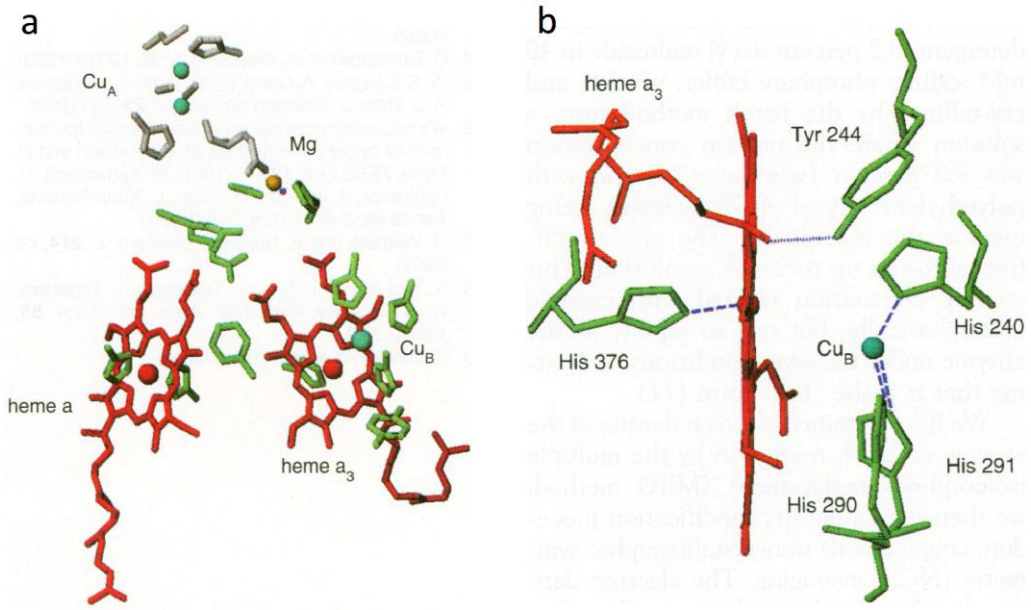

Figure 3: *Representation of the X-ray structure of bovine heart cytochrome c oxidase active site (a) metal centers and (b) the O_2 reaction center*[3,4].

The mechanism of O_2 reduction has been intensely investigated over several decades by using combinations of fast kinetic and sophisticated spectroscopic techniques as well as the study of a wealth of model complexes. The accepted mechanism is briefly summarized in Figure 4[5].

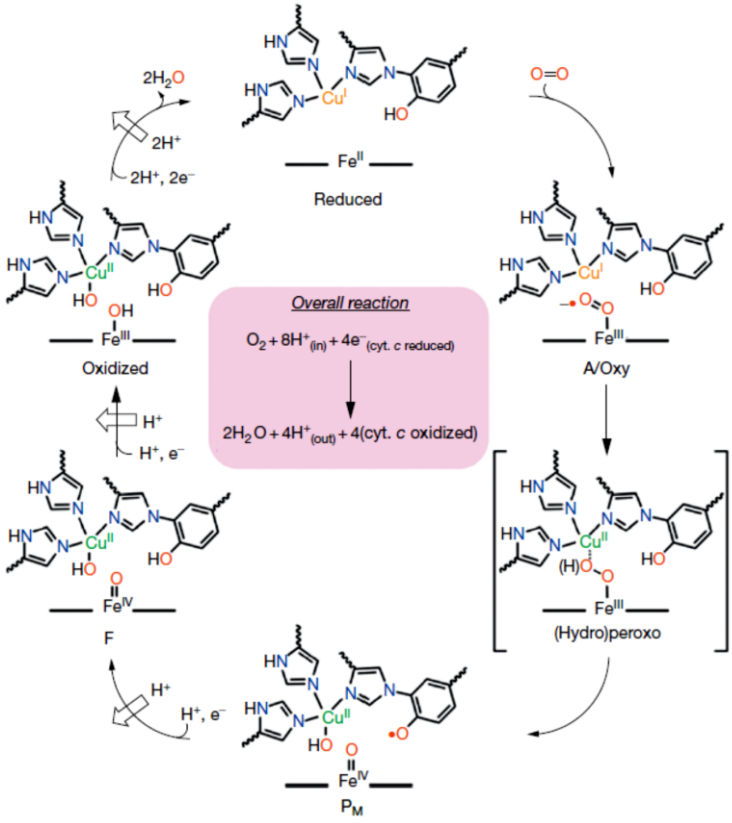

Figure 4: *Schematic representation of cytochrome c oxidase catalytic cycle*[5].

The reduced state reacts with O_2 to give the "A/Oxy" state in which O_2 is bound to $heme_{a3}$ as a superoxide $heme_{a3}$-Fe^{III}-($O_2^{\bullet-}$) Cu^{I}_{B}. Electron transfer from Cu^{I}_{B} then gives a peroxide bridging the two metals that may be protonated ("hydroperoxo" state). The two electrons needed to complete the reduction are afforded by oxidation of the ferric heme to a Fe^{IV} species and of tyrosine to tyrosyl radical ("P_M" state). At this stage, O_2 is reduced to four electrons as an oxide bound to $heme_{a3}$-Fe^{IV} and a hydroxide bound to Cu^{II}_{B}. The successive additions of four electrons through "F" and "oxidized" states regenerate the reduced form and cause the associated proton pumping.

Synthetic models of cytochrome c oxidase were mainly developed by the groups of Collman and Karlin by using slightly different strategies. Collman's strategy was based on the synthesis of binucleating porphyrins, either bis-porphyrins[6] (Figure 5) or porphyrins decorated with a tridentate binding site devoted to copper. Only the latter could be considered a structural model of cytochrome c oxidase[7].

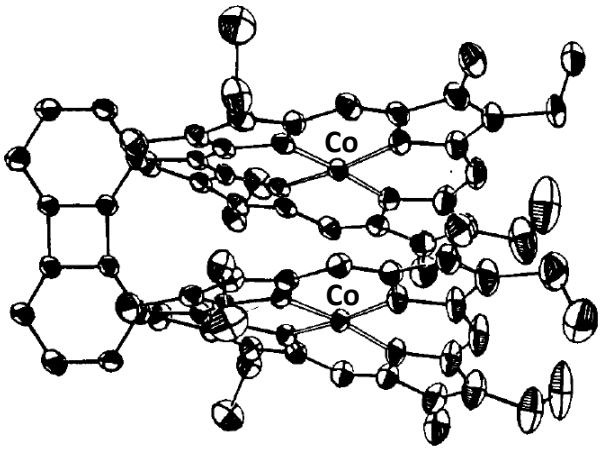

Figure 5: *Representation of the X-ray structure of a dicobalt cofacial diporphyrin designed by Collman and co-workers*[6]*.*

The initial strategy of Karlin involved combination of an iron porphyrin and a tris-amine copper complex but it evolved later to anchor the two moieties through various linkages. As final improvement both groups linked a phenol to a copper ligand as a potential $H^{\bullet}$ donor. This strategy allowed the isolation of crucial potential intermediates such as an Fe-peroxo-Cu entity (Figure 6, left)[8] as well as their spectroscopic characterization and the delineation of their redox properties[9,10]. The efficiency of the catalysts for dioxygen four-electron reduction was thoroughly investigated. Moreover, Collman's group tried to develop electrode materials by linking this kind of catalysts to electrodes[7,11]. The group rationalized the strong dependence of the efficiency of the four-electron reduction of dioxygen on the strategy of grafting of the catalysts on electrodes. In fact when biomimetic complexes are directly adsorbed on edge-plane graphite electrodes the electron transfer is fast and the four-electron reduction is efficient also when the redox centers are not able give the four electrons at once[7]. By contrast, when the complexes are attached to the electrodes by forming self-assembled monolayers, the ability of the catalyst of giving four electrons at once to dioxygen has a capital importance in case of a slow electron transfer from the electrode to the catalyst[11] (Figure 6, right). In fact, if the complex is able to give only two electrons at once to dioxygen and the electron transfer from the electrode surface is slow, the reduction produces a non-negligible amount of hydrogen peroxide, with detrimental effect on the catalytic system.

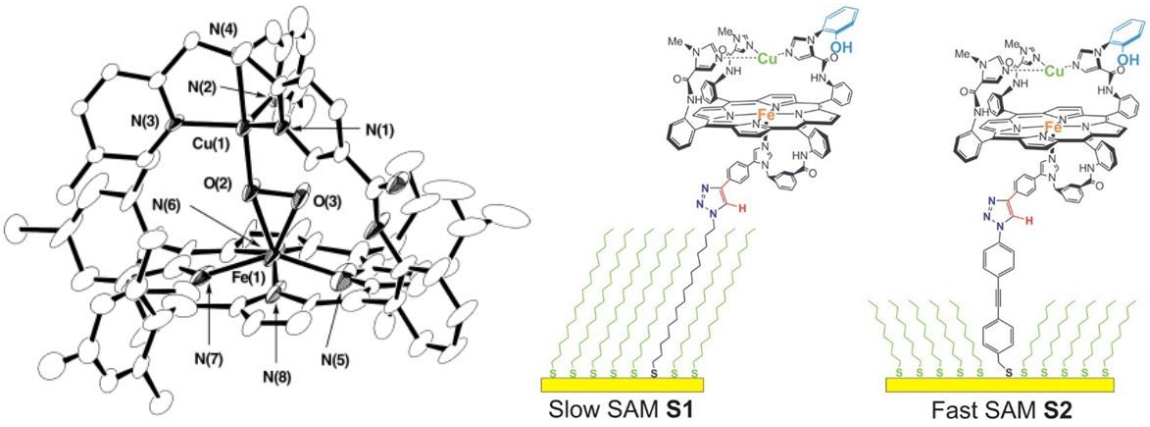

Figure 6: *Representation of the X-ray structure of a synthetic peroxo-bridged iron porphyrin/copper complex isolated by Naruta and co-workers[8] (left) and functionalization of gold electrodes performed by Collman's group with the same class of complexes[11] (right).*

The reduction of molecular oxygen is important for the production of energy not only at cellular level. The fuel cells technology in fact uses the energy generated by the reduction of oxygen at the cathode and the oxidation of hydrogen at the anode to produce electric energy (Figure 7). The fuel cells technology is known for a long time and in the last decades has appeared as a promising source of energy. Unlike polluting power sources as fossil fuels, the only by-product of the reaction is water, without any environmental issues. Moreover, if compared to batteries which normally have long times of charge, fuel cell technology can have the advantage of a quite fast refilling of molecular hydrogen. Different kinds of fuel cells have been developed over time by using different electrolyte systems. The most promising technology for large scale applications is the so called *proton exchange membrane fuel cell* (PEMFC) in which anode and cathode are separated by a proton-conducting polymer membrane (typically Nafion®).

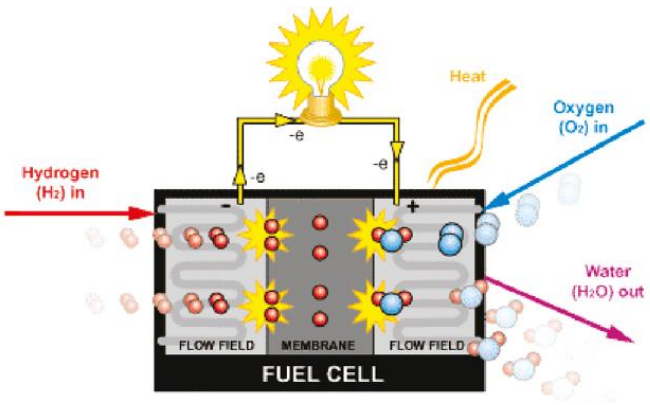

Figure 7: *Working scheme of a fuel cell[12].*

Even if PEMFC technology is known for a long time, its large scale diffusion, for example for automotive applications, has stalemated over the years, owing to two main reasons: the cost of production and the durability. The two are mainly related to the catalytic systems used at both the cathode and the anode, which currently use platinum-based materials. Platinum is one of the scarcest element on Earth (Figure 8), so its high price contributes heavily to the high cost of production and the catalytic system of a fuel cell accounts for up to 30% of its price[12].

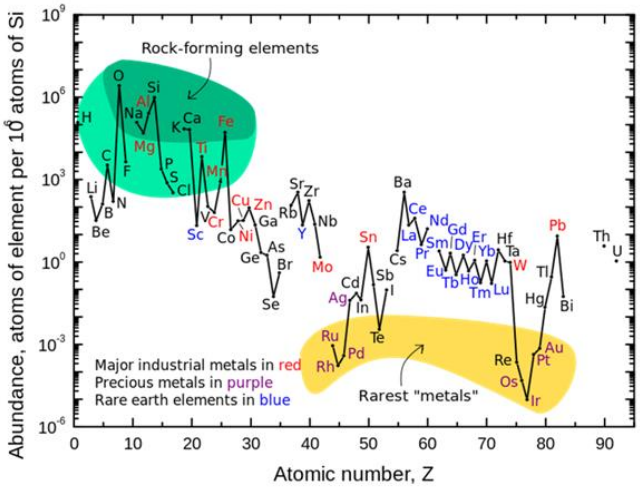

Figure 8: *Relative abundance of elements on Earth crust*

In the last three decades a strong research effort has been devoted to reducing the cost of production of fuel cells catalytic systems, especially regarding the cathodic reaction of reduction of molecular oxygen. In fact, compared to the molecular hydrogen oxidation, dioxygen reduction is six orders of magnitude slower, so it needs more catalyst[13]. This fact has also a consequence on the reduction potential of dioxygen, whose reduction presents an important overpotential (Figure 9). The main approaches used for developing new cheaper oxygen reduction catalytic materials have been the reduction of the amount of platinum in the catalysts and its substitution with non-precious metals[14,15].

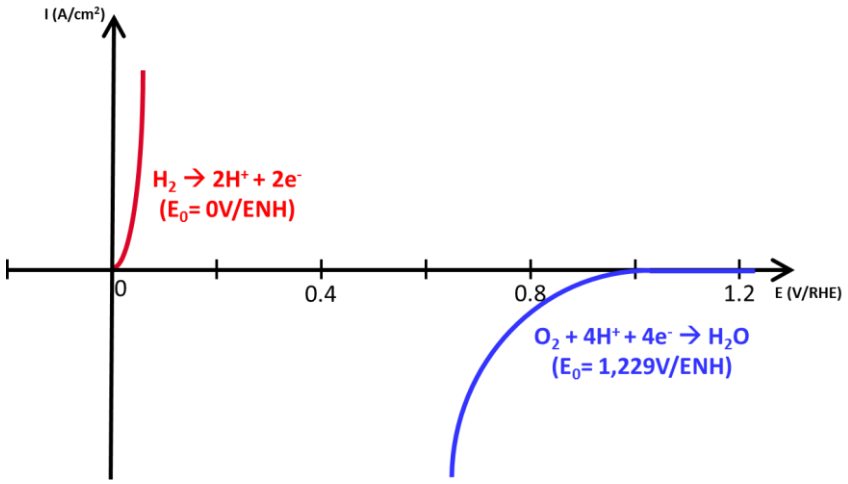

Figure 9: *Comparison between overpotentials of hydrogen oxidation and dioxygen reduction at pH= 0.*

Looking more in depth to the non-precious metals approach, huge efforts have been put in developing systems based on transition metals complexes. The first examples reported in literature were given by Jasinski who described the catalytic behavior of metal phthalocyanins in the reduction of molecular oxygen[16,17]. From these early works, researchers developed a large number of systems based on organometallic complexes[18,19,20], also in the aim of mimicking the activity of enzymes as cytochrome c oxidases and laccases, which are capable of catalyzing the four-electron reduction of dioxygen[21,22]. The work of Collman's group mentioned above about functionalization of electrodes with biomimetic complexes capable of performing dioxygen reduction is a good example of the studies performed with the aim of obtaining alternative catalytic materials for dioxygen reduction[11] (Figure 6, right). Another strategy for the development of catalysts based on non-precious metals consists in supporting and pyrolysing metal precursors on carbon materials, in order to obtain a good dispersion of the active sites on the material and improving the stability of the catalytic system[23].

Another interesting approach for the replacement of platinum-based catalysts is directly inspired by Nature and it consists in using enzymes capable of reducing molecular oxygen[24,25]. The concept is particularly interesting because enzymes, unlike platinum which catalyzes both anodic and cathodic reactions, are selective catalysts and by using them both at anode and cathode the two reactions would not need any membrane for separating them. Unfortunately this approach is difficult to apply in real systems. Enzymes operate in a

narrow range of conditions and they easily undergo degradation in non-natural operating conditions.

From the technological point of view, replacing platinum catalysts with less expensive materials is challenging. In fact, PEMFC with platinum catalysts work in strongly acid media, in which the majority of alternative catalytic materials are not stable, with the loss of their activity. Moreover, small amounts of hydrogen peroxide produced during the reduction of dioxygen can be harmful for the catalytic system, which is easily damaged. A large number of systems based on non-precious metals (e.g. enzymes immobilized on electrodes) is stable at neutral pH but in these conditions the oxygen reduction reaction is inhibited by the poor concentration of H^+ or OH^-, fundamental for carrying on the reaction.

c. The reductive activation of oxygen for chemical transformations: oxidases and oxygenases

The oxygen reduction is involved not only in the production of energy but also in chemical transformations. Oxygenases and oxidases are two classes of enzymes capable of activating and reducing molecular oxygen and coupling this reaction with the oxidation of substrates.

Oxidases are a class of enzymes in which the reduction of molecular oxygen is coupled with the oxidation of substrates. The cytochrome c oxidase described above belongs to this class and it couples the reduction of oxygen with the oxidation of cytochromes in the mitochondria. Another important group of oxidases is represented by the so-called multicopper oxidases counting laccases, ascorbate oxidase and ceruloplasmin as most prominent members[1]. They are able to perform the four-electron reduction of molecular oxygen coupled with the oxidation of substrates such as phenols/anilines or even ferrous ions in the case of ceruloplasmin. Numerous X-Ray structures are available for laccases[26–30], ascorbate oxidases[31], ceruloplasmin[32,33] and bilirubin oxidases[34,35]. All reveal that they have an active site with four copper centers arranged in the same manner (Figure 10):

- A mononuclear center in which a copper ion is coordinated by two histidines, a cysteine and a methionine residue. This copper center is involved in the oxidation of exogenous substrates, storage and delivery of these electrons for dioxygen reduction.

- A trinuclear copper cluster formed by a binuclear entity bridged by a hydroxide, in which each metal is bound by three histidines, and a third copper center coordinated by two histidines and a molecule of water. The four-electron reduction of oxygen occurs here, consuming the electrons provided by the oxidation of exogenous substrates.

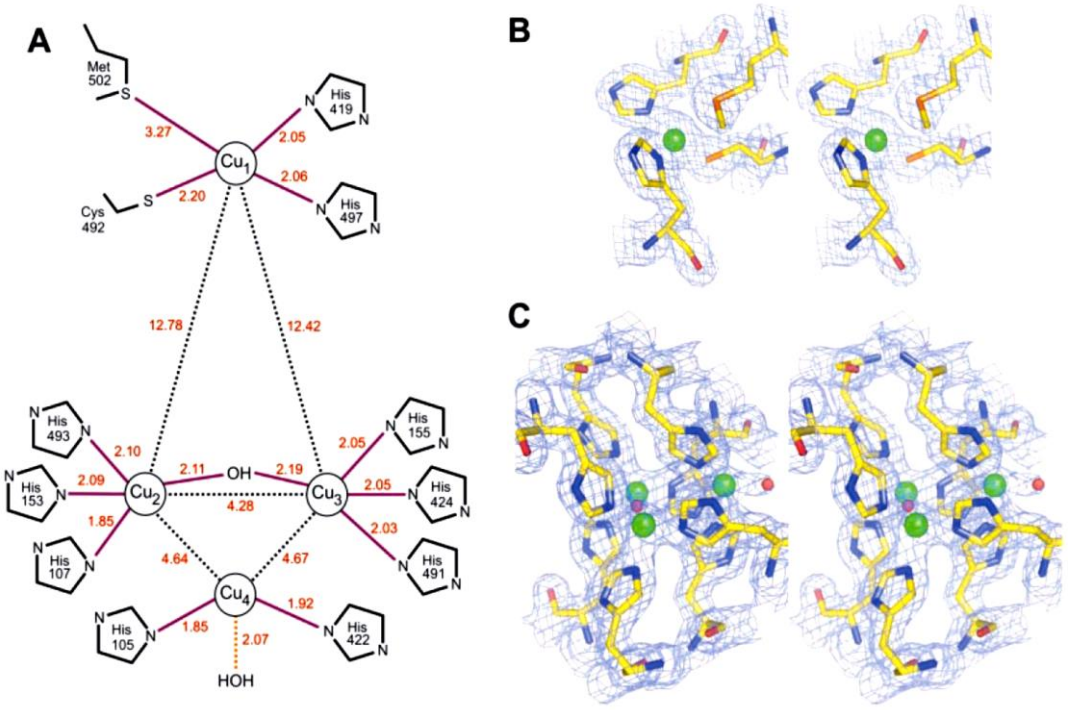

Figure 10: *Representation of the X-ray structure of the bacterial laccase CotA[27]. A) Schematic representation of the copper centers including relevant interatomic distances; B) Stereo view of the mononuclear copper center; C) Stereo view of the trinuclear copper center.*

The mechanism of reaction of multicopper oxidases is not completely established, especially concerning molecular oxygen binding to the trinuclear copper cluster. In fact some crystallographic evidence reported by Bento and co-workers[30] show that molecular oxygen (and also inhibitors of the enzyme like azide) are bound to the trinuclear cluster with a strong interaction with the binuclear copper center and a looser one with the third copper (Figure 11, top). Once the dioxygen is bound, it is reduced to a peroxide intermediate, which is then split by reduction in two hydroxide anions, one bridging between the dinuclear center and the other one bound to the third copper and released as two molecules of water after protonation (Figure 11, bottom).

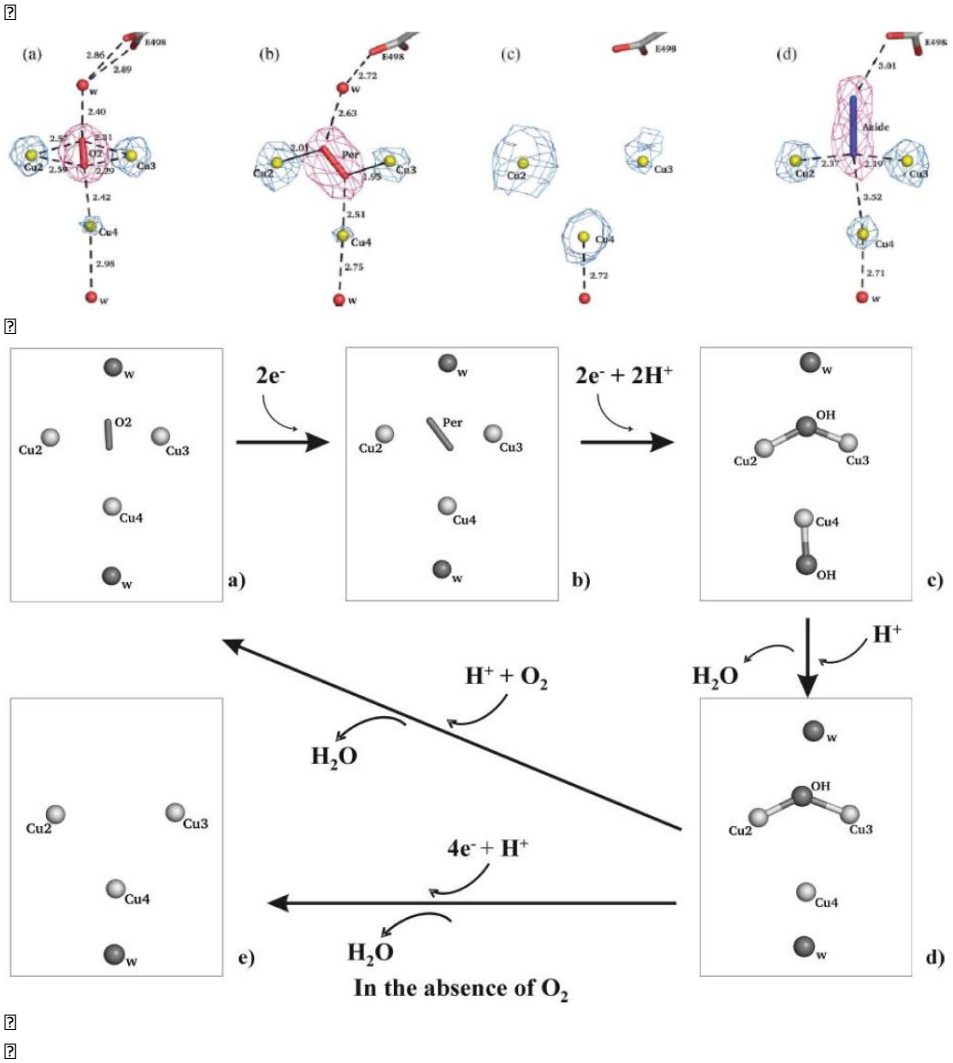

Figure 11: *Top: Representation of the X-ray structures of the trinuclear catalytic site of the bacterial laccase CotA with dioxygen ligands and azide inhibitor[30]. (a) The $CuCl_2$ soaked structure with a bound dioxygen molecule; (b) The peroxide adduct; (c) The fully reduced enzyme; (d) The azide adduct. Bottom: catalytic cycle proposed by Bento and co-workers[30].*

At the same time, Solomon's research group identified slightly different reduction intermediates by using several spectroscopic techniques[36]: i) dioxygen first binds to the tricopper cluster between the mononuclear center and one copper of the binuclear moiety and is reduced to the peroxide level (Figure 12, top); ii) it is then further reduced and split into an oxide bound to the three oxidized copper centers and a hydroxide anion bridged to the binuclear center (Figure 12, bottom).

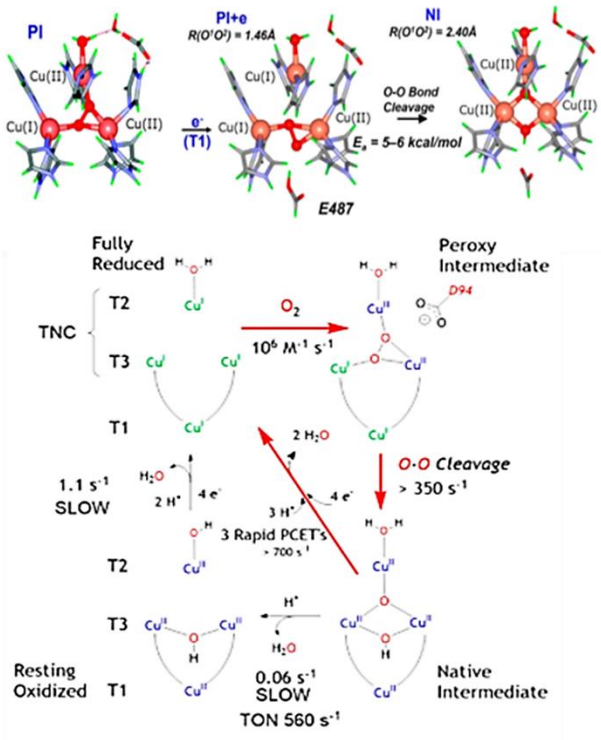

Figure 12: *Reaction intermediates proposed by Solomon and co-workers. Top: reaction coordinate for the reductive cleavage of the O–O bond by the trinuclear copper cluster. Bottom: catalytic cycle proposed by Solomon's group*[36].

Even if the two mechanisms present slightly different reaction intermediates, both agree with the fact that molecular oxygen is reduced using the electrons coming from the oxidation of exogenous substrates and the reduction is performed in two bielectronic steps, with the formation of a peroxide intermediate, unlike what is observed in cytochrome c oxidase. Very recently Solomon reported the influence of chloride anions on the inhibition of bilirubin oxidase[37]. Since the laccase used by Bento was prepared by soaking it with copper chloride, the fact that chlorides can influence the activity of multicopper oxidases could explain the different intermediates observed in the two cases.

As mentioned above, dioxygen does not react with most organic compounds and therefore it needs to be activated for one or both of its oxygen atoms to be inserted in organic substrates either for biosynthesis of specific products or for metabolization of xenobiotics. In nature, these kinds of reactions are catalyzed by the so-called oxygenases, which are capable of performing efficient transformations of many organic substrates.

The most important and studied class of enzymes for oxygenation activity are the cytochromes P450 which are studied intensely for about four decades. In these hemoproteins the iron is bound by an axial cysteinate which is responsible for both their peculiar spectroscopic properties and their outstanding oxidative capacity (Figure 13).

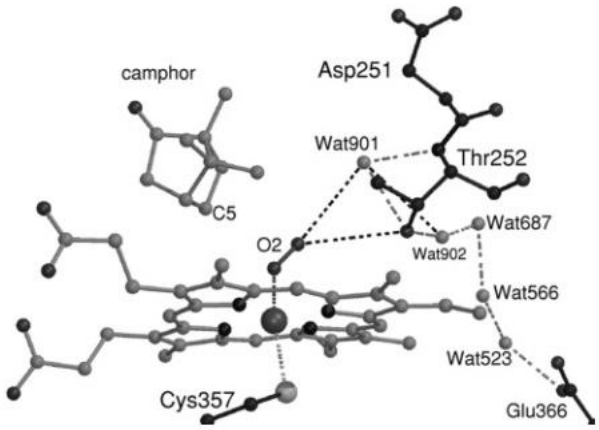

Figure 13: *Representation of the X-Ray structure of cytochrome* $P450_{cam}$[38].

Although their mechanism of action had been understood already in the 1980s, it was fully demonstrated only very recently. The first landmark in this endeavor is the determination of the catalytic pathway of cytochrome $P450_{cam}$ at atomic resolution by Schlichting and co-workers[39] (Figure 14).

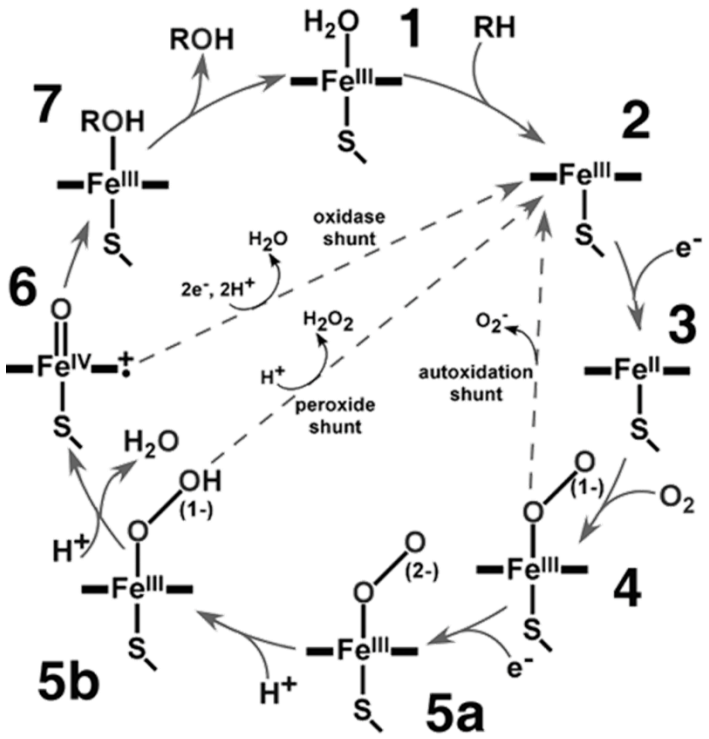

Figure 14: *Mechanism of cytochrome P450$_{cam}$[38].*

This mechanism highlights how O_2 is reduced with three electrons to generate a strongly oxidizing species: i) O_2 is reduced by the ferrous porphyrin (**3**) to give an Fe^{III}-bound superoxide (**4**); ii) addition of a further electron generates the peroxide species (**5a**) which is protonated (**5b**) to an Fe^{III}-bound hydroperoxide; iii) the heterolytic cleavage of the peroxidic O-O bond (Figure 15) is akin to the addition of a third electron (provided by the oxidation of Fe^{III} into Fe^{IV}) with the generation of an oxide (water molecule) and an oxyl anion radical. The latter is stabilized as an Fe^{IV}=O species after internal oxidation of the porphyrin; The resulting species (**6**) is thus best described as an oxo-Fe^{IV} porphyrin radical cation; it is thus akin to a hydroxyl radical confined to the enzyme active site by the Fe-O bond. Such a species was very recently characterized spectroscopically and its reactivity analyzed by Green, what established cytochrome P450 mechanism definitely[40,41].

$$(Por)Fe^{III}—\underline{\bar{O}}—\underline{\bar{O}}H \longrightarrow (Por)Fe^{III}—\underline{\bar{O}}\ \overset{\ominus}{I}\underline{\bar{O}}H$$

$$(Por)Fe^{IV}—\underline{\bar{O}}^{\bullet}$$

$$(Por^{\bullet})Fe^{IV}=\underline{\bar{O}}I$$

Figure 15: *Heterolytic cleavage of peroxidic O-O bond in cytochrome P450 with equivalent formal descriptions of the resulting active species.*

Figure 14 also illustrates that addition of 2 electrons and 2 protons to species **6** generates an equivalent of water, thereby terminating the 4 electron-reduction of O_2. Consistently, treatment of species **5b** by protons releases H_2O_2 (two-electron reduction of O_2). It is of interest that these reactions can operate also in the reverse direction: treatment of the ferric porphyrin (**2**) by hydrogen peroxide generates the hydroperoxide complex **5b** and treatment of **2** by an oxygen donor (such as iodosylbenzene PhI=O or a peracid R-CO_3H) directly generates the active species **6** (Figure 14, species 5a, 5b). These reactions, called respectively *peroxide shunt* and *oxidase shunt*, have been routinely exploited in oxidation catalysis.

As described above for oxidase enzymes, also in the case of oxygenases, it is possible to find active sites of enzymes based on copper clusters. Tyrosinases are one of the most prominent classes of copper oxygenases. They are involved in the hydroxylation of phenols, such as tyrosine, through reductive activation of dioxygen (monoxygenase activity), and their further oxidation to quinones (oxidase activity) (Figure 16). The consecutive polymerization of the synthetized quinones leads to the formation of melanines, involved in all kinds of biological pigmentation processes[1].

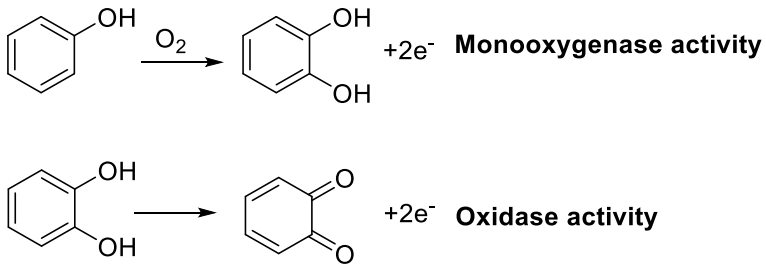

Figure 16: *Catalytic activities of tyrosinase.*

The active site of tyrosinases is formed by a binuclear copper site in which the two metals are both coordinated to three histidine residues and they exhibit antiferromagnetic coupling in the oxidized form of the enzyme (Figure 17, left)[5]. In the catalytic cycle described in Figure 17, right it is possible to observe that the reductive activation of dioxygen leads to the formation of a two-electron reduced peroxo intermediate which is able to perform oxygenation of substrates.

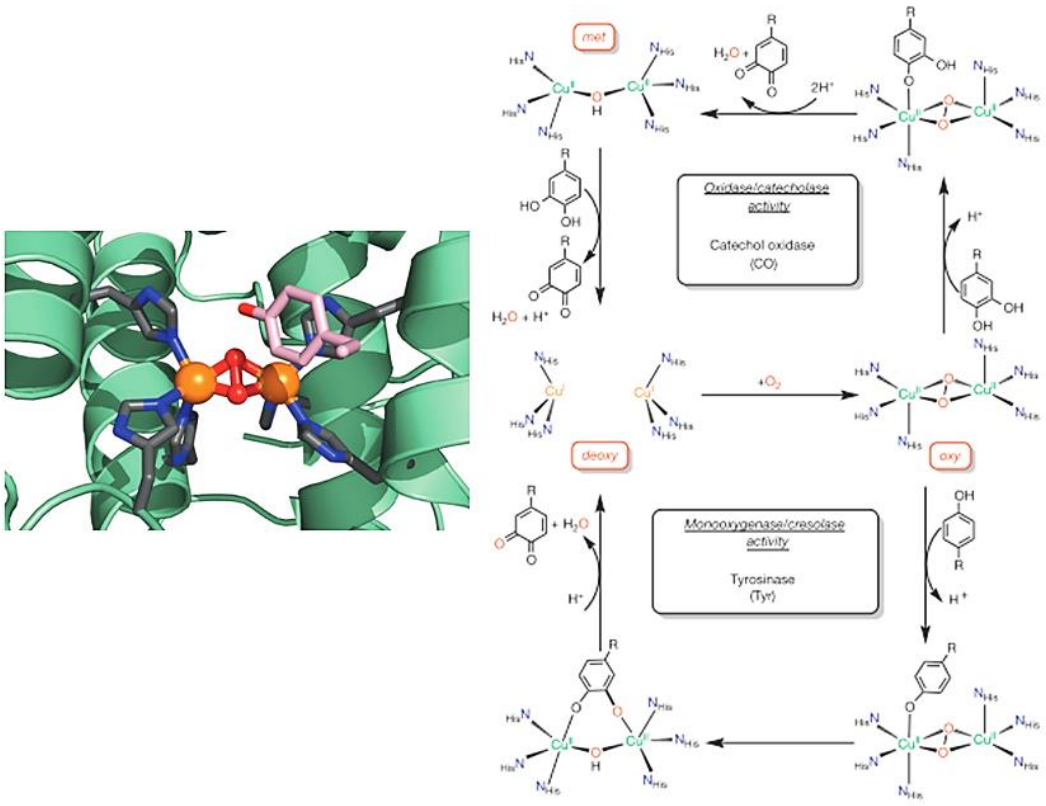

Figure 17: *Representation of the crystal structure of the active site of tyrosinase (left) and its catalytic cycle (right)*[5].

The reaction of dioxygen with copper centers has been thoroughly investigated using synthetic models by several groups and many of the copper-oxygen species illustrated in Figure 17 have been prepared and studied independently. Important contributions by the groups of Karlin[42–44], Stack[45] and Tolman[46] elucidated the mechanism of interaction of dioxygen with binuclear copper complexes. Molecular oxygen can react with reduced binuclear complexes by forming different isomeric Cu_2O_2 cores, whose structures and reactivity have been studied (Figure 18). Moreover, these intermediates can further react with several substrates, giving rise to their oxidation or oxygenation. In the introduction of Chapter 2 the catalytic activity of this kind of complexes will be further discussed with some examples of bioinspired molecular architectures.

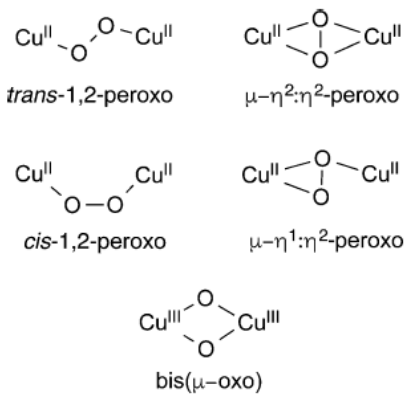

Figure 18: *Isomeric cores of 2:1 Cu:O_2 complexes*[46].

d. The isolobal analogy principle: from oxene transfer to nitrene transfer

This kind of atom-transfer reactions is not restricted to oxygen and can be applied similarly to nitrene transfers. The isolobal principle says that two molecular fragments can be defined as “isolobal” if they have the same number of frontier orbitals, with a similar energy and symmetry and number of electrons. The oxygen atom is isoelectronic with the group "H-N" and this so-called "isolobal analogy" translates into highly similar chemical properties in some instances. This is for example the case for the oxygenase chemistry described above. Indeed, the oxygen atom transfered by the oxygenases and sometimes called an "oxene" (Reactions **a** and **b**) is of the same nature as the "nitrene" often generated in organic chemistry as a means to obtain various kinds of amines.

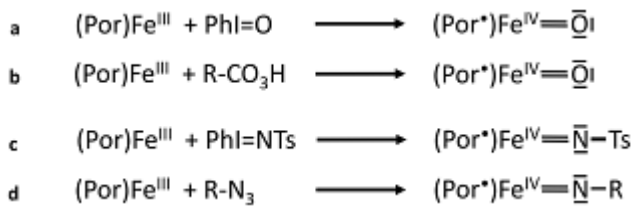

Figure 19: *Oxene and nitrene analogy.*

In these cases, the nitrene transfered is an alkyl or aryl nitrene ("R-N:" or "Ar-N:") rather than the parent "H-N:" which is far more elusive. It is thus possible to generate a species formally equivalent to the active form **6** of cytochrome P450 in Figure 14 by treating a ferric porphyrin by a nitrene precursor as shown in the reactions **c** and **d** in Figure 19. The most

common of these nitrene precursors is the family of iodinanes ArI=NSO_2Ar' based on a hypervalent iodine I^{III} which generate a tosyl nitrene "Ts-N:"[47,48] (Figure 19, Reaction **c**).

These very reactive reagents suffer from two major drawbacks:

- The sulfonamide introduced in the final amine can need harsh conditions to be removed in order to obtain the free amine
- The aryliodide ArI generated as by-product is not optimal in terms of atom economy and green chemistry principles.

These aspects have motivated the research of different kinds of nitrene precursors. In the recent past organic azides, either aliphatic R-N_3 or aromatic Ar-N_3 (Figure 19, Reaction **d**), have been proposed[49–53]. Whereas their use is "eco-friendly" because the only by-product of the reaction is a dinitrogen molecule N_2, it must be kept in mind that the final alkyl or aryl nitrene is less reactive than their tosyl analog and that the starting organic azides are potentially explosives and so more complicated to use on a routine basis.

The discovery that nitrene transfer to an organic substrate can be initiated by the decomposition of an organic azide by a metal salt dates fifty years, with the seminal work of Kwart and Kahn[54,55]. These authors indeed observed that treatment of benzenesulfonylazide ($PhSO_2N_3$) by metallic copper or $CuCl_2$ in presence of DMSO forms the sulfoximine product $(CH_3)_2S(O)(NSO_2Ph)$[54]. Similarly, when the reaction is done in the presence of cyclohexene, the aziridine, enamine and corresponding allylic amine[55] are produced as main aminated products (Figure 20).

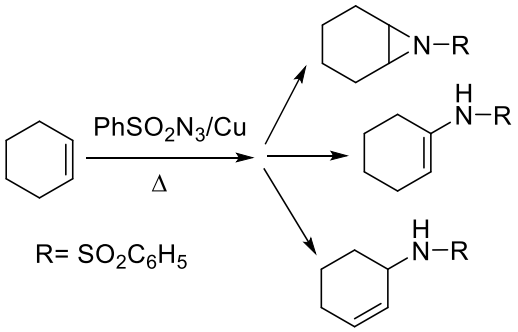

Figure 20: *Products of amination of cyclohexene by benzenesulfonylazide in presence of metallic copper[55].*

In the early 1980s, Breslow reported the intramolecular amination of a predirected substrate functionalized with a nitrene donor upon treatment by an iron or manganese porphyrin[56]

(Figure 21). The same catalyst is also able to perform the intermolecular amination of cyclohexane by reaction using PhI=NTs as nitrene donor[57].

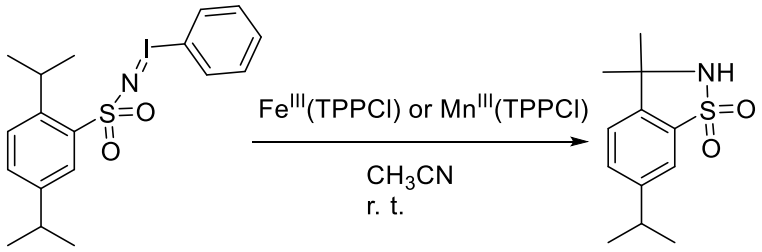

Figure 21: *Intramolecular amination catalyzed by iron and manganese porphyrines[56].*

Soon after, Dawson and Breslow reported that the same intramolecular reaction can be catalyzed by cytochrome P450[58]. However, when an intermolecular aliphatic amination was attempted only formation of oxygenated derivatives was observed[59]. It is generally assumed that their formation results from the fast hydrolysis of the tosylnitrene analog of species **6** of the catalytic cycle of cytochrome P450 (Figure 14) by the water present in the reaction medium. The obtained intermediate is a (Por$^{\bullet}$)Fe(IV)=O, analog to the oxene intermediate obtained by treating P450 with the reactive PhI=O, capable of oxidizing alkanes. (Figure 22)[59].

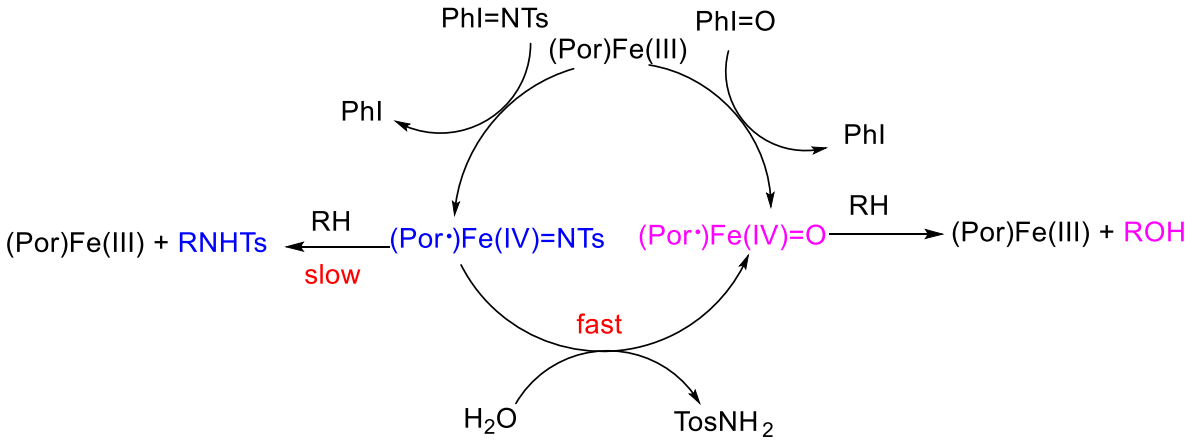

Figure 22: *Possible mechanism of hydrolysis of the Fe(V)=N-Tos intermediate in the catalytic cycle of nitrene transfer catalyzed by P450 (left) compared with the formation of the formation of the active species involved in oxene transfer[59].*

This difficulty has probably been the major reason for stalemating of enzymatic nitrene transfer over three decades. However, green incentives and recent progresses in genetic engineering[60,61] have contributed to their intense revival over the past few years by Arnold's

laboratory. Using as nitrene precursor a sulfonylazide, they have reported several cytochrome P450-catalyzed aminations of various substrates including enantioselective transformations (Figure 23)[62,63].

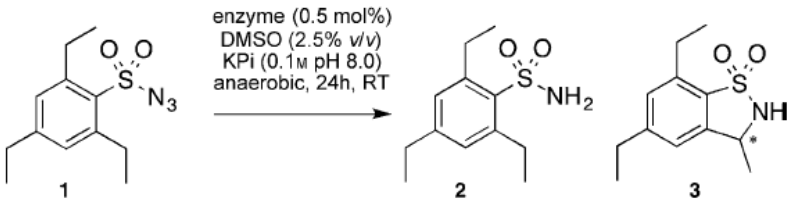

Figure 23: *Enantioselective intramolecular amination catalyzed by cytochrome P450[62].*

Nitrene transfer catalysis presents a huge interest from the point of view of synthetic chemistry because it makes accessible several aminated products otherwise difficult to obtain in good yields or which require harsh experimental conditions. The use of catalysts allows the easier formation of interesting building blocks which can be further used for the synthesis of molecules of commercial interest.

Aziridines are a class of molecules which have a three-member heterocycle with a nitrogen atom. Their structure is often found in biologically active molecules, either natural or synthetic. For example mytomicins are molecules produced by some microorganisms which for a long time bear a huge interest in pharmaceutical chemistry because of their antitumor activity. Their structure presents one aziridine ring which is also the site of interaction with DNA[64] (Figure 24).

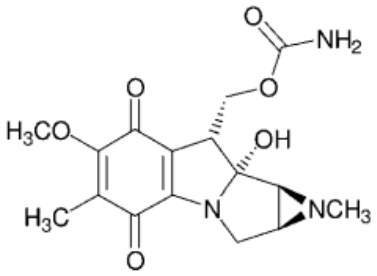

Figure 24: *Structure of mytomicin B.*

In synthetic chemistry aziridines can be obtained by several ways, among which nitrene transfer on alkenes. The classic reaction conditions require harsh conditions for the thermal of photochemical generation of the active nitrene, with the loss of the stereochemical

information[65]. This fact motivated the researchers in finding systems capable of catalyzing the nitrene transfer reaction, with the works described above.

The most efficient catalysts for nitrene transfer currently are based on rhodium and palladium complexes. The major drawbacks of these systems is that they are based on rare and/or toxic metals which make expensive their use in large scale production. Current research is focused on the development of efficient catalysts using earth-abundant metals, such as iron, copper and silver. In the introduction of Chapter 4 nitrene transfer catalysis will be more detailed, focusing on the present examples of catalysts and the main issues in the design of new active systems.

e. Presentation of the subject of the thesis

In the following chapters the results of the thesis will be presented. The work focused on synthesis and characterization of binuclear copper complexes and trinucleating ligands, with investigations about their catalytic applications. Binuclear copper complexes have been conceived as first synthetic models for the creation of trinuclear complexes, in the aim of mimicking trinuclear active sites of enzymes able to perform efficient four-electron reduction of dioxygen. In chapter 2 new binuclear copper complexes will be presented, with a deep description of their synthesis and characterization. An emphasis on the influence of the coordinating environment on electrochemical properties will be placed. The binucleating coordinating entities described in Chapter 2 have been expanded in order to build trinucleating ligands. The isosceles triangular structure of trinuclear copper clusters of multicopper oxidases has been taken as target for the conception of these new ligands. The achieving of these ligands faced some problems for obtaining two key synthetic intermediates. They were finally resolved with an efficient protective strategy which enabled the obtaining of two new trinucleating ligands. The synthetic approach adopted for these ligands will be presented in Chapter 3, with a description of the different strategies followed for their obtention. The ability of one of the binuclear copper complexes as catalyst for reduction of dioxygen was tested, with no remarkable activity. This was then tested in oxidative insertion catalysis. As described above, the oxene intermediate formed during the reduction of dioxygen is isolobal with the nitrene species and both of them are reactive groups which can be transferred on substrates. The Chapter 4 will describe nitrene transfer

catalysis performed with one of the binuclear copper complexes studied in Chapter 2. The studies focused both on catalytic tests of aziridination of styrenes and mechanistic studies of nitrene transfer.

f. Bibliography

(1) Solomon, E. I.; Sundaram, U. M.; Machonkin, T. E. *Chem. Rev.* **1996**, *96*, 2563–2605.
(2) Kaila, V. R. I.; Verkhovsky, M. I.; Wikström, M. *Chem. Rev.* **2010**, *110*, 7062–7081.
(3) Tsukihara, T.; Aoyama, H.; Yamashita, E.; Tomizaki, T.; Yamaguchi, H.; Shinzawa-Itoh, K.; Nakashima, R.; Yaono, R.; Yoshikawa, S. *Science* **1995**, *269*, 1069-1074.
(4) Yoshikawa, S.; Shimada, A. *Chem. Rev.* **2015**, *115*, 1936–1989.
(5) *Comprehensive Inorganic Chemistry II: From Elements to Applications*. 2013, pp 149–177.
(6) Collman, J. P.; Hutchison, J. E.; Lopez, M. A.; Tabard, A.; Guilard, R.; Seok, W. K.; Ibers, J. A.; L'Her, M. *J. Am. Chem. Soc.* **1992**, *114*, 9869–9877.
(7) Collman, J. P.; Fu, L.; Herrmann, P. C.; Zhang, X. *Science* **1997**, *275*, 949-951.
(8) Chishiro, T.; Shimazaki, Y.; Tani, F.; Tachi, Y.; Naruta, Y.; Karasawa, S.; Hayami, S.; Maeda, Y. *Angew. Chem. Int. Ed.* **2003**, *42*, 2788–2791.
(9) Chufán, E. E.; Puiu, S. C.; Karlin, K. D. *Acc. Chem. Res.* **2007**, *40*, 563–572.
(10) Hematian, S.; Garcia-Bosch, I.; Karlin, K. D. *Acc. Chem. Res.* **2015**, *48*, 2462–2474.
(11) Collman, J. P.; Devaraj, N. K.; Decréau, R. A.; Yang, Y.; Yan, Y.-L.; Ebina, W.; Eberspacher, T. A.; Chidsey, C. E. D. *Science* **2007**, *315*, 1565-1568.
(12) Andrew A. Gewirth; Matthew S. Thorum. *Inorg. Chem.* **2010**, *49*, 3557–3566.
(13) Debe, M. K. *Nature* **2012**, *486*, 43–51.
(14) Cheng, F.; Chen, J. *Chem. Soc. Rev.* **2012**, *41*, 2172–2192.
(15) Jaouen, F.; Proietti, E.; Lefevre, M.; Chenitz, R.; Dodelet, J.-P.; Wu, G.; Chung, H. T.; Johnston, C. M.; Zelenay, P. *Energy Environ. Sci.* **2011**, *4*, 114–130.
(16) Jasinski, R. *Nature* **1964**, *201*, 1212–1213.
(17) Jasinski, R. *J Electrochem Soc* **1965**, *112*, 526–528.
(18) Jahnke, H.; Schönborn, M.; Zimmermann, G. In *Physical and Chemical Applications of Dyestuffs*; Schäfer, F. P., Gerischer, H., Willig, F., Meier, H., Jahnke, H., Schönborn, M., Zimmermann, G., Eds.; Springer Berlin Heidelberg: Berlin, Heidelberg, 1976; pp 133–181.
(19) Liu, Y.; Yue, X.; Li, K.; Qiao, J.; Wilkinson, D. P.; Zhang, J. *Coord. Chem. Rev.* **2016**, *315*, 153–177.
(20) Thorseth, M. A.; Tornow, C. E.; Tse, E. C. M.; Gewirth, A. A. *Coord. Chem. Rev.* **2013**, *257*, 130–139.
(21) Tse, E. C. M.; Schilter, D.; Gray, D. L.; Rauchfuss, T. B.; Gewirth, A. A. *Inorg. Chem.* **2014**, *53*, 8505−8516.
(22) Yue-Ting Xi; Ping-Jie Wei; Ru-Chun Wang; Jin-Gang Liu. *Chem. Commun.* **2015**, *51*, 7455–7458.
(23) Lefèvre, M.; Proietti, E.; Jaouen, F.; Dodelet, J.-P. *Science* **2009**, *324*, 71–74.
(24) Lazarides, T.; Sazanovich, I. V.; Simaan, A. J.; Kafentzi, M. C.; Delor, M.; Mekmouche, Y.; Faure, B.; Réglier, M.; Weinstein, J. A.; Coutsolelos, A. G.; Tron, T. *J. Am. Chem. Soc.* **2013**, *135*, 3095–3103.
(25) Mazurenko, I.; Wang, X.; de Poulpiquet, A.; Lojou, E. *Sustain. Energy Fuels* **2017**, *1*, 1475–1501.
(26) Enguita, F. J.; Marçal, D.; Martins, L. O.; Grenha, R.; Henriques, A. O.; Lindley, P. F.; Carrondo, M. A. *J. Biol. Chem.* **2004**, *279*, 23472–23476.
(27) Enguita, F. J.; Martins, L. O.; Henriques, A. O.; Carrondo, M. A. *J. Biol. Chem.* **2003**, *278*, 19416–19425.

(28) Ducros, V.; Brzozowski, A.; Wilson, K.; Brown, S.; Ostergaard, P.; Schneider, P.; Yaver, D.; Pedersen, A.; Davies, G. *Nat. Struct. Biol.* **1998**, *5*, 310–316.
(29) Garavaglia, S.; Cambria, M.; Miglio, M.; Ragusa, S.; Lacobazzi, V.; Palmieri, F.; D'Ambrosio, C.; Scaloni, A.; Rizzi, M. *J. Mol. Biol.* **2004**, *342*, 1519–1531.
(30) Bento, I.; Martins, L. O.; Lopes, G. G.; Carrondo, M. A.; Lindley, P. F. *Dalton Trans.* **2005**, 3507–3513.
(31) Messerschmidt, A.; Ladenstein, R.; Huber, R. *J. Mol. Biol.* **1992**, *224*, 179–205.
(32) Zaitsev, V.; Zaitseva, I.; Papiz, M.; Lindley, P. *J. Biol. Inorg. Chem.* **1999**, *4*, 579–587.
(33) Zaitseva, I.; Zaitsev, V.; Card, G.; Moshkov, K.; Bax, B.; Ralph, A.; Lindley, P. *J. Biol. Inorg. Chem.* **1996**, *1*, 15–23.
(34) Mizutani, K.; Toyoda, M.; Sagara, K.; Takahashi, N.; Sato, A.; Kamitaka, Y.; Tsujimura, S.; Nakanishi, Y.; Sugiura, T.; Yamaguchi, S.; Kano, K.; Mikami, B. *Acta Crystallogr. Sect. F* **2010**, *66*, 765–770.
(35) Cracknell, J. A.; McNamara, T. P.; Lowe, E. D.; Blanford, C. F. *Dalton Trans.* **2011**, *40*, 6668–6675.
(36) Solomon, E. I. *Inorg. Chem.* **2016**, *55*, 6364–6375.
(37) De Poulpiquet, A.; Kjaergaard, C. H.; Rouhana, J.; Mazurenko, I.; Infossi, P.; Gounel, S.; Gadiou, R.; Giudici-Orticoni, M. T.; Solomon, E. I.; Mano, N.; Lojou, E. *ACS Catal.* **2017**, *7*, 3916–3923.
(38) Denisov, I. G.; Makris, T. M.; Sligar, S. G.; Schlichting, I. *Chem. Rev.* **2005**, *105*, 2253–2277.
(39) Schlichting, I.; Berendzen, J.; Chu, K.; Stock, A. M.; Maves, S. A.; Benson, D. E.; Sweet, B. M.; Ringe, D.; Petsko, G. A.; Sligar, S. G. *Science* **2000**, *287*, 1615–1622.
(40) Rittle, J.; Green, M. T. *Science* **2010**, *330*, 933–937.
(41) Yosca, T.; Rittle, J.; Krest, C. M.; Onderko, E. L.; Silakov, A.; Calixto, J. C.; Behan, R. K.; Green, M. T. *Science 342*, 825–829.
(42) Himes R. A.; Karlin K. D. *Curr. Opin. Chem. Biol.* **2009**, *13*, 119–131.
(43) Lee, J. Y.; Karlin, K. D. *Curr. Opin. Chem. Biol.* **2015**, *25*, 184–193.
(44) Quist, D. A.; Diaz, D. E.; Liu, J. J.; Karlin, K. D. *J. Biol. Inorg. Chem.* **2017**, *22*, 253–288.
(45) Citek, C.; Herres-Pawlis, S.; Stack, T. D. P. *Acc. Chem. Res.* **2015**, *48*, 2424–2433.
(46) Elwell, C. E.; Gagnon, N. L.; Neisen, B. D.; Dhar, D.; Spaeth, A. D.; Yee, G. M.; Tolman, W. B. *Chem. Rev.* **2017**, *117*, 2059–2107.
(47) Yamada, Y.; Yamamoto, T.; Okawara, M. *Chem. Lett.* **1975**, *4*, 361–362.
(48) Södergren, M. J.; Alonso, D. A.; Bedekar, A. V.; Andersson, P. G. *Tetrahedron Lett.* **1997**, *38*, 6897–6900.
(49) Katsuki, T. *Chem. Lett.* **2005**, *34*, 1304–1309.
(50) Driver, T. G. *Org. Biomol. Chem.* **2010**, *8*, 3831–3846.
(51) Intrieri, D.; Zardi, P.; Caselli, A.; Gallo, E. *Chem. Commun.* **2014**, *50*, 11440–11453.
(52) Uchida, T.; Katsuki, T. *Chem. Rec.* **2014**, *14*, 117–129.
(53) Jenkins D. M. *Synlett* **2012**, 1267–1270.
(54) Kwart, H.; Kahn, A. A. *J. Am. Chem. Soc.* **1967**, *89*, 1950–1951.
(55) Kwart, H.; Khan, A. A. *J. Am. Chem. Soc.* **1967**, *89*, 1951–1953.
(56) Breslow, R.; Gellman, S. H. *J. Am. Chem. Soc.* **1983**, *105*, 6728–6729.
(57) Breslow, R.; Gellman, S. H. *J. Chem. Soc. Chem. Commun.* **1982**, 1400–1401.
(58) Svastits, E. W.; Dawson, J. H.; Breslow, R.; Gellman, S. H. *J. Am. Chem. Soc.* **1985**, *107*, 6427–6428.
(59) White, R. E.; McCarthy, M. B. *J. Am. Chem. Soc.* **1984**, *106*, 4922–4926.

(60) McIntosh, J. A.; Farwell, C. C.; Arnold, F. H. *Curr. Opin. Chem. Biol.* **2014**, *19*, 126–134.
(61) Arnold, F. H. *Q. Rev. Biophys.* **2015**, *48*, 404–410.
(62) McIntosh, J. A.; Coelho, P. S.; Farwell, C. C.; Wang, Z. J.; Lewis, J. C.; Brown, T. R.; Arnold, F. H. *Angew. Chem. Int. Ed.* **2013**, *52*, 9309–9312.
(63) Farwell, C. C.; McIntosh, J. A.; Hyster, T. K.; Wang, Z. J.; Arnold, F. H. *J. Am. Chem. Soc.* **2014**, *136*, 8766–8771.
(64) Lowden, P. A. S. In *Aziridines and Epoxides in Organic Synthesis*; Wiley-VCH Verlag GmbH & Co. KGaA, 2006; pp 399–442.
(65) Sweeney, J. B. In *Aziridines and Epoxides in Organic Synthesis*; Wiley-VCH Verlag GmbH & Co. KGaA, 2006; pp 117–144.

Chapter 2: synthesis and electrochemical studies of binuclear copper complexes

In this chapter, studies on binuclear copper complexes will be presented. First of all, examples of binuclear systems reported in literature will be introduced. Studies on three binuclear copper complexes will be then presented, with a description of synthesis and characterization of the ligands and their complexes. The characterization will focus on studies of the electrochemical behaviour of the complexes, performed by coupling electrochemical techniques (cyclic voltammetry, RDE analysis, coulometry) and EPR spectroscopy.

a. Introduction

Over the past fifty years a huge number of binuclear copper complexes have been studied both for their magnetic properties, catalytic applications and first binuclear copper complexes were obtained by using μ-phenoxo-imine ligands. Binucleating ligands incorporating a bridging phenolate were introduced independently in the early 1970s by R. Robson[1,2], H. Okawa[3] and S. Kida[4] who reported the syntheses of numerous (μ-phenoxo)(μ-X)dicopper complexes (Figure 1). These reports led to the development of many kinds of ligand systems acyclic or macrocyclic[5,6], symmetrical or unsymmetrical, homo- or heterobinuclear[6–8] by using lateral complexing arms with various denticities and aromatic or aliphatic organic bridges. All these works focused on studies about structural and magnetic properties of the complexes.

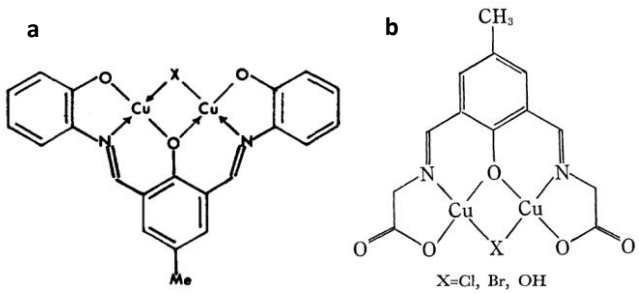

Figure 1: *Dicopper complexes reported by Robson[1] and Okawa and Kida[4].*

More recent works are oriented to bioinspired studies in order to mimic the activity of copper enzymes and better understand their reactivity[9]. Binuclear copper complexes have been used so far especially in two major domains: hydrolysis of phosphate esters aiming at DNA cleavage and oxidation of phenols and catechols in relation with the activities of tyrosinase and catechol oxidase[10,11].

These studies focused on synthetic models of tyrosinase and catechol oxidase with high number of dinuclear copper complexes obtained from dinucleating ligands bearing polyamine side-arms. Karlin and co-workers firstly reported the intramolecular oxygenation of a m-xylyl dinuclear Cu(I) complex upon reaction with molecular oxygen, with the formation of a μ-phenoxo bridgded complex (Figure 2)[12]. This first study paved the way to investigations on the interaction between copper complexes and molecular oxygen, with important contributions by the groups of Karlin, Stack and Tolman[9].

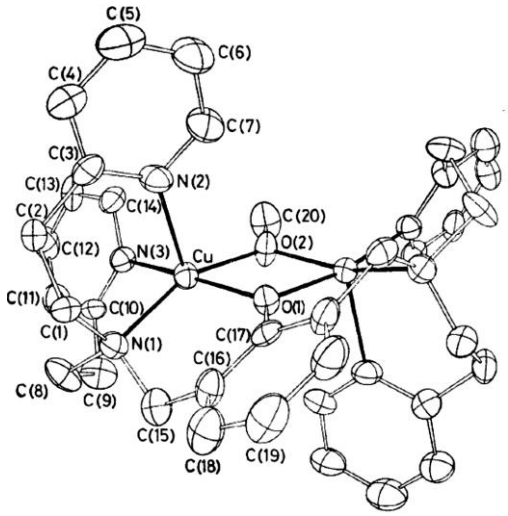

Figure 2: *μ-phenoxo bridged complex obtained by Karlin and co-workers[12].*

As mentioned in Chapter 1, copper-oxygen adducts can react by giving rise to oxidation or oxygenation of substrates. Literature reports a huge number of binuclear copper complexes capable of mimicking the activity of tyrosinase and catechol oxidase, with several complexes based on μ-phenoxo bridging polyamine ligands. Systems developed by the groups of Krebs[13], Mukherjee[14] and Belle[15] have been used for studying the influence of the coordinating environment on catalytic activity, especially in catalytic oxidation of catechols. Historically the oxidation of catechols has been more explored than oxygenation of phenols because the former reaction is easier to study for two main reasons. First of all, oxidation of catechols does not involve any atom transfer but only electron transfer between substrate and catalyst. Moreover, catechols have lower oxidation potentials than phenols so they can be more easily oxidised.

While catecholase activity was found to be relatively easy to mimic, a smaller number of binuclear copper complexes proved able to oxygenate substrates[16]. As mentioned above,

Karlin's group first used a m-xylyl ligand for performing intramolecular oxygenation. Several binuclear complexes with different molecular architectures have been developed for performing hydroxylation of phenols. Casella and co-workers developed in the 1990s efficient catalysts able to hydroxylate phenols, following a reaction mechanism similar to tyrosinase[17] (Figure 3). This is based on a m-xylyl ligand like the system developed by Karlin's group but this latter does not show intramolecular hydroxylation of the ligand but oxygenation of phenols and sulfides[18].

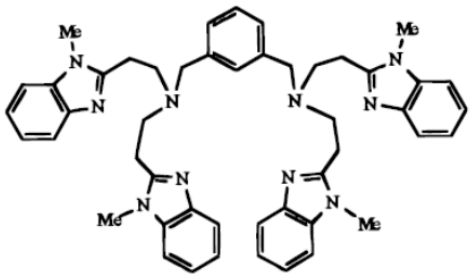

Figure 3: *m-xylyl ligand developed by Casella and co-workers for performing intermolecular oxygenations[17,18].*

Three new binuclear copper complexes will be presented here. They have been obtained by using a m-xylyl and a μ-phenolato motifs, both of them bearing piperazine side arms. They have been conceived as first models for the design of biomimetic trinuclear copper complexes for reduction of dioxygen.

b. Design and synthesis of bioinspired binuclear complexes

As stated in Chapter 1, binuclear copper centers in enzymes and in complexes are able in principle to perform only a two-electron reduction of molecular oxygen, producing hydrogen peroxide and its derivatives, which can be detrimental for the catalytic systems. Looking at issues of the catalysis of oxygen reduction from a broader point of view, these kinds of catalysts would not be used for reactivity in solution but they would be immobilized on electrodes. They could be able to continuously supply the electrons needed to perform catalysis, avoiding the formation of harmful by-products. As described in Chapter 1, Collman and co-workers demonstrated that when complexes are directly adsorbed on electrodes in which the electron transfer is fast, the four-electron reduction is efficient also when they are not capable of giving the four electrons at once[19].

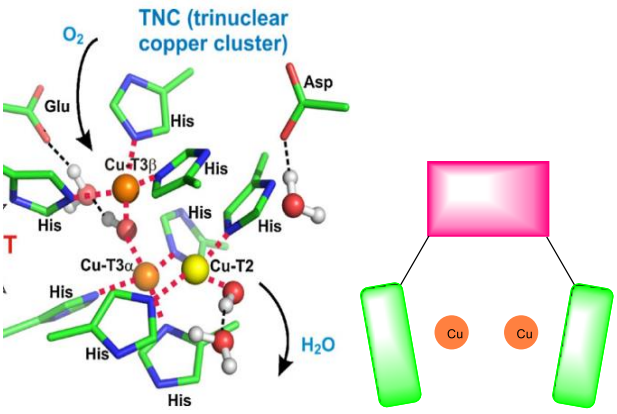

Figure 4: *Trinuclear copper cluster of multicopper oxidases (left) and design of bioinspired binuclear complexes (right).*

Binuclear copper complexes here presented have been designed as elementary part of more elaborated catalysts for dioxygen reduction (see Chapter 3). The designed ligands are symmetric, with two identical arms, separated by a m-xylyl spacer, capable of binding two copper centers with the same coordinating environments (Figure 4). This design has been chosen to mimic the coordination environment of dicopper enzymes, in which the two metal centers are often bound by the same ligands, with the formation of symmetric clusters. Moreover, symmetric ligands are often more easily accessible from the synthetic point of view.

The coordinating units have been chosen in order to tune the redox behaviour of the copper centers. The two oxidation states of copper have different coordination geometries (tetrahedral for Cu(I), square-pyramidal for Cu(II)), with important molecular rearrangements of the complexes when they undergo a redox phenomenon. As a result electron transfer in copper complexes is often slow and irreversible. A slow electron transfer is highly undesirable for performing efficient electrocatalysis, so, in order to minimize the rearrangements of the complexes, the ligands were designed with groups capable of stabilising copper in both oxidation states but leaving conformational flexibility. Moreover, the ligands should stabilize the Cu(I) state, in order to increase its reduction potential close to that of dioxygen and for preventing the disproportionation of Cu(I), a common phenomenon in copper complexes. Piperazines have been chosen as coordinating groups because they are able to coordinate each copper center with their two amine groups and leaving the other coordinating positions occupied by solvent molecules or coordinating anions. These latter can be easily coordinated/decoordinated when the metal complex

undergoes a redox phenomenon, with a minimization of the rearrangements and a fostering of fast electron transfers. The major difference between the two synthetized binucleating ligands mXBMP and mXBMP-OH (Figure 5) is the presence of a phenolic group between the two piperazine arms. The presence of the hydroxo-bridging group would increase the stability of the Cu(II) complexes and the interactions between the two copper ions.

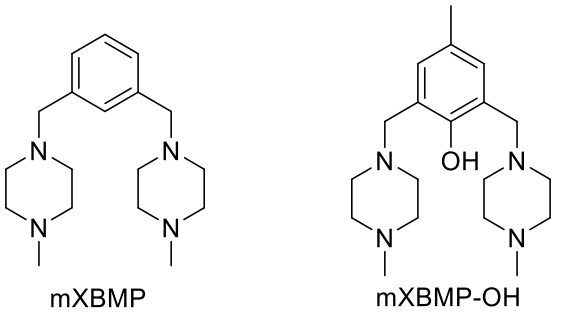

Figure 5: *Structure of the binucleating ligands mXBMP (left) and mXBMP-OH (right).*

As it is possible to observe in the retrosynthetic path shown in Scheme 1, the ligands are quite easy to obtain. Indeed they are synthetized by nucleophilic substitution between their dichloride precursors and 2 equivalents of N-methyl piperazine. In the case of the synthesis of the ligand mXBMP-OH, the dichloride precursor is not commercial and it is obtained by chlorination of 2,6-bis(hydroxymethyl)-p-cresol, by following a literature protocol[20]. The ligand mXBMP is already known in literature as ligand for bismuth complexes[21] but no copper complexes using this ligand are reported. Several copper complexes with ligands similar to mXBMP-OH are reported in literature but no one of them has a methyl substituent as para substituent of the phenol[13,22,23].

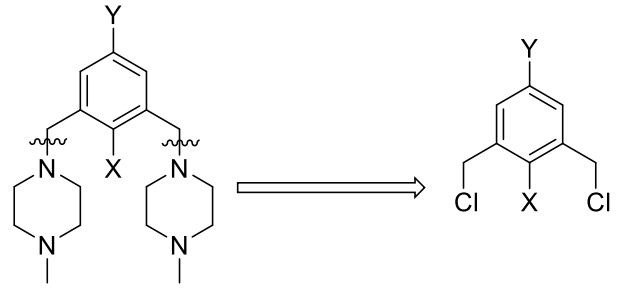

mXBMP: X= H, Y= H
mXBMP-OH: X= OH, Y= CH_3

Scheme 1: *Retrosynthetic path of the ligands mXBMP and mXBMP-OH.*

1. *Synthesis of the ligands*

The ligand mXBMP **(1)** has been obtained in one step, through a nucleophilic substitution between dichloro-m-xylene and N-methyl piperazine (Scheme 2), following a modified version of a published experimental protocol[21]. Since the reaction between dichloro-m-xylene and N-methyl piperazine is slow, the reaction mixture was heated and an excess of amine is necessary to drive the formation of the disubstituted product.

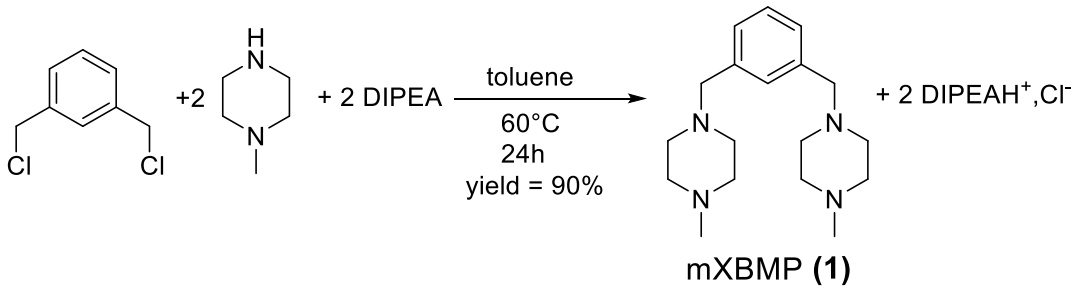

Scheme 2: *Synthesis of mXBMP* ***(1)****.*

The ligand was obtained pure and in good yields and white crystals of mXBMP suitable for single crystal X-ray diffraction were obtained by slow evaporation of a concentrated solution of the ligand in dichloromethane (Figure 6).

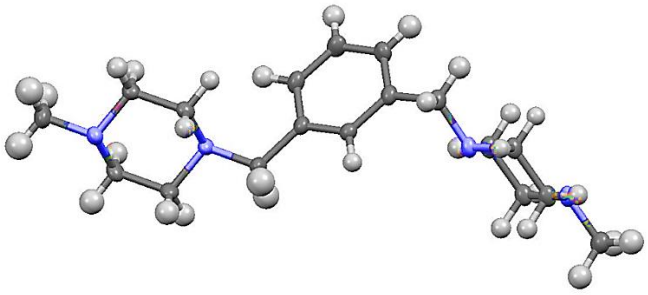

Figure 6: *Mercury drawing of the ligand based on crystalline structure of the ligand mXBMP (blue = N, dark grey = C, pale grey = H).*

The ligand crystallizes in the monoclinic system, with space group $P2_1/n$. It is possible to observe that the two arms of the ligand are not coplanar and the two piperazine moieties adopt a chair conformation.

The ligand mXBMP-OH was obtained in a way similar to mXBMP. As described above, the dichloride precursor is not commercial and it is synthetized by chlorination of 2,6-bis(hydroxymethyl)-p-cresol with thionyl chloride[20] (Scheme 3).

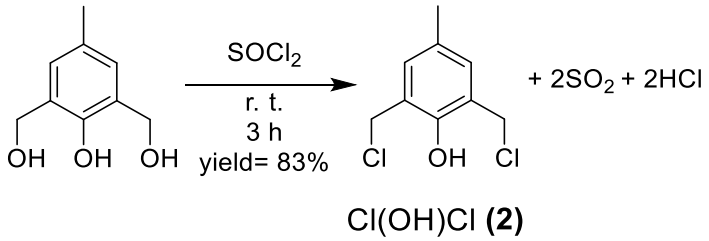

Cl(OH)Cl **(2)**

Scheme 3: *Synthesis of the dichloride precursor Cl(OH)Cl* ***(2)****.*

The obtained dichloride is then used for a step of nucleophilic substitution with N-methyl piperazine. In this case the chloride appears more reactive and the reaction is performed in stoichiometric conditions and without heating (Scheme 4).

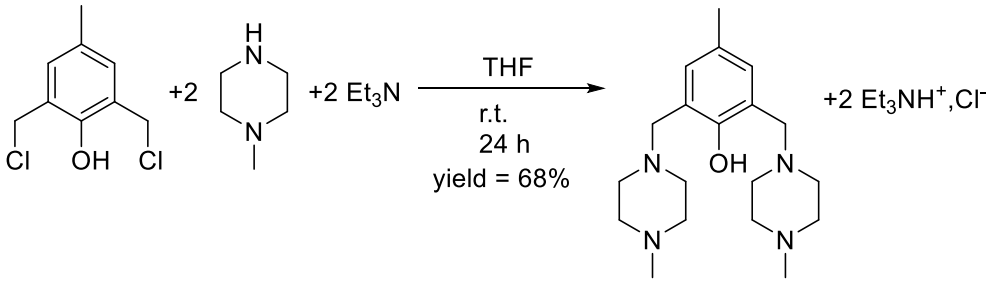

mXBMP-OH **(3)**

Scheme 4: *Synthesis of the ligand mXBMP-OH* ***(3)****.*

The two ligands are quite accessible from the synthetic point of view and both have been obtained in good yields. One of the major drawbacks in synthesizing these piperazine ligands is the basicity of their tertiary amine groups. In fact they have a basicity close to the basicity of triethylamine and di-isopropylethylamine (DIPEA) and in the reactions of nucleophilic substitution an excess of base as proton scavenger is always necessary in order not to lose the reactivity of the amino groups by protonation. Moreover, the obtained molecules are highly polar and hydrophilic, therefore their purification can be laborious and with loss of a part of product.

2. Synthesis and characterization of the binuclear complexes

The binuclear complexes have been obtained by adding the two equivalents of Cu(II) salts. The ligand mXBMP-OH is previously treated with NaH, in order to obtain the sodium salt of the salt (mXBMP-ONa, **(4)**), in which the phenolic group is deprotonated and can act as a better ligand (Scheme 5).

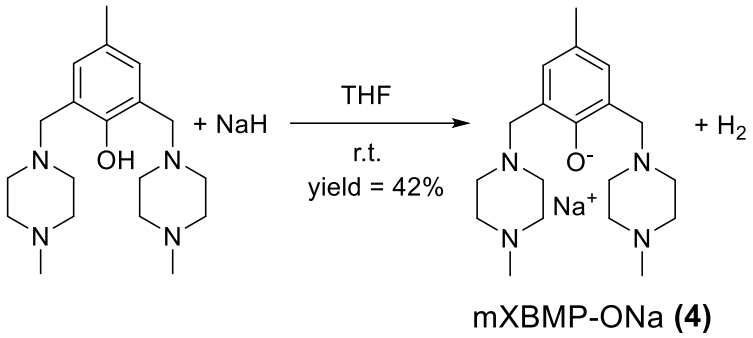

mXBMP-ONa **(4)**

Scheme 5: *Synthesis of the sodium salt mXBMP-ONa* ***(4)****.*

a. Synthesis and characterization of the complex CxCl **(5)**

For the synthesis of this complex the ligand mXBMP was used for the complexation adding two equivalents of $CuCl_2.2H_2O$ to its solution in acetonitrile (Scheme 6). The complex was obtained as a pale green/yellowish powder.

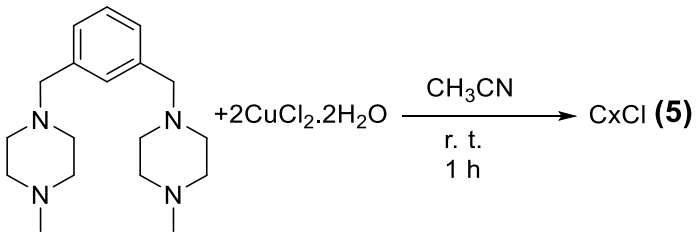

Scheme 6: *Synthesis of the complex CxCl* ***(5).***

The exact nature of the obtained complex was difficult to state; no single crystal could be obtained and Cu(II) complexes are not suitable for NMR studies. Upon performing a UV-vis titration of the ligand with $CuCl_2.2H_2O$ it was possible to affirm that the complex has a 2:1 stoichiometry Cu(II) : mXBMP. The titration was performed by adding from 0 to 4 equivalents of copper salt to the ligand. The recorded spectra show the increase of the absorbance of a peak at 303 nm during the whole titration, while the appearance of a peak at 256 nm is observed only after addition of 2 equivalents of copper salt (Figure 7, top left, continuous lines). Dashed line spectra in Figure 7 show that copper chloride has intense absorptions in the same domain, at 313 nm and 467 nm. For this reason the obtained data were treated to subtract the contribution of copper chloride. Treated spectra (Figure 7, top right) show the increase of a peak at 296 nm ($\varepsilon = 4800\ M^{-1}\ cm^{-1}$) between 0 and 2 eqv. of Cu(II) and then no changes in spectra recorded between two and four equivalents of Cu(II) (Figure 7, bottom, right). This characteristic band of the complex suggests a charger transfer transition $Cl^- \rightarrow$ Cu(II) close in energy to the one of the copper salt alone, so it is possible that the

coordination sphere of copper is completed by chloride anions. d-d transitions confirm the formation of a binuclear Cu(II) complex with absorption peaks at 659 nm and 836 nm (Figure 7, bottom left), close to the ones of the copper salt alone. The absorption peaks in this region are broad and not intense and it is not possible to make investigations about the coordination geometry through them.

To check the validity of the hypothesis about the coordination sphere of the complex, the spectrum of copper chloride was recorded at the concentration corresponding to two equivalents of Cu(II). Both the energy and intensity of the absorbance match those reached during the titration. These observations thus support the coordination of two chloride anions to each copper. It is possible to hypothesize that the formula of the complex is $Cu_2(mXBMP)Cl_4$

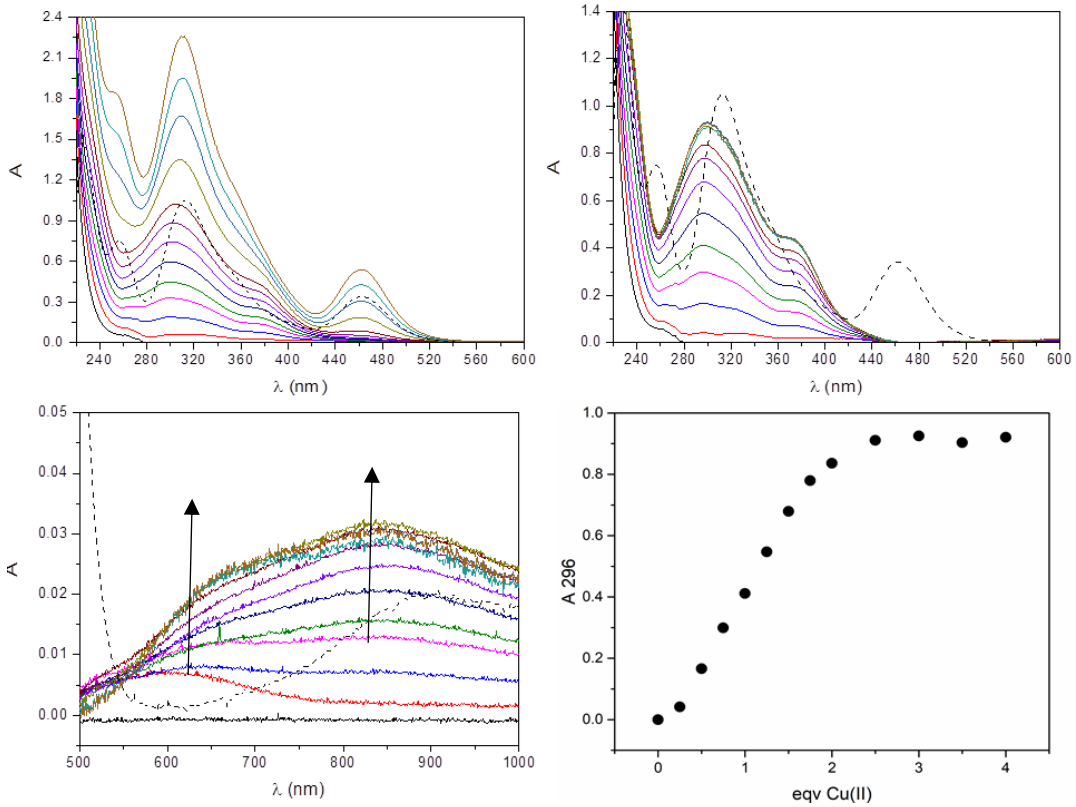

Figure 7: *Titration of mXBMP with $CuCl_2.2H_2O$ in acetonitrile ([mXBMP]= 2 10^{-4} M). Top: monitoring of the titration from 0 to 4 eqv. of Cu(II) (continuous lines) and spectrum of $CuCl_2.2H_2O$ (dashed lines); left: spectra before subtraction of the copper salt contribution, right: spectra after subtraction of the copper salt contribution. Bottom, left: view of the evolution of the d-d transitions region during the titration (spectra after subtraction of the copper salt contribution). Bottom, right: evolution of the absorbance at 296 nm during the titration.*

b. Synthesis and characterization of the complex Cx(pheno)Cl **(6)**

The sodium salt of mXBMP-OH was used for the synthesis of its copper complex by dissolving it in anhydrous THF and adding at room temperature two equivalents of copper chloride (Scheme 7). The complex was afforded as a brown powder after its precipitation with hexane from a brown solution.

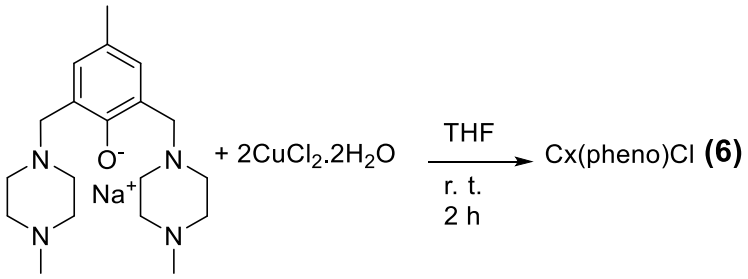

Scheme 7: *Synthesis of Cx(pheno)Cl* ***(6)****.*

Also in this case the nature of the obtained complex is difficult to state. Through UV-vis titration of the sodium salt of the ligand in THF it was possible to state that the complex is a 2:1 species Cu(II) : ligand. During the titration it is possible to observe the increase of a peak at 450 nm (Figure 8, top left, continuous lines) and also in this case it is possible to observe that copper chloride has important absorption peaks in the same zone. These can influence the characteristic peaks of the complex when the copper salt is in excess. For this reason also in this case collected data were treated by subtracting the spectrum of copper chloride to the recorded spectra. Treated spectra in Figure 8, top right show the increase of a characteristic peak at at 454 nm (ε= 1800 M^{-1} cm^{-1}) between 0 and 2 equivalents of copper salt (Figure 8, right). This absorption can be assigned to a charge transfer transition between the phenolate group and the copper ions[24] and since the band grows until two equivalents of copper chloride it is possible to affirm that the two metal centers are bound by the phenolate. Looking and considering the part at higher energy of the UV-vis spectrum it is possible to observe that the ligand alone has an important transition at 290 nm, which increases during the titration until two equivalents of copper chloride. As noted above this absorption is assigned to a Cl^- → Cu(II) charge transfer transition, so also in this case it is possible to affirm that chloride anions are present in the coordination sphere of the two metals. Unlike for the complex CxCl previously described in this case it is not possible to estimate the number of chlorides present in the complex because of the superposition of the absorption of the ligand. For respecting the stoichiometry and the electroneutrality of

the complex a reasonable formula of it can be Cu_2(mXBMP-O)Cl_3.

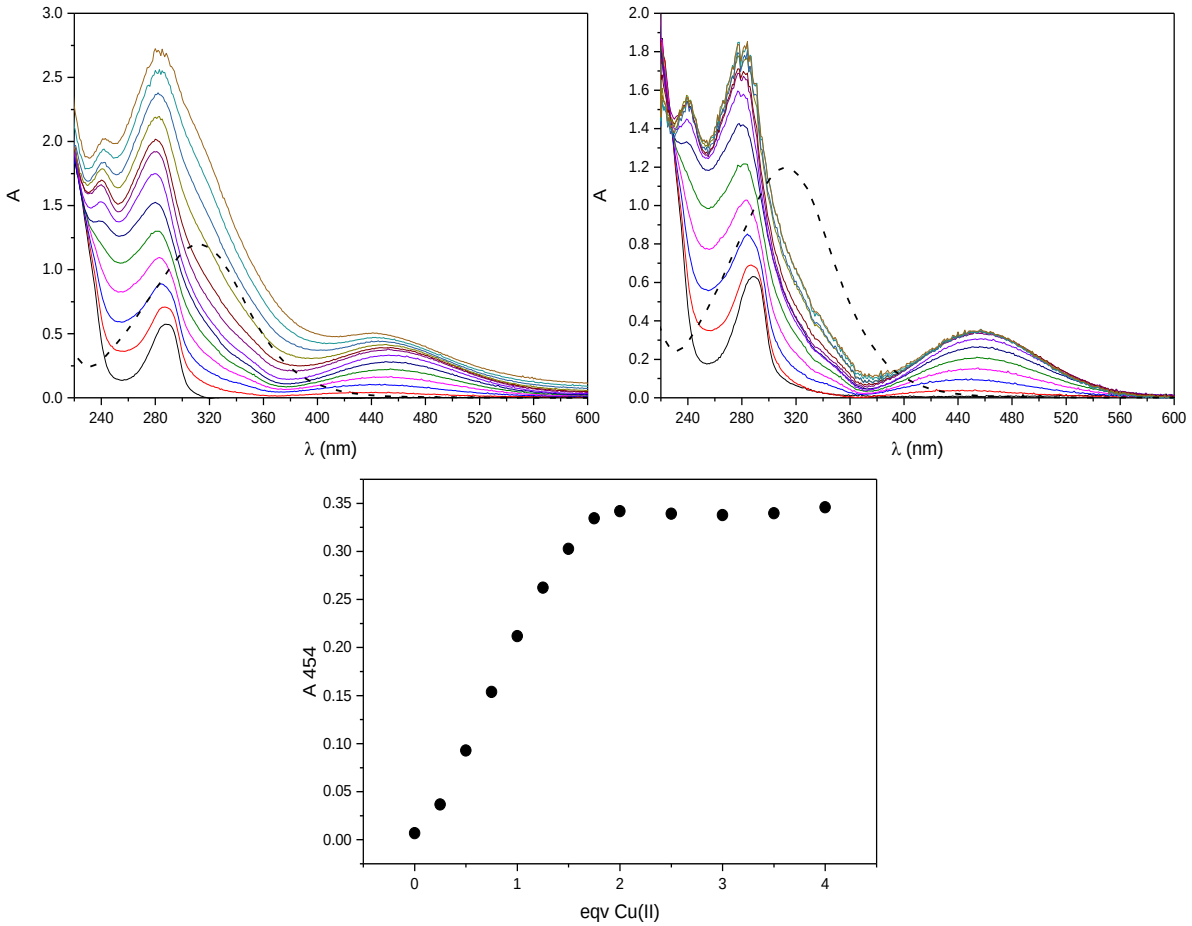

Figure 8: *Titration of mXBMP with $CuCl_2.2H_2O$ in THF ([mXBMP-ONa]= 2 10^{-4} M). Top: monitoring of the titration from 0 to 4 eqv. of Cu(II) (continuous lines) and spectrum of $CuCl_2.2H_2O$ (dashed lines); left: spectra before subtraction of the copper salt contribution, right: spectra after subtraction of the copper salt contribution. Bottom: evolution of the absorbance at 296 nm during the titration.*

c. Synthesis and characterization of the complex [Cu_2(mXBMP-O)($CH_3COO)_2$](ClO_4).(CH_3CN).(MeOH) **(7)**

This complex was synthesized by using the sodium salt of mXBMP-OH, like Cx(pheno)Cl. Copper acetate was used as Cu(II) salt, as it can give bridging anions to the complex. Two equivalents of copper acetate monohydrate was added to a solution of ligand in a mixture 50:50 v/v acetonitrile : methanol stirred at room temperature. The binuclear copper complex was obtained in good yield as a green powder (Scheme 8).

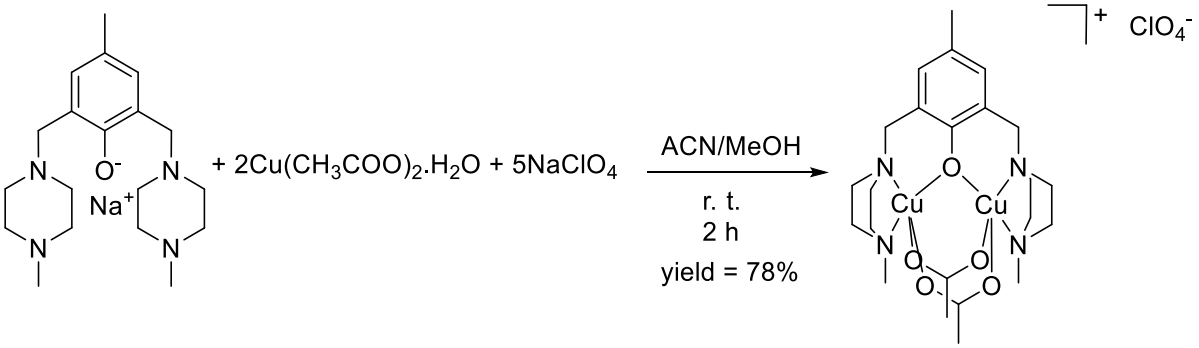

Scheme 8: *Synthesis of $[Cu_2(mXBMP\text{-}O)(CH_3COO)_2]ClO_4.(CH_3CN).(MeOH)$* ***(7)****.*

In this case green crystalline needles suitable for single crystal X-ray diffraction were obtained by slow evaporation of a concentrated solution of the complex in an acetonitrile: methanol mixture 50:50 v/v. The complex crystallizes in the monoclinic system, space group $P2_1/n$. (Figure 9). The structure shows the presence of a binuclear Cu(II) complex, in which each metal center is pentacoordinated by the two piperazine units in a boat conformation, the bridging phenolate of the ligand and two exogeneous bridging acetate anions. The two metal centers are not strictly equivalent because of slightly different bond lengths with piperazine and acetate ligands. The distance between the two metal centers is 3.253 Å, the angle $Cu(II)_1\text{-}O_{phenolate}\text{-}Cu(II)_2$ is of 113.96° and the distance between the two metal centers and the oxygen of phenolate is 1.940 Å. A non-coordinated perchlorate is present as a counteranion and the two solvents used for the synthesis are also found in the crystalline structure, with the methanol molecule hydrogen bonded to an acetate ligand. These crystallographic results are very close to those reported in literature for similar triply-bridged complexes with a phenolato ligand and two exogenous coordinating acetate anions[23,22]. The structural properties of the complex have an influence also on its spectroscopic behaviour. The presence of two bridging acetate anions results in a broadening of the angle $Cu(II)_1\text{-}O_{phenolate}\text{-}Cu(II)_2$ from 90°. As a consequence, there is a good overlap between the magnetic orbitals of the copper centers and molecular orbitals of the ligand, which promotes the antiferromagnetic coupling of the two metals, resulting in the absence of EPR signal.

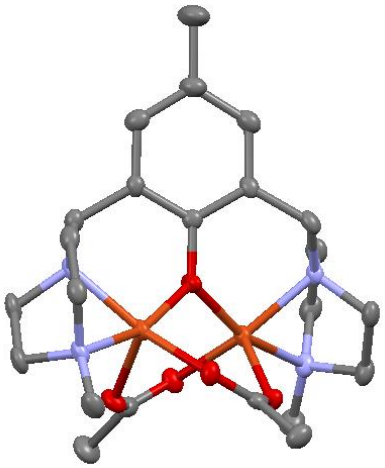

Figure 9: *Mercury drawing of the cation based on crystalline structure of* $[Cu_2(mXBMP\text{-}O)(CH_3COO)_2]^+$. Grey= C, red= O, light blue= N, orange= Cu. Hydrogen atoms are omitted for clarity.

The UV-vis spectrum of the complex in acetonitrile solution (Figure 10) is dominated by two main transitions. The more intense band at 402 nm (ε= 916 M^{-1} cm^{-1}) can be attributed to a charge transfer transition from the bridging phenolate to the two metallic centers, while the broad absorption in the visible region of the spectrum (λ_{max}= 666 nm, ε= 420 M^{-1} cm^{-1}) is due to the d-d transitions of the coordinated Cu(II) centers.

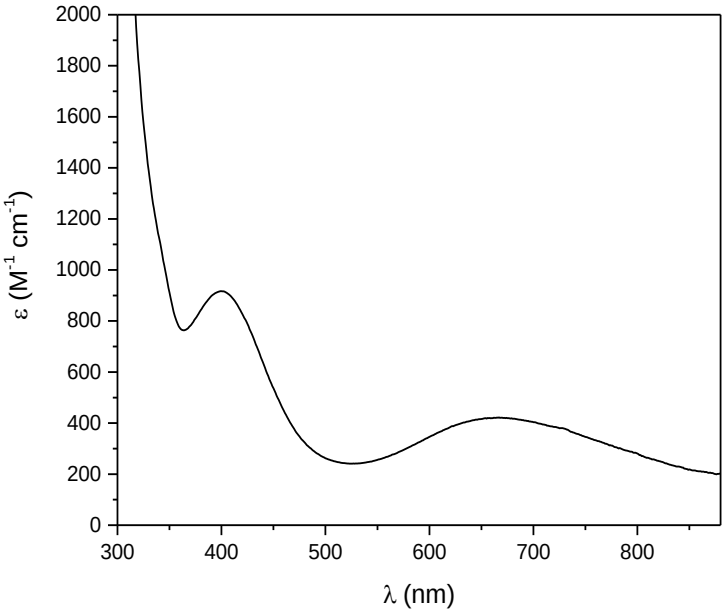

Figure 10: *UV-vis spectrum of the complex* $[Cu_2(mXBMP\text{-}O)(CH_3COO)_2]ClO_4.(CH_3CN).(MeOH)$ *in acetonitrile. [complex]= 4* 10^{-4} *M.*

c. Study of the electrochemical properties of the complexes

The three obtained complexes were studied by electrochemical techniques in order to correlate their electrochemical behaviour with the coordinating environment of the copper centers. CxCl and Cx(pheno)Cl were studied by cyclic voltammetry, RDE and coulometry. The experiments have been performed with a 1mM acetonitrile solution of the complex, using tetrabutylammonium hexafluorophosphate ($TBAPF_6$) as supporting electrolyte. Moreover, after each electrolysis of the two complexes a sample was collected and analysed by EPR spectroscopy. $[Cu_2(mXBMP\text{-}O)(CH_3COO)_2]ClO_4.(CH_3CN).(MeOH)$ was studied only by cyclic voltammetry and since it appeared less soluble in acetonitrile the experiments were carried out in DMF, with $TBAPF_6$ as supporting electrolyte. For all experiments ferrocene was used as internal standard for the calibration[25] and the potentials are here reported to the Fc^+/Fc couple.

1. Study of the electrochemical behavior of complex CxCl

The electrochemical experiments were performed as above. The complex was not completely soluble in acetonitrile in presence of the electrolyte, and a green solution with some tiny solid was observed. Since the exact nature of the complex was not known, for all the electrochemical calculations the molecular weight was calculated taking into account the presence of a 2:1 Cu(II) : mXBMP complex, in which each copper is bound to both the nitrogen atoms of a piperazine and two chloride anions (MW= 571.36 $g.mol^{-1}$).

The RDE analysis (Figure 11, top left) shows the presence of a wave which starts from positive current. Moreover, the wave appears ill-defined which suggests that several waves are superimposed. This means that several species at different redox states are present in solution. Cyclic voltammetry (Figure 11, top right) confirms the presence of an equilibrium between a mixture of species at different oxidation states. Starting the scan from the open circuit potential towards positive potentials it is possible to observe a small, not well defined oxidation peak and, from the second cycle, an oxidation peak at 0.46 V, coupled with a reduction at 0.21 V vs. Fc+/Fc. The two peaks are broadened, suggesting a slow electron transfer or the presence of more than one species with close reduction potentials. The linear variation of the current intensity with the square root of the scan rate indicates that the electrochemical process takes place in solution (Figure 11, bottom left).

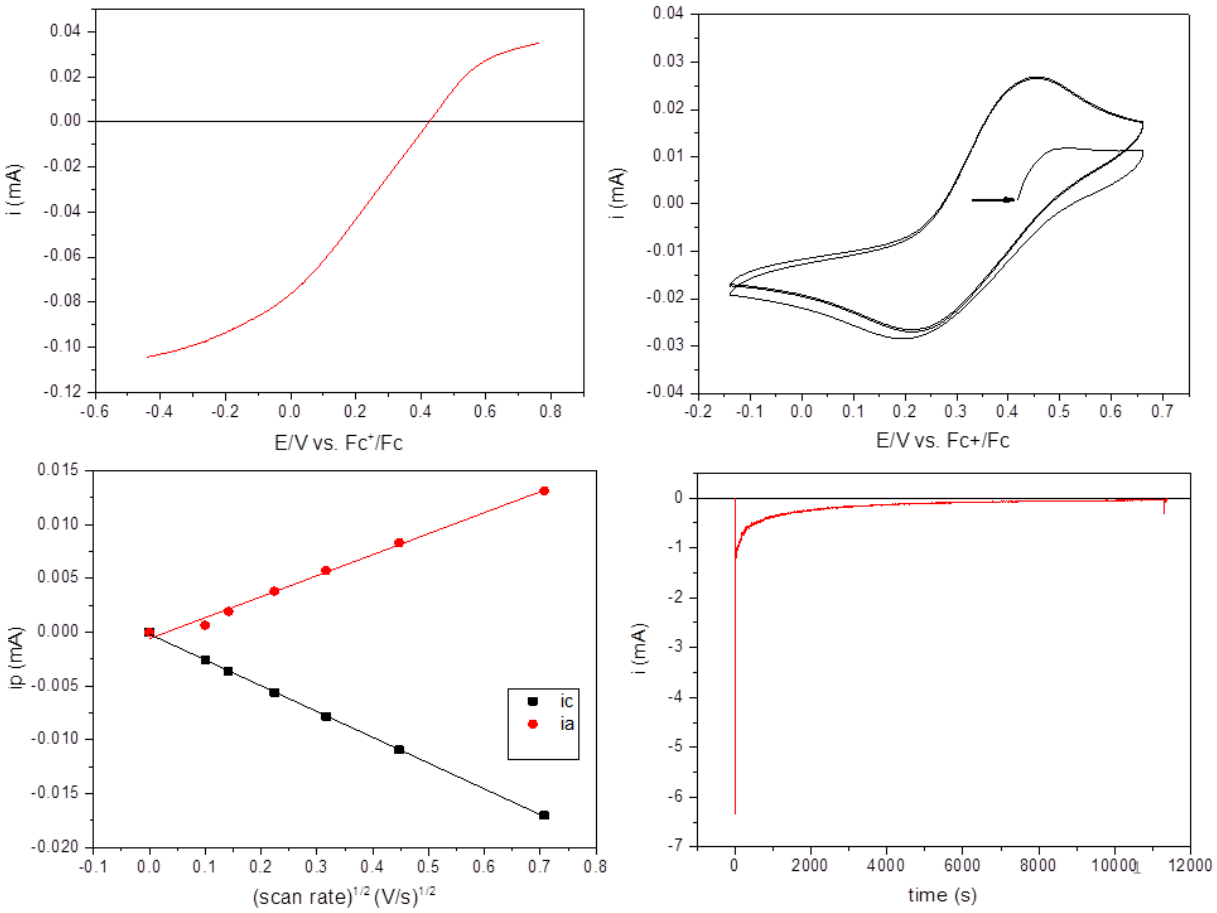

Figure 11: *Electrochemical behaviour of the complex CxCl in acetonitrile (0.1 M $TBAPF_6$ as supporting electrolyte). Top left: RDE analysis (1000 rpm, 10 mV/s). Top right: cyclic voltammetry (100 mV/s). Bottom left: tracing of peak currents vs. square root of scan rate. Bottom right: electrolysis of CxCl at -0.4 V vs. Fc+/Fc. Counter electrode= Pt wire, reference electrode= homemade Ag/AgCl electrode, working electrode= glassy carbon electrode (3 or 5 mm).*

The complex was then electrolysed at -0.4 V vs. Fc+/Fc (Figure 11, bottom right) and the solution turned from green to pale yellow, with dissolution of the precipitate observed before. Integration of the current passed over time resulted in 1.76 C exchanged during the electrolysis, which corresponds approximatively to 1.13 electrons per molecule. Owing to the presence of solid which dissolved during the electrolysis, it is difficult to determine the exact number of electrons exchanged.

The RDE analysis of the electrolysed solution (Figure 12, top left) confirms the presence of a completely reduced species, which shows only a well-defined oxidation wave. The recorded cyclic voltammogram after the reduction (Figure 12, top right) shows an oxidation peak at 0.50 V vs. Fc+/Fc coupled with a reduction peak at 0.32 V. By observing narrow peaks both in

oxidation and reduction it is possible to state that after reduction only one species is present in solution. This observation is consistent with the RDE experiment.

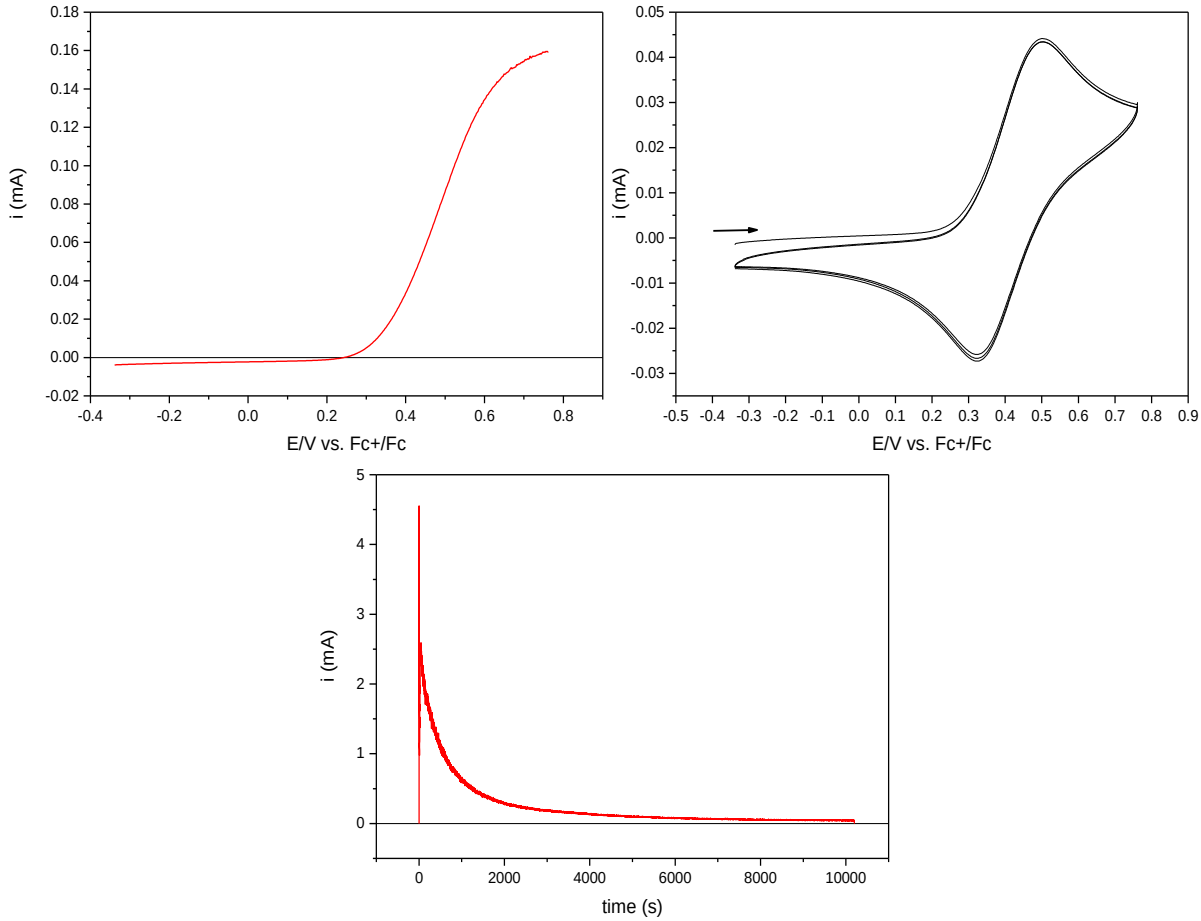

Figure 12: *Electrochemical analysis of the product of the first electrolysis of CxCl in acetonitrile (0.1 M $TBAPF_6$ as supporting electrolyte). Top left: RDE analysis (1000 rpm, 10 mV/s). Top right: cyclic voltammetry (100 mV/s). Bottom: electrolysis of the reduced product at 0.6 V. Counter electrode= Pt wire, reference electrode= homemade Ag/AgCl electrode, working electrode= glassy carbon electrode (3 or 5 mm).*

The reduced complex was then re-oxidized at 0.6 V vs Fc+/Fc for three hours (Figure 12, bottom). The potential chosen to perform this electrolysis is not much higher than the oxidation potential of the complex because at more positive potential chloride anions can be oxidized and interfere with the measurements. The solution passed from pale yellow to yellowish-green, indicating the re-oxidation of copper, but it did not come back to the original colour before the first electrolysis and no formation of precipitate was observed. Integration of the current passed over time resulted in 2.47 C exchanged during the electrolysis, which resulted in 1.59 electrons per molecule.

The RDE analysis performed after the re-oxidation of the complex (Figure 13, left) shows a reduction wave which confirms the presence of an oxidized species. The recorded cyclic voltammogram shows a reduction peak at 0.22 V vs. Fc+/Fc which moves to 0.30 V after oxidation at 0.52 V (Figure 13, right). Thus it is possible to say that the oxidized species generated by electrolysis during the cyclic voltammetry underwent a chemical transformation after the first reduction which changed its reduction potential. Like in the previous case, the peaks appear quite narrow, indicating the presence of only one species after electrolysis.

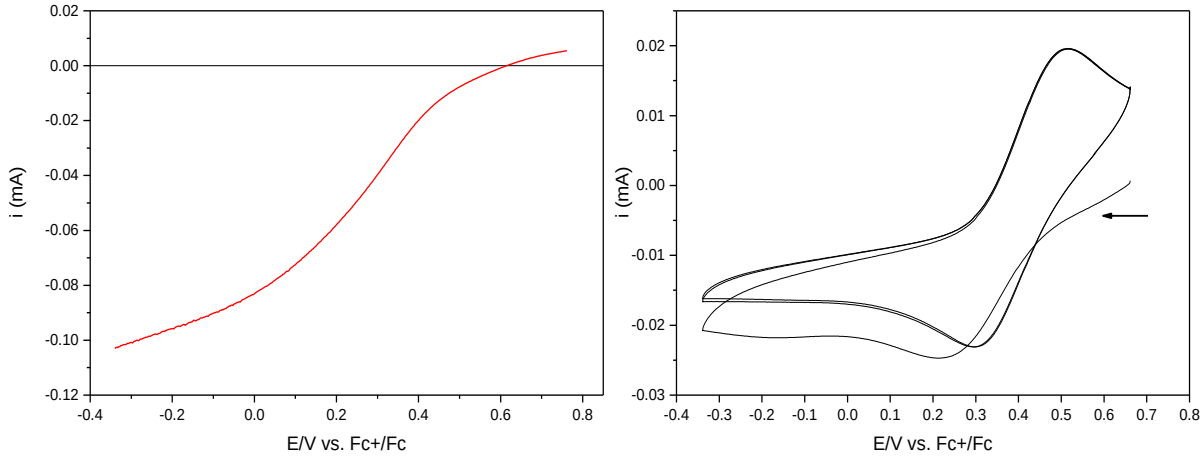

Figure 13: *Electrochemical analysis of the product of the electrolysis at 0.6 V vs. Fc+/Fc in acetonitrile (0.1 M $TBAPF_6$ as supporting electrolyte). Left: RDE analysis (1000 rpm, 10 mV/s). Right: cyclic voltammetry (100 mV/s). Counter electrode= Pt wire, reference electrode= homemade Ag/AgCl electrode, working electrode= glassy carbon electrode (3 or 5 mm).*

Looking at the summarising figures (Figure 14), it is possible to observe that the system does not come back to the starting conditions after a cycle of reduction/reoxidation. The starting complex seems in fact a mixture of several species, in which a part of the copper is reduced. After reduction and successive oxidation of the solution it seems that it exists only one species in solution in one oxidation state.

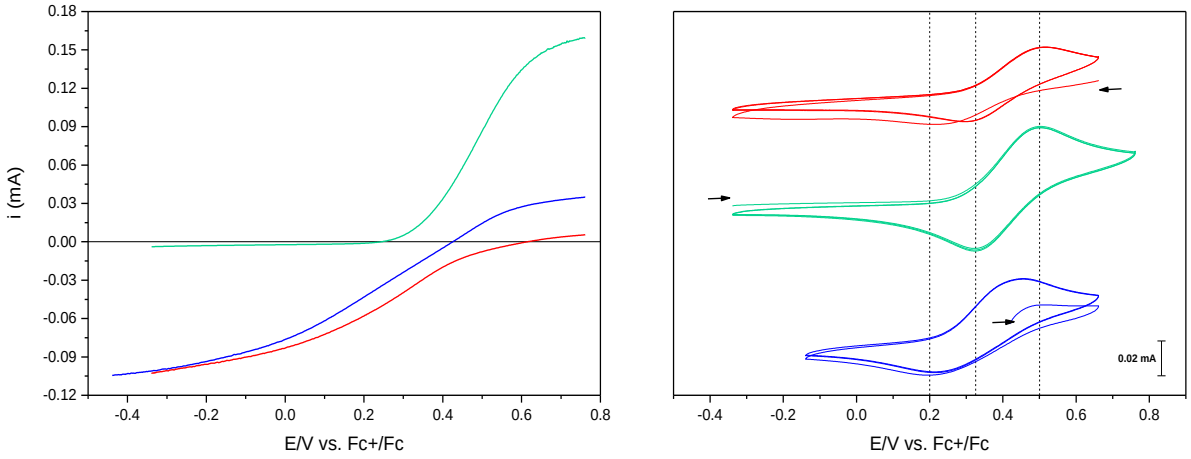

Figure 14: *Summarising figures of the electrolysis of the complex CxCl. Blue lines: starting complex; green lines: after reduction at -0.4 V; red lines: after reoxidation at 0.6 V. Left: RDE analysis. Right: cyclic voltammetry.*

Samples for EPR of the different species generated during the electrolysis were collected, frozen in liquid nitrogen and analysed in frozen solution. As it is possible to observe in Figure 15, the starting solution, has a complex spectrum, with two kinds of signal in the parallel region (blue line). The hyperfine lines in the parallel region of the spectrum spread over a limited magnetic field range which is generally indicative of a tetrahedrally distorted Cu(II). Their lack of resolution is probably due to the presence of several species leading to overlap of the lines.

After reduction at -0.4 V vs. Fc^+/Fc, a sample of the obtained solution was collected and analysed by EPR in the same experimental conditions. The recorded spectrum (Figure 15, green line) shows a very small signal, confirming the almost complete reduction of copper observed by electrochemical analysis. The solution was then electrolyzed at 0.6 V vs. Fc^+/Fc and another sample collected for EPR analysis. In this case (Figure 15, red line) the spectrum shows a broadened signal. This can be attributed to the presence of aggregates of Cu(II) complex, formed by bridging chloride anions. Since chloride anions promote not very strong antiferromagnetic coupling between copper centers, these present a signal even if they are coupled.

The electrochemical experiments coupled with EPR analysis gave important information about the nature of the complex CxCl. Firstly, it is possible to observe that in the electrochemical solution, the complex exists as a mixture of several species with close reduction potentials and EPR spectra, in which a part of copper is reduced to Cu(I). This

mixture is completely reduced upon electrolysis, giving rise to a species which presents only one redox wave and is EPR-silent. Reoxidation of the product gives rise to a completely oxidized product which presents a single quasi-reversible wave. This product has a broadened EPR spectrum, without any hyperfine pattern so it is possible to suppose that after oxidation an aggregate of Cu(II) species bridged by chloride anions is obtained. The formation of these species can be explained by supposing that after reduction a part of chloride anions which coordinated Cu(II) at the beginning are released in solution and replaced by solvent molecules; once the complex is reoxidized chlorides come back coordinating Cu(II) but bridging metal centers coordinated by different molecules of ligand and giving rise to the formation of polymers of the complex and other aggregates.

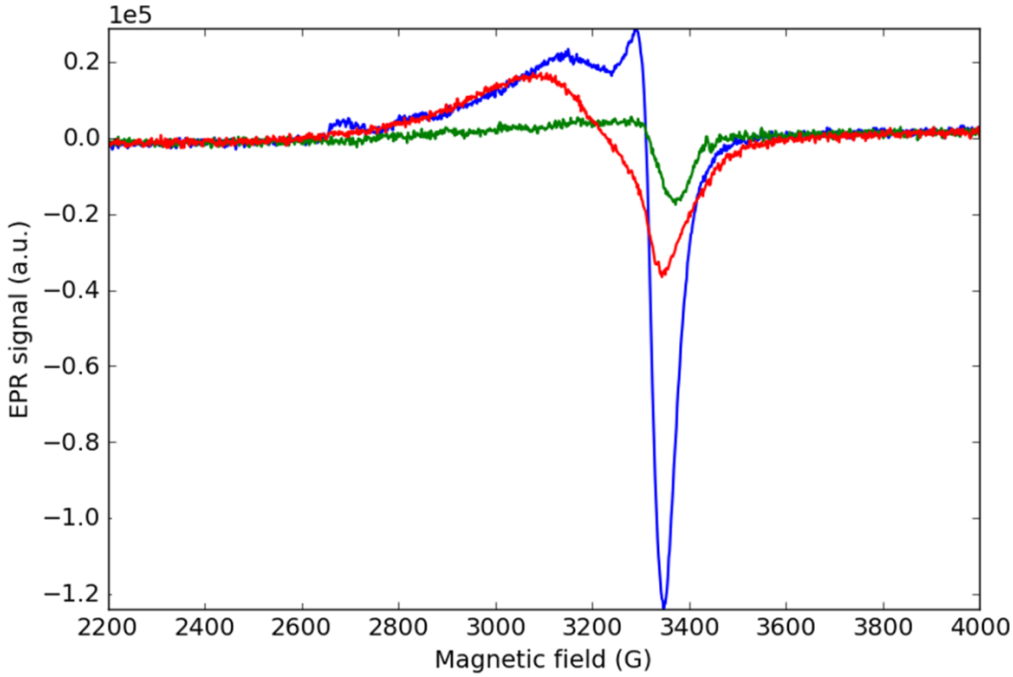

Figure 15: *EPR analysis of the samples collected during the coulometric analysis of CxCl (T= 30K, P= 33 dB, solvent= acetonitrile, 0.1 M $TBAPF_6$). Blue= starting sample, green= sample collected after reduction at -0.4 V vs. Fc^+/Fc, red= sample collected after reoxidation at 0.6 V vs Fc^+/Fc.*

2. *Study of the electrochemical behavior of the complex Cx(pheno)Cl*

The electrochemical behaviour of the complex Cx(pheno)Cl has been studied in a similar way as CxCl seen above. A 1 mM solution of the complex in acetonitrile with $TBAPF_6$ 0.1 M as supporting electrolyte is studied by RDE analysis, cyclic voltammetry and coulometry. Also in this case the exact nature of the complex is not known, its molar weight used in the experiments was calculated by taking into account the presence of a 2:1 Cu(II): mXBMP-O in

which each copper is coordinated to two nitrogen atoms of piperazine, the bridging phenolate of the ligand and three chloride anions (MW= 564.93 g mol^{-1}).

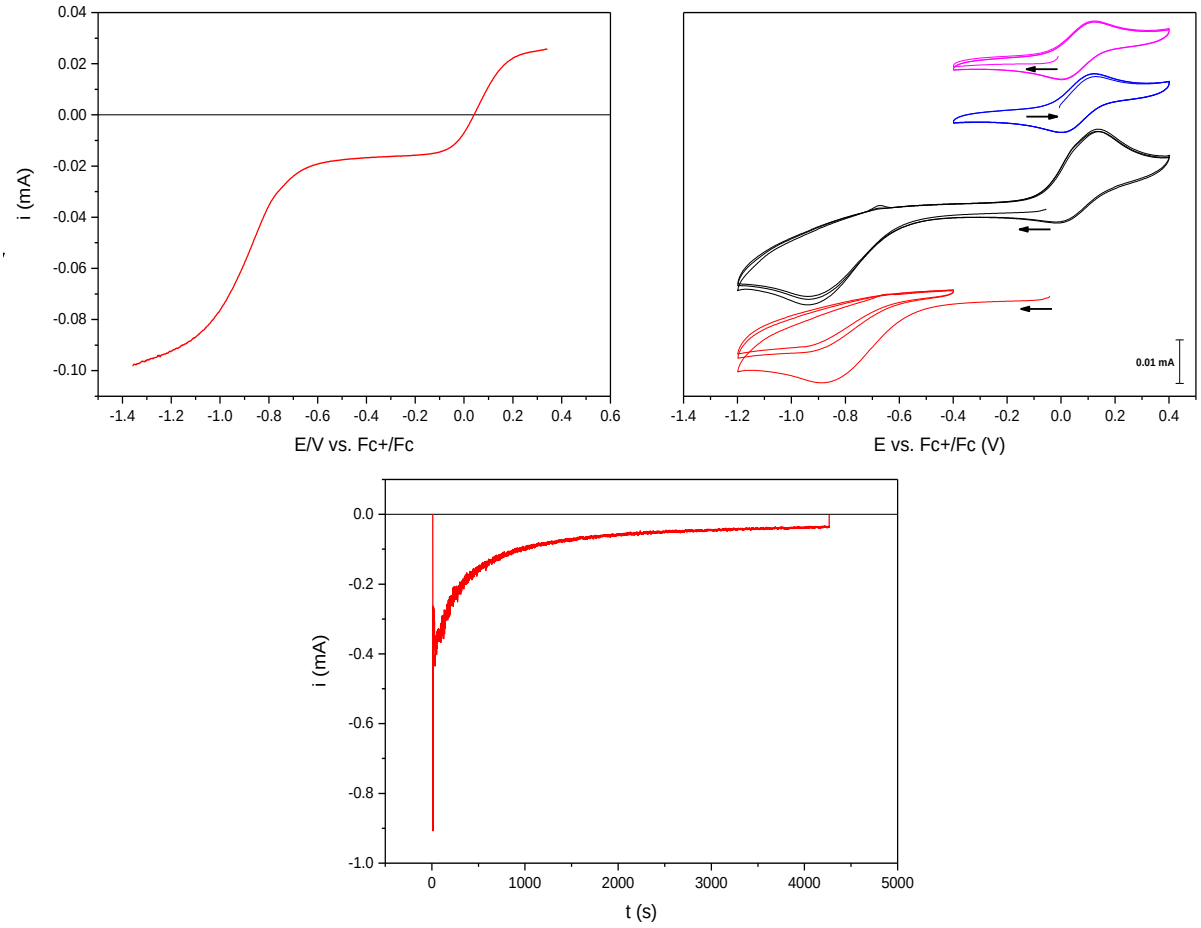

Figure 16: *Electrochemical analysis of the complex Cx(pheno)Cl in acetonitrile (0.1 M $TBAPF_6$ as supporting electrolyte). Top left: RDE analysis (1000 rpm, 10 mV/s). Top Right: cyclic voltammetry in different scan windows (100 mV/s). Bottom: electrolysis of the complex at -0.3 V. Counter electrode= Pt wire, reference electrode= homemade Ag/AgCl electrode, working electrode= glassy carbon electrode (3 or 5 mm).*

It is possible to observe a more complex electrochemical behaviour compared to the complex CxCl described before (Figure 16). The RDE analysis (Figure 16, top left) starts from positive current like for CxCl and it shows the presence of two reduction waves and one oxidation wave. The complexity of the phenomenon was confirmed by cyclic voltammetry (Figure 16, top right). Starting the scan from the open circuit potential towards negative potentials (black line), it is possible to observe an irreversible reduction peak at -0.92 V vs. Fc^+/Fc reference and, reversing the scan two nearly overlapping oxidation peaks at 0.04 V and 0.13 V. From the second cycle another reduction peak is observed at -0.01 V. This means that during the oxidation scan a new species is produced and it is reduced in the second

cycle. The fact that there is a partially reduced species is more evident looking at the blue and magenta lines. The two scans are performed in the same potential range and they are superimposable; in the magenta line there is no reduction at the beginning of the scan but it appears at -0.01 V after the first oxidation at 0.13 V, while in the blue line the oxidation peak at 0.13 V is noticeable at the beginning of the scan and it is coupled with the reduction at -0.01 V. This means that a partially reduced species is present in solution and it can be oxidized at 0.13 V and further reduced at -0.92 V, as it is possible to observe in the red line. This reduced species is then re-oxidized at 0.04 V. Also in this case the presence of broadened peaks suggests a slow electron transfer or the presence of more species with near reduction potentials. The complex was firstly reduced at -0.3 V vs. Fc+/Fc (Figure 16, bottom). No important changes in the appearance of the solution are observed. Integration of the current passed over time resulted in 0.35 C exchanged during the electrolysis, which corresponded to 0.21 electrons per molecule.

The cyclic voltammetry (Figure 17) of the obtained product shows more or less the same behaviour as that before the electrolysis. The RDE analysis (Figure 17) is more interesting because it is possible to observe two well-defined waves in reduction and oxidation, starting from zero current. This indicates the presence of a species in a well-defined redox state capable of undergoing one oxidation and one reduction process. This would be compatible with the presence of a mixed valence Cu(II)Cu(I) species. Moreover, in this RDE analysis it is possible to observe the beginning of a further reduction process at -1.2 V vs. Fc+/Fc.

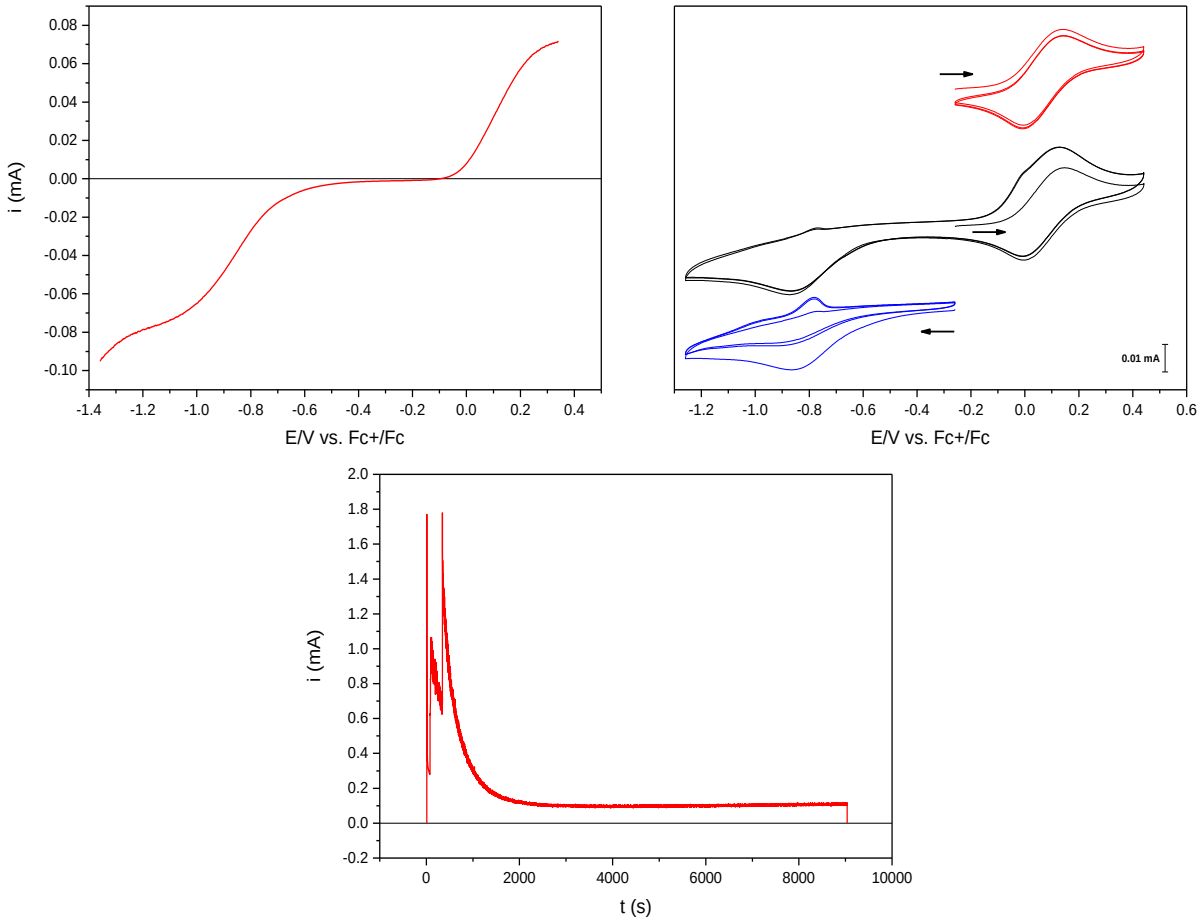

Figure 17: *Electrochemical analysis of the product of reduction of CxCl at -0.3 V in acetonitrile (0.1 M $TBAPF_6$ as supporting electrolyte). Top left: RDE analysis (1000 rpm, 10 mV/s). Top right: cyclic voltammetry with different scan windows (100 mV/s). Bottom: oxidation of the product at 0.4 V. Counter electrode= Pt wire, reference electrode= homemade Ag/AgCl electrode, working electrode= glassy carbon electrode (3 or 5 mm).*

The reduced solution was then re-oxidized at 0.4 V vs. Fc+/Fc (Figure 15), and the solution became yellow-greenish. Integration of the current passed over time resulted in 1.56 C exchanged during the electrolysis, which corresponded to 0.92 electrons per molecule. Also in this case the potential for the re-oxidation of the complex was chosen close to the oxidation peak of the complex in order to avoid the oxidation of chloride anions.

The RDE analysis of the oxidized product (Figure 18, left) shows the presence of a first well-defined reduction wave, while the second one at more negative potentials is less well defined than before, with a very short plateau followed by a further reduction. The cyclic voltammetry (Figure 18, right) now shows a completely oxidized species which undergoes two reductions but the oxidation peak at 0.04 V vs. Fc^+/Fc has disappeared, leaving only the oxidation peak at 0.13 V.

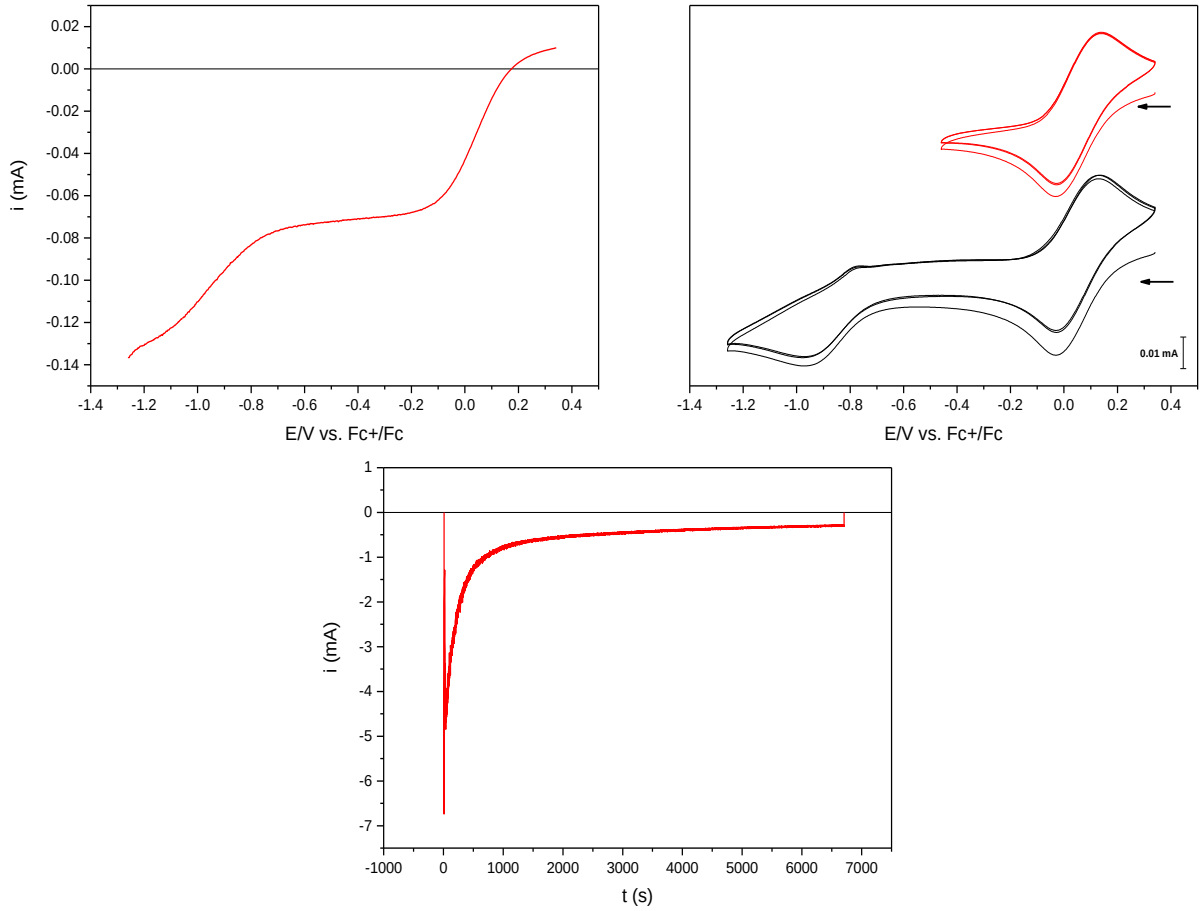

Figure 18: *Electrochemical analysis of the product of oxidation at 0.4 V in acetonitrile (0.1 M $TBAPF_6$ as supporting electrolyte). Top left: RDE analysis (1000 rpm, 10 mV/s). Top right: cyclic voltammetry (100 mV/s). Bottom: reduction of the product at -1 V. Counter electrode= Pt wire, reference electrode= homemade Ag/AgCl electrode, working electrode= glassy carbon electrode (3 or 5 mm).*

The solution was further electrolysed at -1 V vs. Fc+/Fc (Figure 18, bottom). It is possible to observe the complete bleaching of the solution, in agreement with a complete reduction of the complex. At the same time an important quantity of metallic copper was deposited on the electrode, making impossible any other electrochemical or spectroscopic analysis.

Looking at the summarizing figures (Figure 19) it is possible to observe that also in this case the system does not come back to the original state after a cycle of reduction/reoxidation. Unfortunately the deposition of metallic copper made impossible any analysis of the second reduction phenomenon.

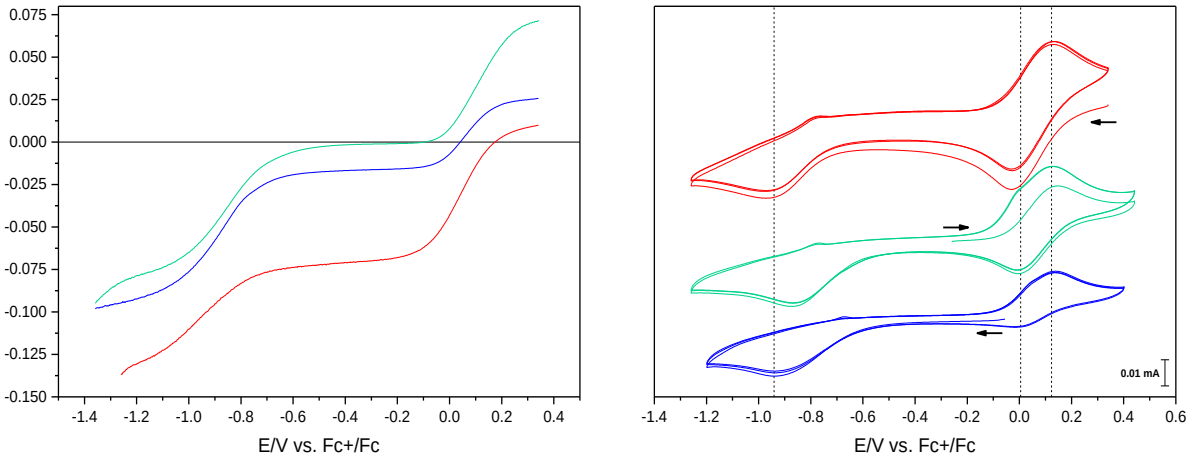

Figure 19: *Summary of the electrochemical analysis performed during the electrolysis of Cx(pheno)Cl. Blue lines: before electrolysis. Green lines: after reduction at -0.3 V vs. Fc+/Fc. Red lines: after re-oxidation at 0.4 V vs. Fc+/Fc. Left: summary RDE analysis. Right: summary cyclic voltammetry*

Samples of the different products of electrolysis were collected and analysed by EPR in frozen solution (Figure 20). At the beginning of the experiments (Figure 20, blue line) the product presents a broadened and not very intense spectrum. This could belong to antiferromagnetically coupled Cu(II) species present in the mixture or a mixture of similar species, as observed for the complex CxCl. The solution then underwent reduction at -0.3 V vs. Fc^{+}/Fc and the sample collected for EPR analysis shows a slightly more intense spectrum (Figure 20, green line) in which it is possible to observe some hyperfine coupling. This is compatible with the formation of a mixed valence species after reduction, previously observed in the electrochemical measurements. Unfortunately the poor resolution of the spectrum does not allow to clearly state if this mixed valence is localised or delocalised. The solution was then oxidized and the sample collected for the EPR analysis shows a more intense spectrum (Figure 20, red line) with a less well defined hyperfine coupling compared to the spectrum of the reduced sample. This may indicate the presence of several species whose hyperfine lines overlap.

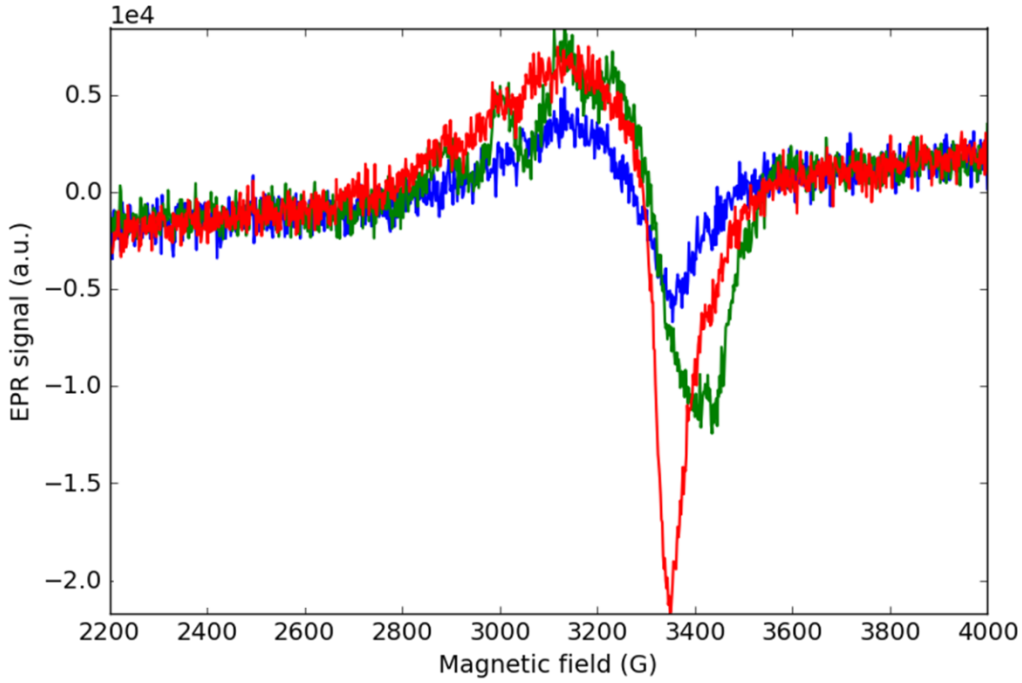

Figure 20: *EPR analysis of the samples collected during the coulometric analysis of Cx(pheno)Cl (T= 30K, P= 33 dB, solvent= acetonitrile/TBAPF$_6$ 0.1 M). Blue= starting sample, green= sample collected after reduction at -0.3 V vs. Fc$^+$/Fc, red= sample collected after reoxidation at 0.4 V vs Fc$^+$/Fc.*

Also in this case, electrochemical experiments coupled with spectroscopic analysis gave insights into the nature of the complex Cx(pheno)Cl. As for the complex CxCl, the electrochemical solution of the complex comprises a mixture of at least two species, in which a part of Cu(II) is spontaneously reduced. In this case the electrochemical behaviour is more complex. Reduction of the solution at -0.3 V vs Fc+/Fc generates a mixed-valent species, but complete reduction at -1 V leads to generation of metallic copper.

3. *Study of the electrochemical behavior of the complex [Cu$_2$(mXBMP-O)(CH$_3$COO)$_2$]ClO$_4$.(CH$_3$CN).(MeOH)*

For reasons of solubility the electrochemistry of this complex was studied in DMF solution instead of acetonitrile. Also in this case TBAPF$_6$ was added as supporting electrolyte and ferrocene used as internal reference for the potentials. The cyclic voltammetry of the complex shown in Figure 21 presents a broad reduction peak at -1.25 V coupled with a broad oxidation peak at -0.40 V vs. Fc$^+$/Fc. Moreover, it is interesting to observe another oxidation peak at -0.77 V at slow scan rates. This can be attributed to the stripping of metallic copper deposited on the electrode when it is formed at slow scan rates, similarly to what was observed when Cx(pheno)Cl was electrolysed at -1 V with the deposition of metallic copper.

The presence of broad cyclic voltammetry peaks suggests a slow electron transfer due to important rearrangements in the structure of the complex during the redox processes. If this cyclic voltammetry is compared to the one of the complex Cx(pheno)Cl before the electrolysis, it is possible to observe the effect of the presence of oxygenated anions as ligands in the shift of the oxidation peak towards negative potentials. In this case the complex was not further analysed by coulometry and RDE because of its tendency to deposit metallic copper on the electrode, which would make impossible any electrolysis.

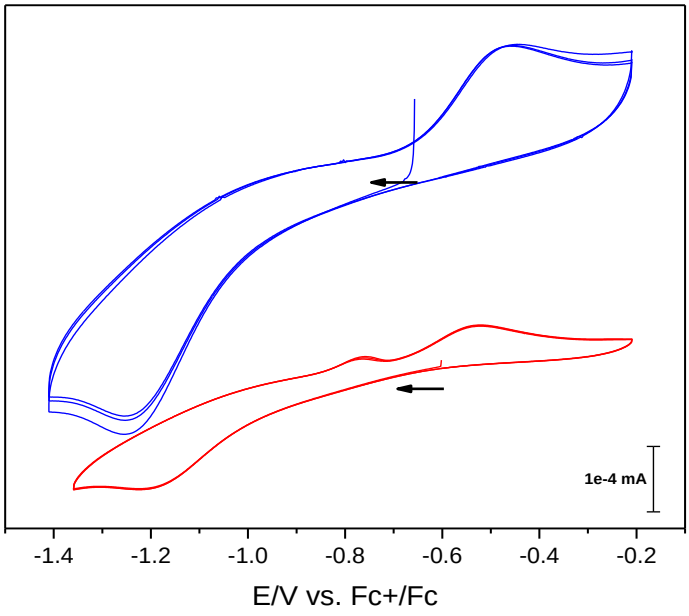

Figure 21: *Cyclic voltammetry analyisis of the complex [Cu_2(mXBMP-O)($CH_3COO)_2$]ClO_4.(CH_3CN).(MeOH) in DMF (0.1 M $TBAPF_6$ as supporting electrolyte). Red: scan rate= 20 mV/s, blue: scan rate= 100 mV/s.*

d. Conclusions

The results here presented show the strong influence of the coordination environment on stability and electrochemical properties of copper complexes. As stated in the introduction of the chapter, the ligands have been conceived with the aim of obtaining flexible bis-Cu(II) complexes capable of undergoing fast electron transfer, potentially efficient in electrocatalysis of dioxygen reduction. The two ligands mXBMP and mXBMP-OH were easily accessible from the synthetic point of view and they were obtained in good yields. The two ligands have been used for binding Cu(II) and through electrochemical and spectroscopic analysis it is possible to observe the effect of the coordination environment on the chemical properties of the obtained complexes.

The two complexes CxCl and Cx(pheno)Cl, respectively obtained by reaction of mXBMP and the sodium salt of mXBMP-OH presented a non-simple chemistry. In fact, even if UV-vis spectroscopy suggested in both cases the formation of 2:1 Cu(II): ligand species, electrochemical and EPR analysis revealed the presence of more than one species, with some reduced copper. This phenomenon of reduction is not completely understood and it can be due to several reasons. The coordination environment seems to have an important role, because probably in the two complexes the copper centers have an incomplete coordination sphere, and a part of Cu(II) undergoes reduction. Morover, the copper salt chosen for the synthesis of the complexes contained chlorides as counterions. As stated before, they can undergo oxidation at a potential close to the reduction potentials of the complexes CxCl and Cx(pheno)Cl so during the synthesis of the complexes a phenomenon of oxidation of chlorides can occur, resulting in the formation of Cu(I). All these phenomena would be enhanced by the fact that the reaction of synthesis took place in acetonitrile, which notably stabilises Cu(I).

The complex $[Cu_2(mXBMP\text{-}O)(CH_3COO)_2]ClO_4.(CH_3CN).(MeOH)$ was obtained from the sodium salt of mXBMP-OH but in this case the presence of bridging acetate as counteranions stabilises the complex in a triply-bridged structure, in which both Cu(II) ions are pentacoordinated. Oxygenated anions stabilise Cu(I) less than chlorides present in CxCl and Cx(pheno)Cl and this results in a negative shift of reduction potentials. Moreover, the triply-bridged structure of the complex undergoes important rearrangements during a redox process. Electron transfer becomes slow, resulting in broad and irreversible peaks in cyclic voltammetry.

To sum up, this studies on these new binuclear copper complexes shows that ligands capable of leaving flexibility in the coordination sphere of copper can enhance rapid electron transfer but at the same time they can have problems in the stabilisation of the copper centers. On the other hand, when the structure is well stabilised with bridging coordinating groups, the electrochemistry of the complex becomes dominated by slow electron transfer, less promising for electrocatalytic applications. Some preliminary tests of reduction of oxygen were performed without any remarkable results. It is clear that for obtaining more efficient complexes, more complex ligands are needed. In the next chapter the synthesis of more complex trinucleating ligands will be presented.

e. Experimental section

Synthesis of 1,3-bis((4-methylpiperazin-1-yl)methyl)benzene (mXBMP) (1)

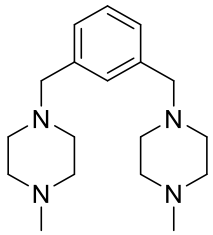

0.500 g of 1,3-bis-(chloromethyl)-benzene (MW= 175.16, 2.85 mmol) were dissolved in 15 mL of toluene with 2.7 mL of DIPEA (MW= 129.25, d= 0.742 g/mL, 15.7 mmol) and 1.6 mL of N-methyl piperazine (MW= 100.17, d= 0.903 g/mL, 14.3 mmol). The mixture was stirred at 60°C under argon for 24 hours, leading to the formation of a white precipitate in a yellow solution. After 24 hours the precipitate was filtered off and washed several times with toluene. Evaporation of the solvent left a yellow oil. This was purified by column chromatography on alumina (mobile phase Hexane : 2-propanol 10:1, Rf = 0.4). The pure product appears as a white powder and white crystals suitable for single crystal X-ray diffraction can be obtained by slow evaporation of a concentrated solution of mXBMP in dichloromethane.

m = 0.775 g

MW = 302.46 g mol^{-1}

Yield = 90%

^{1}H-NMR (δ, ppm, $CDCl_3$, 400 MHz): 7.25 (m, 4H), 3.50 (s, 4H), 2.45 (bs, 16H), 2.28 (s, 6H)

^{13}C-NMR (δ, ppm, $CDCl_3$, 100 MHz): 137.82 (Q), 129.57 (CH), 127.80 (CH), 127.59 (CH), 62.71 (CH_2), 54.91 (CH_2), 52.80 (CH_2), 45.86 (CH_3)

(+)-ESI-MS (m/z): 303 $(M+H^+)^+$, 152 $(M+2H^+)^{2+}$

Synthesis of 2,6-bis(chloromethyl)-4-methylphenol (Cl(OH)Cl) (2)

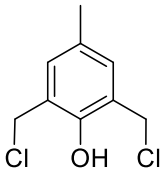

The molecule was synthetized following a published experimental protocol[20]. 3.4 g of 2,6-bis(hydroxymethyl)-p-cresol (MW= 168.19 g mol^{-1}, 20 mmol) were suspended in 60 mL of diethyl ether and stirred at room temperature under argon. 3 mL of thionyl chloride (d= 1.631 g mL^{-1}, MW= 118.97 g mol^{-1}, 41 mmol) were added dropwise to the suspension, causing the dissolution of the solid and the formation of a pale yellow solution. This was stirred for 3 hours at room temperature and then the tiny precipitate formed during the reaction was filtered off. The clear yellow solution was then evaporated, affording a yellowish/white solid. This was dissolved in 30 mL of dichloromethane, then 30 mL of hexane were added and the solution evaporated, in order to remove the residuals of thionyl chloride. The obtained white solid was recrystallized in diethyl ether and washed with a 20:80 v/v diethyl ether : hexane mixture. The product was afforded as white crystals.

m = 0.820 g

MW = 205.08 g mol^{-1}

Yield = 83%

^{1}H-NMR (δ, ppm, CD_2Cl_2, 400 MHz): 7.11 (s, 2H), 5.58 (bs, 1H), 4.67 (s, 4H), 2.27 (s, 3H)

Synthesis of 4-methyl-2,6-bis((4-methylpiperazin-1-yl)methyl)phenol (mXBMP-OH) (3)

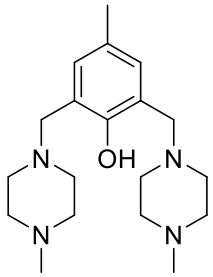

A solution of **2** (1.040 g MW= 205.08, 4.5 mmol) in 40 mL of THF was added dropwise to a solution of 1 mL of N-methyl piperazine (MW= 100.17, d= 0.903 g/mL, 9 mmol) and 7.5 mL of Et_3N (MW= 101.19, d= 0.728 g/mL, 54 mmol) in 200 mL of THF. During the addition, performed at room temperature, it was possible to observe the formation of a white precipitate of Et_3NCl. The mixture was stirred at room temperature for 24 hours, then the precipitate was filtered off and washed with some THF. The solution was then evaporated leaving a pale yellow oil, which was dissolved in 20 mL of CH_2Cl_2 and washed twice with 5 mL of a saturated solution of NH_4Cl. The organic phase was then dried over Na_2SO_4, filtered and evaporated, giving a pale yellow oil.

m = 1.16 g

MW = 332.49 g mol^{-1}

Yield = 68%

^{1}H-NMR (δ, ppm, $CDCl_3$, 400 MHz): 6.84 (s, 2H), 3.59 (s, 4H), 2.52 (bs, 16H), 2.28 (s, 6H), 2.22 (s, 3H)

^{13}C-NMR (δ, ppm, $CDCl_3$, 100 MHz): 153.86 (Q), 129.49 (CH), 127.49 (Q), 122.24 (Q), 58.86 (CH_2), 54.99 (CH_2), 52.74 (CH_2), 45.96 (CH_3), 20.48 (CH_3)

(+)-ESI-MS (m/z): 333 $(M+H^+)^+$

Synthesis of the sodium salt of mXBMP-OH (mXBMP-ONa) (4)

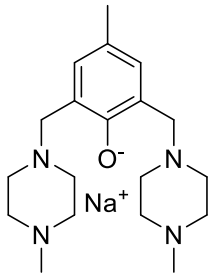

The synthesis was performed in glovebox, using anhydrous solvents. 0.611 g of **3** (MW = 332.49, 1.838 mmol) were dissolved in 80 mL of anhydrous THF and stirred at room temperature, giving a yellow solution. 0.045 g of NaH (MW = 23.99, 1.838 mmol) were carefully added to the solution of ligand. The progressive dissolution of NaH was observed during prolonged stirring of the suspension at room temperature. The product was then recuperated after 24 hours by evaporating the solvent to around 1/3 of the starting volume, adding 20 mL of hexane and cooling the mixture. A white precipitate was formed, recuperated by centrifugation and washed with hexane.

m = 0.2742 g

MW = 354.47 g mol^{-1}

Yield = 42%

Synthesis of the complex CxCl (5)

71.9 mg of **1** (MW= 302.46 g mol^{-1}, 0.238 mmol) were dissolved in 30 mL of acetonitrile and stirred at room temperature. 81.0 mg of $CuCl_2.2H_2O$ (MW= 170.48 g mol^{-1}, 0.476 mmol) were dissolved in 18.8 mL of acetonitrile and added dropwise to the stirred solution of ligand. During the addition it was possible to observe that the reaction mixture passes from colourless to green, with the formation of a yellowish/green precipitate. The reaction mixture was left stirring at room temperature for 1 hour and then left standing for decantation. The solvent was then removed after centrifugation of the suspension and the precipitate recuperated and washed with THF, affording a yellowish/green solid.

m= 38.3 mg

Synthesis of the complex Cx(pheno)Cl (6)

35.7 mg of **4** (MW= 354.47 g mol^{-1}, 0.1007 mmol) were dissolved in 30 mL of anhydrous THF and stirred at room temperature, giving a pale yellow solution. 34.3 mg of $CuCl_2.2H_2O$ (MW= 170.48 g mol^{-1}, 0.201 mmol) were dissolved in 10.2 mL of THF and added dropwise to the ligand solution, causing a colour change of the solution to orange and then brown. The reaction mixture was left stirring at room temperature for 2 hours, then some hexane was added and the mixture cooled at low temperature, causing the precipitation of a brown powder which was recuperated by centrifugation and washed with some hexane.

m= 20.7 mg

Synthesis of the complex $[Cu_2(mXBMP\text{-}O)(CH_3COO)_2]ClO_4.(CH_3CN).(MeOH)$ (7)

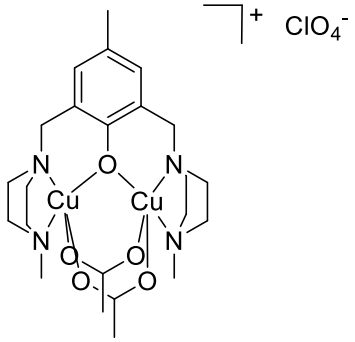

19.3 mg of **4** (MW= 354.47 g mol^{-1}, 0.0544 mmol) were dissolved in 16 mL of a 50:50 v/v mixture acetonitrile/methanol and stirred at room temperature. 21.7 mg of $Cu(CH_3COO)_2.H_2O$ (MW= 199.65 g mol^{-1}, 0.1089 mmol) were dissolved in 3.4 mL of a 50:50 v/v acetonitrile/methanol mixture and added dropwise to the solution of the ligand; the reaction mixture turns from colourless to yellow and then green. 0.0382 g of $NaClO_4$ were then dissolved in 4.8 mL of 50:50 v/v acetonitrile/methanol mixture and added to the reaction mixture, which was left stirring at room temperature for 2 hours. The reaction mixture was then filtered and evaporated, leaving a green powder, which was washed with cold THF and cold diethyl ether. The purified product appears as a green powder. Crystals suitable for X-ray diffraction can be obtained by slow evaporation of a concentrated solution of the complex in a 50:50 v/v acetonitrile/methanol mixture.

m = 29.7 mg

MW = 749.19 g mol^{-1}

Yield = 78%

(+)-ESI-MS (m/z): 575 $[Cu_2(mXBMP\text{-}O)(CH_3COO)_2]^+$, 553 $[Cu_2(mXBMP\text{-}O)(CH_3COO)Cl]^+$, 258 $[Cu_2(mXBMP\text{-}O)(CH_3COO)]^{2+}$

UV-vis titration of mXBMP with $CuCl_2.2H_2O$

2.545 mL of a solution 2 10^{-4} M of mXBMP in anhydrous acetonitrile were put in a UV-vis cuvette at room temperature. The titration was performed by adding from 0 to 4 eqv. of a solution 2.5 10^{-2} M of $CuCl_2.2H_2O$ in dry acetonitrile. Recorded spectra were then treated by mathematic subtraction of the contribution of the spectrum of $CuCl_2.2H_2O$ recorded in the same conditions.

UV-vis titration of mXBMP-ONa with $CuCl_2$ $2H_2O$

2.545 mL of a solution 2 10^{-4} M of mXBMP-ONa in anhydrous THF were put in a UV-vis cuvette at room temperature. The titration was performed by adding from 0 to 4 eqv. of a solution 2.5 10^{-2} M of $CuCl_2$ $2H_2O$ in dry THF. Recorded spectra were then treated by mathematic subtraction of the contribution of the spectrum of $CuCl_2.2H_2O$ recorded in the same conditions.

General method of correction of UV-vis spectra collected during the titrations of mXBMP and mXBMP-ONa with $CuCl_2.2H_2O$

At the end of the UV-vis titrations spectra were treated as follows. First of all the spectrum registered after the addition of 3 eqv. of $CuCl_2.2H_2O$ was subtracted to the spectrum registered at 4 eqv. of $CuCl_2.2H_2O$. The spectrum corresponding to the concentration of 1 eqv. of $CuCl_2.2H_2O$ was then obtained and subtracted to all the spectra of the titration, by multiplying it by a suitable coefficient, in order to put equal to zero the absorbance in a point in which only absorptions of the copper salt are present. For the titration of mXBMP the subtractions were performed by putting A_{460}= 0 and for the titration of mXBMP-ONa by putting A_{370}= 0.

Electrochemistry experiments

All the electrochemistry experiments were performed by using a Biologic or Origalys potentiostat with a three electrode system. A platinum wire was used as counter electrode, a homemade Ag/AgCl electrode as reference electrode and a glassy carbon electrode (3 or 5 mm) as working electrode. In the coulometry experiments the glassy carbon electrode was substituted with a carbon felt as working electrode. All the measurements were performed under an argon atmosphere and ferrocene was used as internal standard for calibrating the potentials.

For the analysis of CxCl and Cx(pheno)Cl, the complexes were dissolved in 25 mL of dry acetonitrile, in order to obtain a solution 1 mM in complex with the addition of $TBAPF_6$ 0.1 M. The prepared solutions were firstly analysed by rotating disk electrode (1000 rpm) and cyclic voltammetry, then they underwent electrolysis. After each electrolysis the solution was analysed by rotating disk electrode, cyclic voltammetry and a sample was collected, frozen in liquid nitrogen for EPR analysis.

For the analysis of the complex $[Cu_2(mXBMP\text{-}O)(CH_3COO)_2]ClO_4.(CH_3CN).(MeOH)$, this was dissolved in 1 mL of dry DMF, in order to obtain a 1 mM solution, with the addition of $TBAPF_6$ 0.1 M as supporting electrolyte.

f. Bibliography

(1) Robson, R. *Inorg. Nucl. Chem. Lett.* **1970**, *6*, 125–128.
(2) Robson, R. *Aust. J. Chem.* **1970**, *23*, 2217–2224.
(3) Okawa, H. *Bull. Chem. Soc. Jpn.* **1970**, *43*, 3019.
(4) Okawa, H.; Kida, S. *Bull. Chem. Soc. Jpn.* **1971**, *44*, 1172.
(5) Guerriero, P.; Tamburini, S.; Vigato, P. A. *Coord. Chem. Rev.* **1995**, *139*, 17–243.
(6) Okawa, H.; Furutachi, H.; Fenton, D. E. *Coord. Chem. Rev.* **1998**, *174*, 51–75.
(7) Zanello, P.; Tamburini, S.; Vigato, P. A.; Mazzocchin, G. A. *Coord. Chem. Rev.* **1987**, *77*, 165–273.
(8) Casellato, U.; Vigato, P. A. *Chem. Soc. Rev.* **1979**, *8*, 199–220.
(9) Elwell, C. E.; Gagnon, N. L.; Neisen, B. D.; Dhar, D.; Spaeth, A. D.; Yee, G. M.; Tolman, W. B. *Chem. Rev.* **2017**, *117*, 2059–2107.
(10) De, A.; Mandal, S.; Mukherjee, R. N. *J. Inorg. Biochem.* **2008**, *208*, 1170–1189.
(11) Koval, I. A.; Gamez, P.; Belle, C.; Selmeczi, K.; Reedijk, J. *Chem. Soc. Rev.* **2006**, *35*, 814–840.
(12) Karlin, K. D.; Dahlstrom, P. L.; Cozzette, S. N.; Scensny, P. M.; Zubieta, J. *J. Chem. Soc. Chem. Commun.* **1981**, 881–882.
(13) Reim, J.; Krebs, B. *J. Chem. Soc. Dalton Trans.* **1997**, 3793–3804.
(14) Mandal, S.; Mukherjee, J.; Lloret, F.; Mukherjee, R. *Inorg. Chem.* **2012**, *51*, 13148–13161.
(15) Belle, C.; Beguin, C.; Gautier-Luneau, I.; Hamman, S.; Philouze, C.; Pierre, J. L.; Thomas, F.; Torelli, S.; Saint-Aman, E.; Bonin, M. *Inorg. Chem.* **2002**, *41*, 479–491.
(16) Hamann, J. N.; Herzigkeit, B.; Jurgeleit, R.; Tuczek, F. *Small Mol. Act.* **2017**, *334*, 54–66.
(17) Casella, L.; Monzani, E.; Gullotti, M.; Cavagnino, D.; Cerina, G.; Santagostini, L.; Ugo, R. *Inorg. Chem.* **1996**, *35*, 7516–7525.
(18) Gamba, I.; Palavicini, S.; Monzani, E.; Casella, L. *Chem. Eur. J.* **2009**, *15*, 12932–12936.
(19) Collman, J. P.; Fu, L.; Herrmann, P. C.; Zhang, X. *Science* **1997**, *275*, 949-951.
(20) Carlsson, H.; Haukka, M.; Bousseksou, A.; Latour, J.-M.; Nordlander, E. *Inorg. Chem.* **2004**, *43*, 8252–8262.
(21) Soran, A.; Breunig, H. J.; Lippolis, V.; Arca, M.; Silvestru, C. *Dalton Trans* **2009**, 77–84.
(22) Anekwe, J.; Hammerschmidt, A.; Rompel, A.; Krebs, B. *Z. Für Anorg. Allg. Chem.* **2006**, *632*, 1057–1066.
(23) Bertoncello, K.; Fallon, G. D.; Hodgkin, J. H.; Murray, K. S. *Inorg. Chem.* **1988**, *27*, 4750–4758.
(24) Rajendiran, T. M.; Venkatesan, R.; Rao, P. S.; Kandaswamy, M. *Polyhedron* **1998**, *17*, 3427–3432.
(25) Pavlishchuk, V. V.; Addison, A. W. *Inorg Chim Acta* **2000**, *298*, 97–102.

Chapter 3: Synthesis and characterization of bioinspired trinucleating ligands

In this chapter the obtaining of new trinucleating ligands will be presented. First of all, a digression with a description of the principal strategies for the elaboration of trinuclear clusters will be made, in order to define the underlying ideas on the conception of new trinuclear copper complexes. The synthesis of two new trinucleating ligands then will be presented, with a description of the different strategies applied for obtaining them.

a. Introduction

Trinuclear metallobiosites have appeared in the late 1980s and modelling the trinuclear active site of multicopper oxidases[1] has been for the past twenty years and is still a strong motivation for many groups in the bioinorganic community both for the academic challenge and the potential rewards in terms of energy conversion. Three different approaches have been developed to assemble the three copper ions which can be distinguished on the basis of the corner stone of their elaboration: (i) use of a trinucleating template, (ii) assembly of a three-fold symmetric macrocycle and (iii) association of a mononuclear site to a binucleating unit.

1. Trinucleating templates

This approach is the most developed probably because it is intrinsically the easiest to carry out, which by no way means that it is easy. Indeed elaborating symmetric molecules appears generally less complicate than dissymetric ones. However, this approach bears the intrinsic drawback that it will probably generate an equilateral triangular unit, whereas the biological site corresponds to an isosceles arrangement [2 + 1] of the three copper ions. It involves branching three identical copper binding sites onto a node which can be an atom (either a nitrogen or carbon-2 of an ethyl group) or a 1,3,5-substituted hexaatomic molecule (generally a benzene).

Single atom node. The first such system was elaborated by Karlin and colleagues[2,3] using a tris-aminoethylamine to associate three pyridylethylamine branches. They were thus able to isolate a tris-Cu^{I} and a tris-Cu^{II} complex (Figure 1).

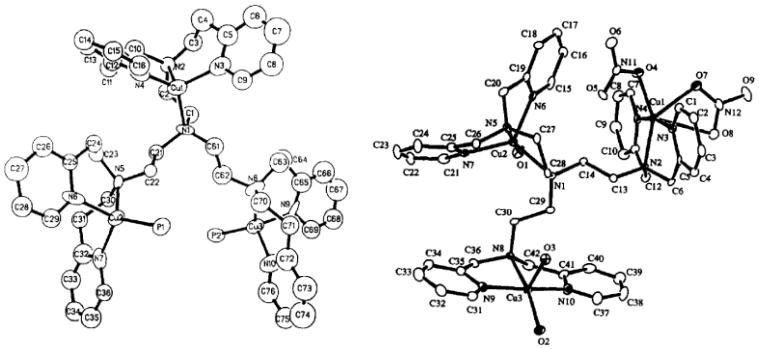

Figure 1: *Representation of the crystalline structure of tris-copper(I) and copper(II) complexes obtained by Karlin and co-workers[2,3].*

This approach was further developed by Tolman, Casella and colleagues[4] who compared ligands with the N or the "CH_3-C" node. With the ethyl-based system the three branches have the tendency to orient apart from each other and the three copper ions to behave independently. By contrast, with the amine-based system, a central copper ion can be bound that serves as a template to avoid this effect (Figure 2).

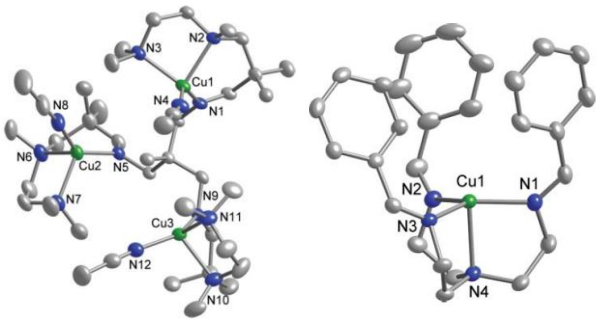

Figure 2: *Representation of the crystalline structures of tris-copper(I) complex and templating copper(I) obtained by Tolman and co-workers[4].*

This latter strategy was recently used by Agapie and colleagues[5] who used a lanthanide as a templating metal to maintain the three copper ions in close vicinity. Indeed, by reacting the Cu^{I}_3 complex with dioxygen at low temperature they were able to isolate a bis-μ-oxo Cu^{II}_3 complex, thereby proving that the copper ions can act together (Figure 3).

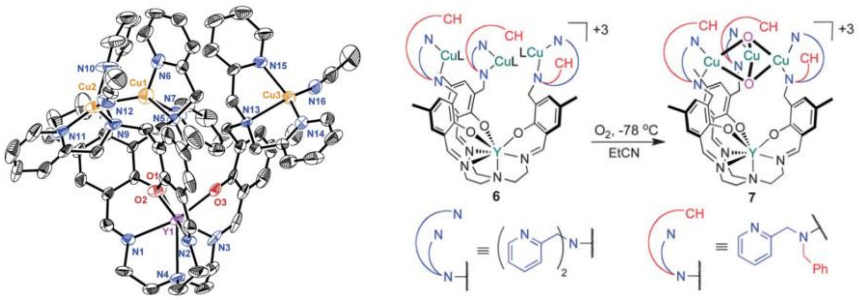

Figure 3: *Tris-copper(I) complex obtained by Agapie and coll.*[5] *and its oxygenation.*

To avoid the copper binding branches to orient outwardly, Murray and colleagues[6] locked them with two triphenymethyl units thereby constituting a cryptate binding three $Cu^{II}Cl$ units (Figure 4).

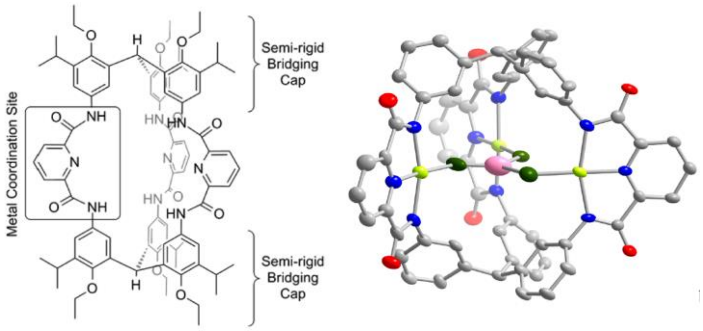

Figure 4: *Scheme of ligand (left) and representation of the crystalline structure (right) of trichlorocopper(I) complex obtained by Murray and co-workers*[6]*.*

Hexaatomic node. Suh and colleagues[7] were the first to report such a system using a 1,3,5-triazacyclohexane where each couple of nitrogens anchors a four-nitrogen aliphatic chain. The whole ligand is therefore able to host a μ-oxoCu_3 cluster (Figure 5).

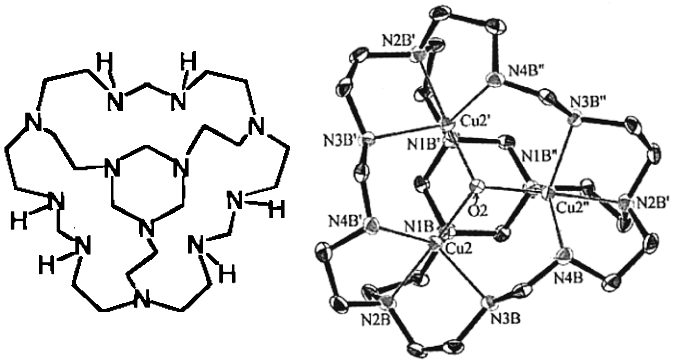

Figure 5: *Trinucleating ligand (left) and representation of the crystalline structure (right) of tris-copper(II) complex obtained by Suh and co-workers[7].*

But the nodes most used for this purpose have been 1,3,5-trisubstituted benzenes. A first generation of systems was introduced by Karlin's group[8] based on the anchoring of polyamines to the template through methylene groups. Oxygenation of the tris-Cu^{I} complex led to hydroxylation of the benzene and the formation of a μ-phenoxido bis-Cu^{II} entity (Figure 6).

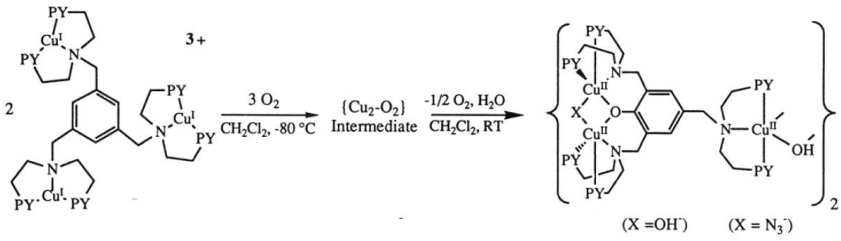

Figure 6: *Tris-copper(I) complex obtained by Karlin's group and its oxygenation[8].*

To avoid this reaction, Itoh and colleagues[9,10] and Karlin and colleagues[11] used a 1,3,5-trisubstituted-2,4,6-trisethylbenzene. This gave rise to flexible systems in which each of the three copper ions has a tendency to behave independently of the two others or form a dinuclear unit through anion bridging (Figure 7).

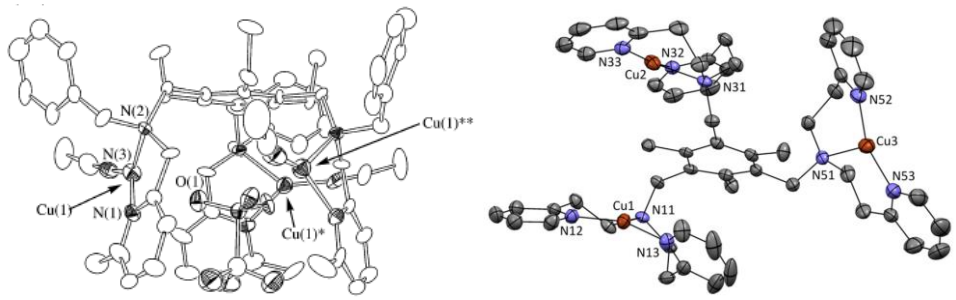

Figure 7: *Representation of crystalline structures of tris-copper(I) and copper(II) complexes obtained, respectively, by the groups of Itoh[10] and Karlin[11].*

To counter this effect, Agapie and coll.[12,13] used a phenyl group as rigid linker between the template and the coordinating site. The latter associates both nitrogen donors and an alcohol group. Deprotonation of the latter is required for the three-copper unit to converge and assemble as a metallacrown. Further stabilization is provided by capping the three copper ions by a μ_3 bridge (Figure 8).

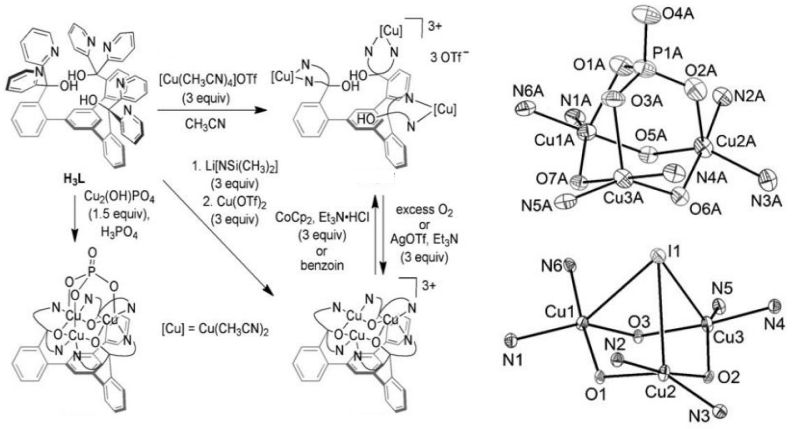

Figure 8: Synthesis and representation of the crystalline structure of tris-copper(I) complexes obtained by Agapie and co-workers[13].

Very recently a further development has been introduced by Murray and colleagues[14,15] who connected two templating units by three diketimine ligands therefore providing three copper ions with a N_2 donor set within the cage. Binding of anion and even dinitrogen within the Cu_3 unit was reported (Figure 9).

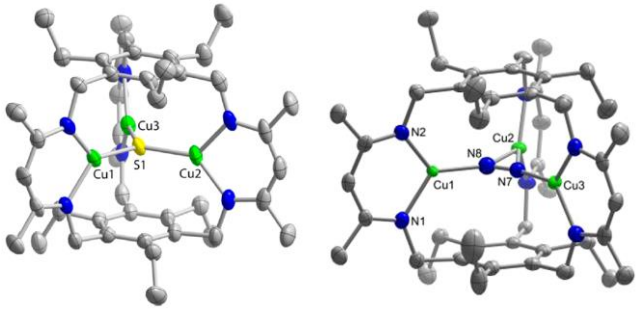

Figure 9: Representation of the crystalline structure of tris-copper(I) complexes obtained by Murray and co-workers[14,15].

2. *Macrocycles*

Macrocycles are well-known to be able to host several metal ions in close proximity and this property has been used by a few groups to assemble three copper ions. Fenton and colleagues[16] took advantage of a specifically designed macrocyclic compartmental ligand to synthesize a tris-copper(II) complex with a hydroxo-bridged pair and a third Cu ion in close proximity (Figure 10).

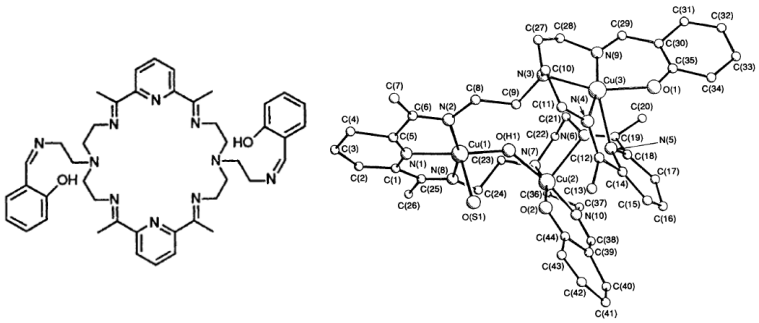

Figure 10: Macrocyclic ligand and representation of the crystalline structure of tris-Cu(II) complex obtained by Fenton and co-workers[16].

A similar approach was used by Lloret and colleagues[17] who built a three-fold symmetric macrocycle by the alternation of a pyridine and a trans-diaminocyclohexane (Figure 11). This ligand could bind three copper(II) ions bridged by two hydroxides.

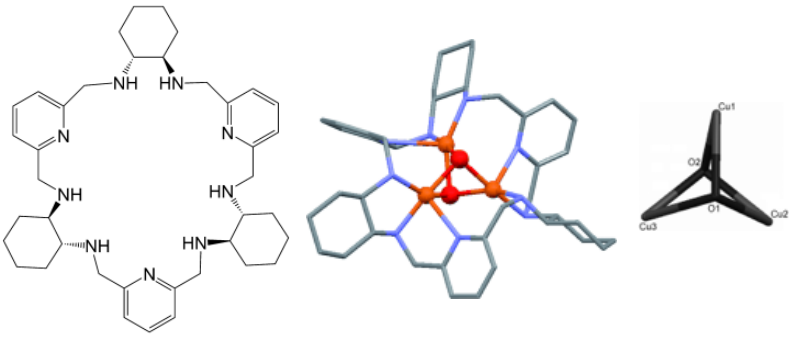

Figure 11: *Macrocyclic ligand, X-ray structure and central $Cu_3(OH)_2$ core of tris-copper(II) complex obtained by Lloret and co-workers*[17].

Osuka and colleagues developed the synthetic access to calix[3]dipyrrins by countering the formation of the corresponding porphyrins by adding water to the reaction mixture. Subsequent metallation afforded the tris-copper(II) complex in which the three copper ions are bridged by alcoxides and form an equilateral triangle (Figure 12).

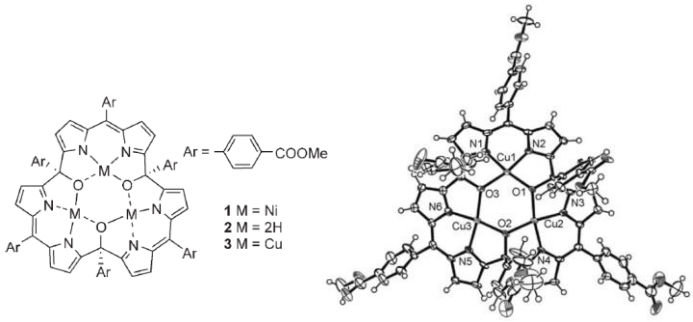

Figure 12: *Macrocyclic ligand and representation of the crystalline structure of tris-copper(II) complex obtained by Osuka and co-workers*[18].

3. *Combination of mononucleating and binucleating sites*

As detailed above, all attempts at building trinuclear sites have relied on three-fold symmetric systems which do not allow to access an isosceles triangular arrangement of the copper ions. The only exception was described by Fenton and colleagues with the aid of serendipity.[16] A specific design of an isosceles arrangement (Scheme 1) was pursued by three groups who anchored to a mononuclear site (T2 in copper enzymes) two identical arms suited to form the two halves of the binuclear site (T3 in copper enzymes).

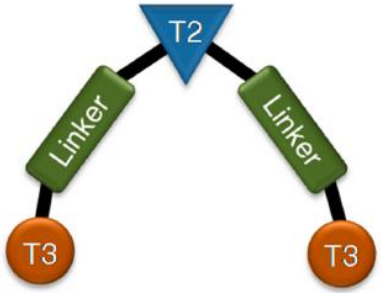

Scheme 1: *Design principle for models of the multicopper oxidase tris-copper site*[19].

The first to address this problem was the group of Casella who used a piperazine for the mononuclear site and attached to its nitrogen atoms various triamino ligands (Figure 13).[20,21]

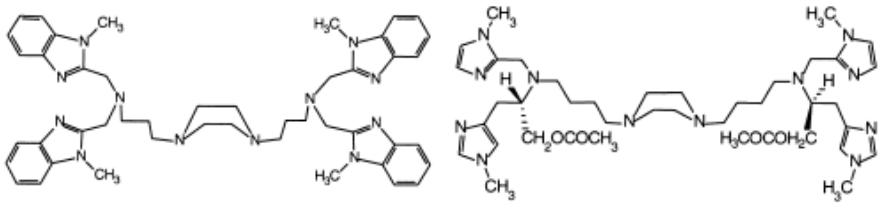

Figure 13*: Trinucleating ligands designed by Casella and co-workers*[20,21].

A similar approach was used by Gewirth and colleagues[19] using bipyridine or terpyridine as central motif (Figure 14). Both groups faced the same problem to bring in close proximity the two lateral copper ions.

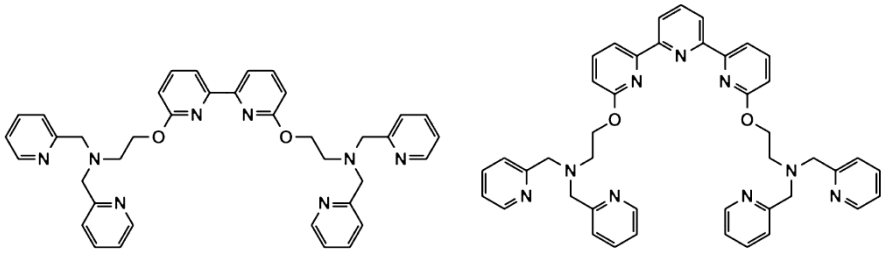

Figure 14: *Trinucleating ligands designed by Gewirth and co-workers*[19].

The group of Chan[22,23] developed trinucleating ligands to mimic the structure and the reactivity of the active site of the particulate methane monoxygenase (pMMO). However, the most recent crystallographic results do not support the occurrence of a tris-copper site[24]. Whatsoever, they used the same approach as Fenton and Gewirth and their coworkers: starting from a central diazepine, they incorporated, within the linker to the lateral binding

sites, an alcoxide which can bridge each lateral copper to the central one and thereby the two lateral copper ions comes in close proximity of each other so that a hydroxo bridge can form (Figure 15).

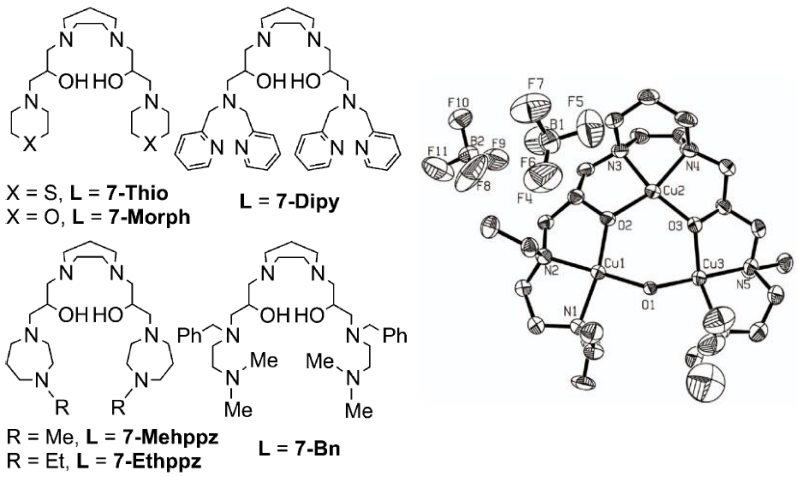

Figure 15: *Trinucleating ligands and representation of the crystalline structure of a tris-copper(II) complex obtained by Chan and co-workers*[22,23].

4. Summary of the structural parameters of some tris-copper complexes

The inter-copper distances of these model complexes and two enzymes are summarized in Table 1, which highlights a large dispersion of these data. It is noteworthy that the biological sites themselves show substantial variations according to the redox state of the trinuclear site (Cu^{II}_3 vs Cu^{I}_3) and its coordination by diverse anions in the oxidized states. Careful consideration of the models data reveals several interesting features: (i) systems not providing a bridge between the copper ions give long and variable interatomic distances, (ii) the best defined systems (i.e. the most rigid) approach an equilateral triangle,[7,13,14,17,18,22] (iii) a few isosceles arrangement have been achieved sometimes with the help of serendipity,[11,15,16,22] but the geometrical parameters differ from those of the enzymes.

System		Cu-Cu intra	Cu-Cu inter. 1	Cu-Cu inter. 2	Ref.
Laccase	Cu^{I}_3	5.10	4.20	4.22	25
Asc. Oxidase oxidized Asc. Oxidase reduced	Cu^{II}_3 Cu^{I}_3	 5.01	3.6 to 3.9 4.1	 4.4	26 27
Karlin	Cu^{I}_3 Cu^{II}_3		6.0 to 7.7 5.8 to 8.8		2 3
Tolman	Cu^{I}_3		5.67 to 5.82		4
Agapie	Cu^{I}_3		8.90		5
Murray	Cu^{I}_3		6.5 to 6.7		6
Suh	Cu^{II}_3		3.105		7
Karlin	Cu^{I}_3		5.9 to 9.4		8
Itoh	Cu^{I}_3		5.8 to 6. 3		10
Karlin	Cu^{II}_3	3.1	7.7 to 9.6	7.4 to 10.1	11
Agapie	Cu^{II}_3		3.3 to 3.5		13
Murray	$Cu^{I}Cu^{II}_2S$ $Cu^{I}Cu^{I}_2(N_2)$	 4.24	3.65 3.70	 3.76	14 15
Fenton	Cu^{II}_3	3.62	4.95	5.89	16
Lloret	Cu^{II}_3		2.83		17
Osuka	Cu^{II}_3		3.52(5)		18
Chan	Cu^{II}_3	3.65	3.50	3.52	22

Table 1: *Inter-copper distances (Å) within the dinuclear center (Cu-Cu intra.) and between each of its copper and the third one of the triangular center (Cu-Cu inter. 1-2). Where only one distance is indicated, this is referred to the average value between the three distances.*

It is worth noting also that the studies most focused on generating isosceles arrangements by the groups of Casella[20] and Gewirth[19] have faced significant difficulties. They were based

on the anchoring of two identical binding sites onto the mononuclear site but these lateral sites did not assemble easily into a binuclear one. The groups of Tolman and Casella[4] and Agapie[13] faced similar difficulties when they used a templating metal to assemble the trinuclear unit.

To try and enforce the constitution of the binuclear site, we resorted to elaborate the isosceles triangular arrangement by starting from a binucleating unit (m-xylyl derivative or 2,6-disubstituted phenol) on which terminal ligands would be added to organize the mononuclear site (Figure 16, right). We chose to use the synthon 1-(2-ethylamino)piperazine because it provided both a piperazine group for the dinucleating site already used by others[20,22] and a two-atom linker to the mononuclear binding site.

b. Synthesis of trinucleating ligands

1. Design of the ligands - the biomimetic approach

As described before, the ligands here described have been conceived for obtaining trinuclear copper complexes which mimic the active sites of multicopper oxidases. They have been designed as [2 + 1] arrangements of the three coordinating entities, with the expansion of the binucleating systems described in Chapter 2. The third coordinating unit was added with the aim of putting the third copper center farther in the space. In this way, the metal centers should form an isosceles triangle, like observed in multicopper oxidases but seldom successfully reproduced in biomimetic complexes (Figure 16).

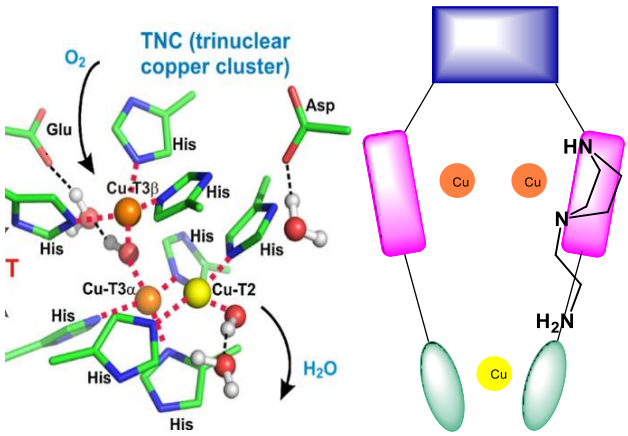

Figure 16: *Trinuclear copper cluster of multicopper oxidases (left) and scheme of designed biomimetic copper complexes.*

For building the three coordinating units 1-(2-ethylamino)piperazine was considered a key synthon. It can provide at the same time the piperazine groups for building the first two coordinating entities and a linking unit with a primary amine group (Figure 16). This can be functionalized for building the third site of coordination. As for binucleating ligands, the unities for the third coordinating group have been chosen in order to obtain flexible ligands which can easily adapt to the coordination geometries of the different redox states of copper. Pyridine groups have good affinity for both Cu(II) and Cu(I) and they have been chosen as ligands for the third coordinating unit. The presence of three coordination entities in flexible ligands would enable fast electron transfers and the presence of a third redox center would change the electrochemical activity of the complexes compared to the binuclear complexes described in Chapter 2.

In the two synthesized ligands BPBPyr and BPBPyrOH (Figure 17) the coordinating arms are linked by the same aromatic spacers used in binuclear complexes. As observed in the Chapter 2 and in the introduction of this chapter, the presence phenol bridging groups between the metals has a capital importance for the stabilization and the properties of this kind of complexes.

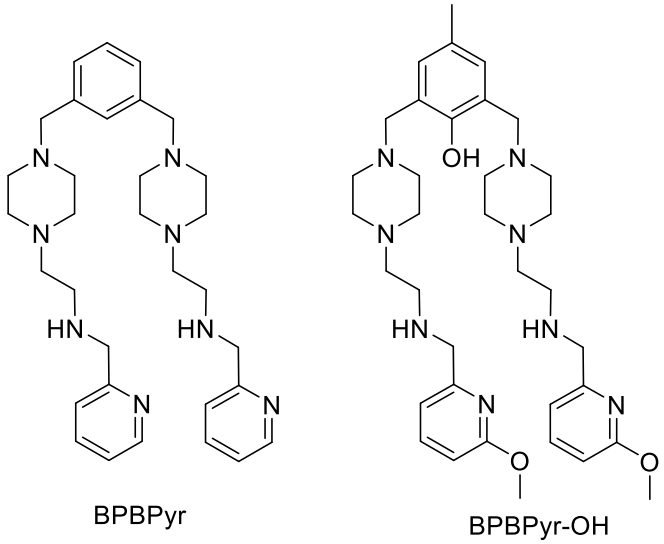

Figure 17: *Trinucleating ligands BPBPyr (left) and BPBPyr-OH (right).*

2. General synthetic strategy

The synthesis of the designed trinucleating ligands was planned starting from a retrosynthetic analysis of the two final molecules (Scheme 2). The ligand BPBPyr was obtained by reductive amination of pyridine-2-carboxyaldehyde with the diamine mXBAEP. This could be obtained by nucleophilic substitution between dichloro-m-xylene and aminoethylpiperazine. The ligand BPBPyr-OH was similarly obtained by reductive amination of 6-methoxy-2-pyridinecarboxyaldehyde with the diamine mXBAEP-OH. This could be obtained by nucleophilic substitution between aminoethylpiperazine and the dichloride Cl(OH)Cl, whose synthesis from 2,6-bis(hydroxymethyl)-p-cresol has been already described in Chapter 2. As it is possible to observe in the retrosynthetic analysis, the key issue in the synthesis of the two ligands was the obtention of the primary diamine fragments. The isolation of this two synthons was challenging; this kind of diamines in fact are strongly basic and polar, making their purification tough. In the following section the different strategies adopted for obtaining the diamines mXBAEP and mXBAEP-OH will be described.

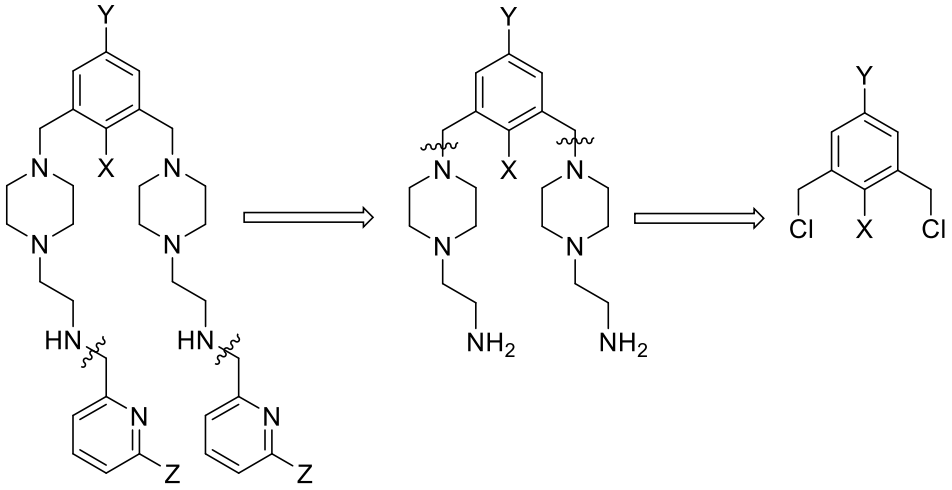

BPBPyr: X= H, Y= H, Z= H
BPBPyr-OH: X= OH, Y= CH_3, Z= OCH_3

Scheme 2: *Retrosynthetic analysis for the design of the ligands.*

3. Synthesis of the diamine precursors

The first strategy adopted for the synthesis of the ligands considered the direct nucleophilic substitution between the dichloride precursors and aminoethylpiperazine, in order to obtain in the two cases the diamine (Scheme 3). Several conditions of reactions were tested by using a common experimental protocol typical of organic nucleophilic substitutions, which will be detailed in the following paragraphs.

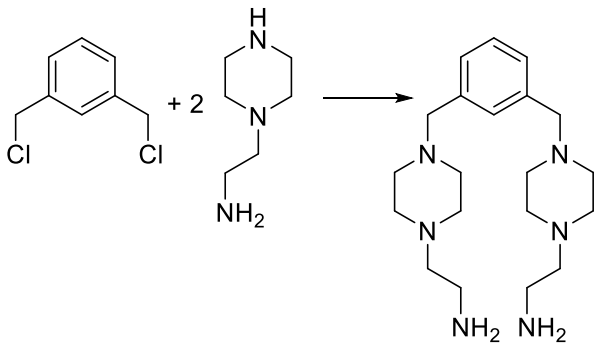

Entry	Solvent	Time (h)	Temperature (°C)	Base	eqv. aminoethylpiperazine
1	toluene	48	room temperature	DIPEA	2
2	toluene	48	room temperature	no base	4
3	toluene	24	60	DIPEA	2
4	ethanol	24	65	Cs_2CO_3	2
5	THF	48	room temperature	Et_3N	2

Scheme 3: *First strategy adopted in the synthesis of the trinucleating ligands with the different reaction conditions tested.*

Unfortunately this strategy faced some problems of selectivity in the first step of nucleophilic substitution; in fact the aminoethylpiperazine used for the reaction is capable of reacting with the dichloride precursors using both the primary and the secondary amine, giving rise to a mixture of by-products from which it was not possible to separate the desired product (Scheme 4).

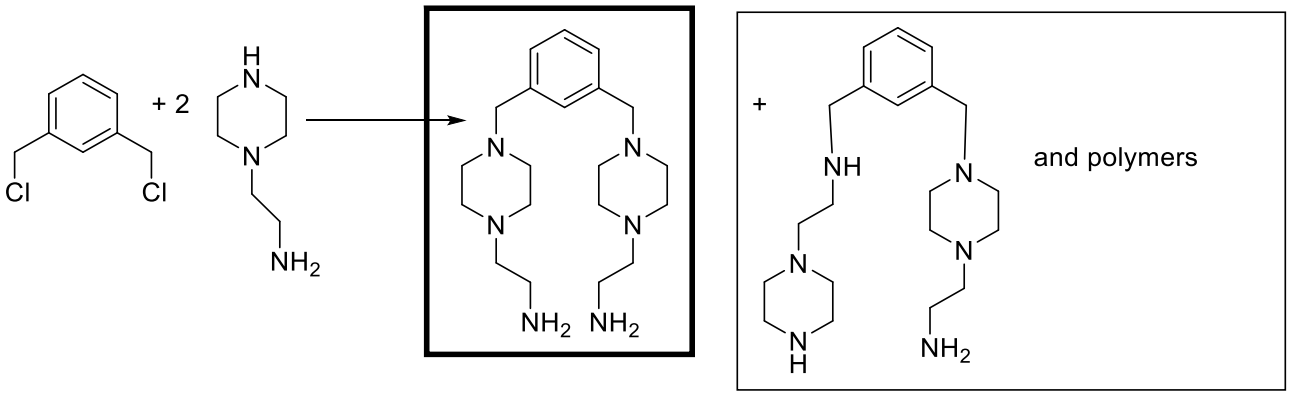

Scheme 4: *By-products of direct nucleophilic substitution between dichloro-m-xylene and aminoethylpiperazine.*

Since the direct nucleophilic substitution between dichloride precursors and aminoethylpiperazine failed in giving the diamine building blocks, another synthetic path

was tested. The aminoethylpiperazine unit can be splitted in two, by forming firstly the piperazine units which can be further functionalized by adding the primary amine arms (Scheme 5).

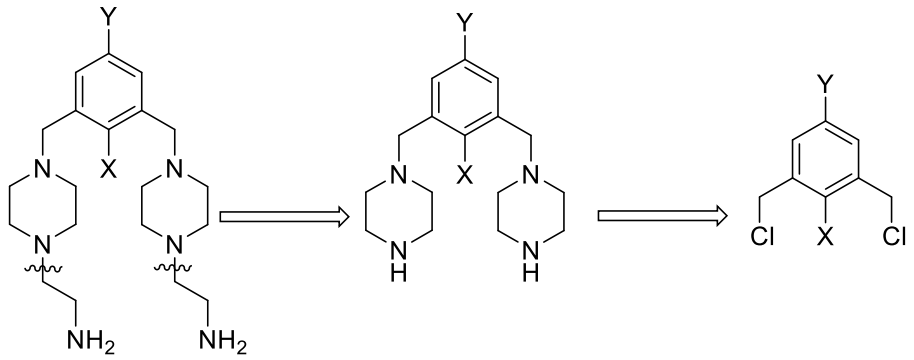

BPBPyr: X= H, Y= H, Z= H
BPBPyr-OH: X= OH, Y= CH_3, Z= OCH_3

Scheme 5: *Alternative retrosynthetic path for the obtention of the diamine building blocks.*

The bis-piperazine unity (mXBP, **(8)**) was synthetised by nucleophilic substitution between dichloro-m-xylene and homopiperazine. Homopiperazine can react with both its secondary amines giving rise to the formation of polymers. A selective reaction with good yields was achieved by mixing equimolar quantities of homopiperazine and its dihydrochloride before the addition of dichloro-m-xylene. In this way, the monohydrochloride of piperazine was formed in situ, enabling the reaction only on the free base side. The pure product was then recuperated as its tetrahydrochloride after treatment of the reaction mixture with gaseous hydrogen chloride at the end of the reaction (Scheme 6).

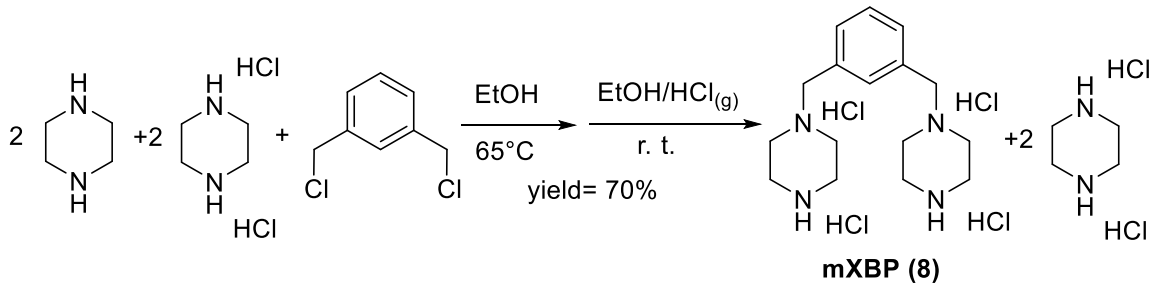

Scheme 6: *Synthesis of mXBP* ***(8)****.*

The obtained molecule, as its free base, was then functionalized by reaction with two equivalents of chloroacetaldehyde dimethyl acetal for obtaining a dialdehyde after acid

deprotection (Scheme 7). This could be then converted into the corresponding diamine. Unfortunately this reaction did not afford the desired product because the acid treatment of the diacetal formed after nucleophilic substitution resulted in the decomposition of the product, precluding the continuation of the synthesis of the diamine.

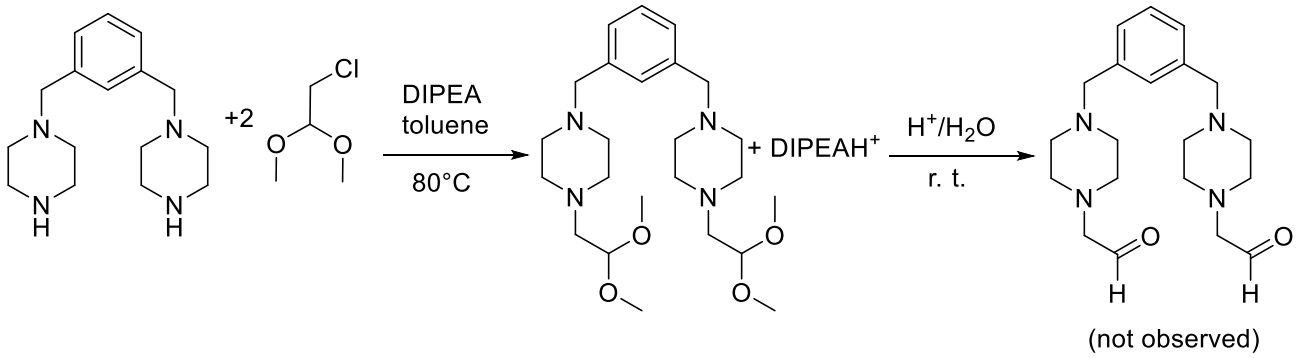

Scheme 7: Functionalization of mXBP for obtaining the dialdehyde.

The two diamines were finally obtained by selective protection of the primary amine of aminoethylpiperazine through the formation of the 2,5-dimethyl pyrroles derivative (Pip-P, 2) with a Paal-Knorr reaction between aminoethylpiperazine and 2,5-hexandione, according to a published experimental protocol (Scheme 8)[28].

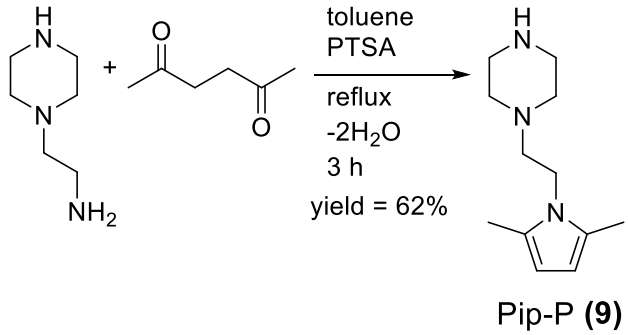

Scheme 8: *Protection of the primary amine group of aminoethyl piperazine via synthesis of Pip-P* ***(9)****.*

The protection consists in a double nucleophilic attack of the primary amine on the two carbonyl groups followed by the elimination of two molecules of water per primary amine group (Scheme 9). For this reason the formation of the protected product is enhanced by distilling away the water formed during the reaction using a Dean-Stark apparatus. In this way it is also possible to know when the reaction is completed by measuring the quantity of water collected in the system.

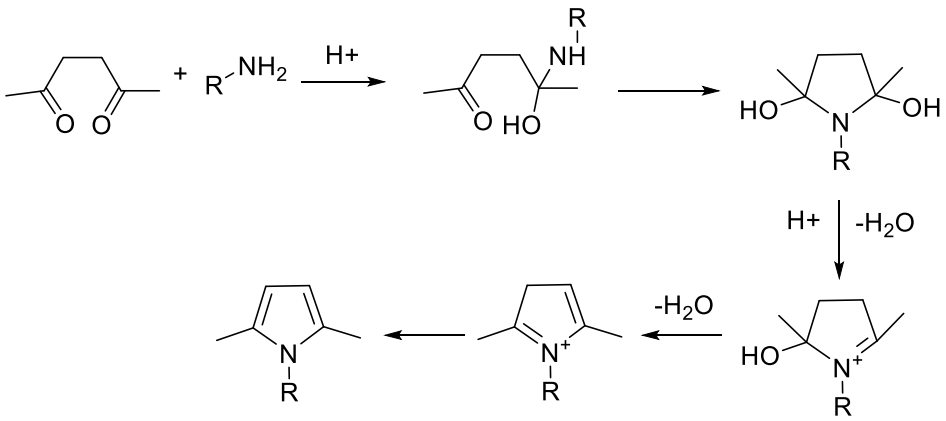

Scheme 9: *Mechanism of protection of primary amines via formation of 2,5-dimethyl pyrrole.*

The protected aminoethylpiperazine (Pip-P) was then used as building block for the synthesis of the trinucleating ligands, enabling selective nucleophilic substitutions on the same chloride precursors used for the synthesis of binucleating ligands.

The protected product was used in a step of nucleophilic substitution with dichloro-m-xylene, in order to synthetize the disubstituted derivative mXB(Pip-p) **(10)**. The reaction appeared to be slow and the formation of the disubstituted product was driven by heating the reaction mixture for 48 hours and adding an excess of protected amine (Scheme 10).

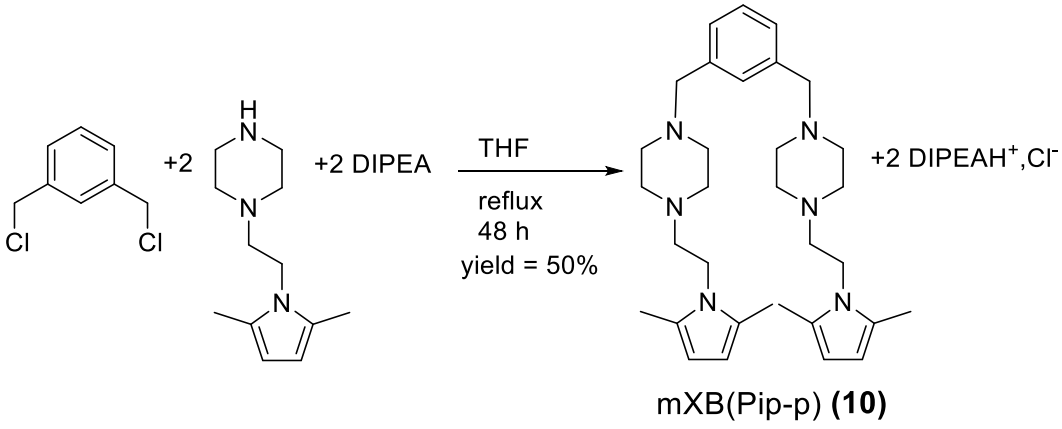

Scheme 10: *Synthesis of mXB(Pip-P)* ***(10)****.*

The same reaction was performed using the dichloride precursor Cl(OH)Cl (Scheme 11). This dichloride precursor seems more reactive than dichloro-m-xylene in the nucleophilic substitution with Pip-P. The disubstituted product product mXB(Pip-P)-OH **(11)** was easily obtained in quantitative yields without heating nor adding an excess of Pip-P.

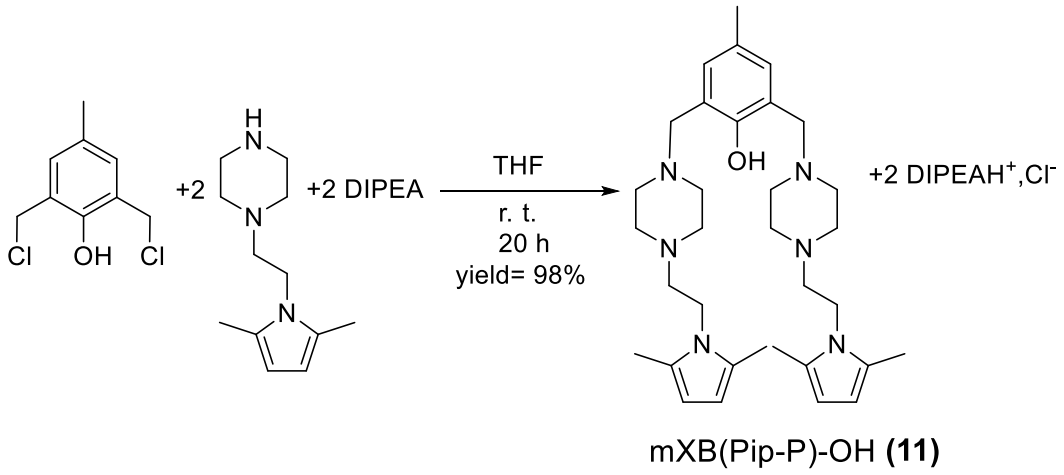

Scheme 11: *Synthesis of mXB(Pip-P)-OH* ***(11)****.*

The primary amine group can be recovered by a deprotection through opening of the pyrrolic rings using hydroxylamine, which attacks the pyrrole ring, to give the free amine and 2,5-hexanedioxime coming from the opening of the cycle (Scheme 12).

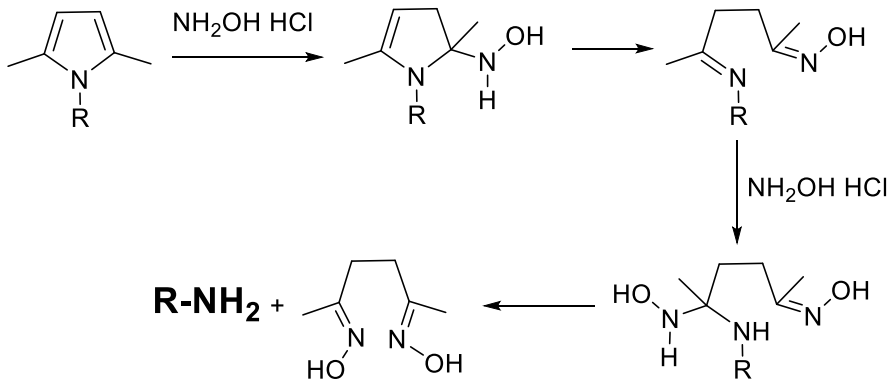

Scheme 12: *Mechanism of deprotection of the primary amine via opening of the pyrrolic ring by hydroxylamine hydrochloride.*

The deprotection of the two disubstituted products mXB(Pip-P) and mXB(Pip-P)-OH was made through opening of the two pyrrolic rings with an excess of hydroxylamine hydrochloride in basic medium (Scheme 13). The two diamines mXBAEP **(12)** and mXBAEP-OH **(13)** were obtained in good yields and also in this kind of reaction the presence of the phenol group seemed to accelerate the reaction.

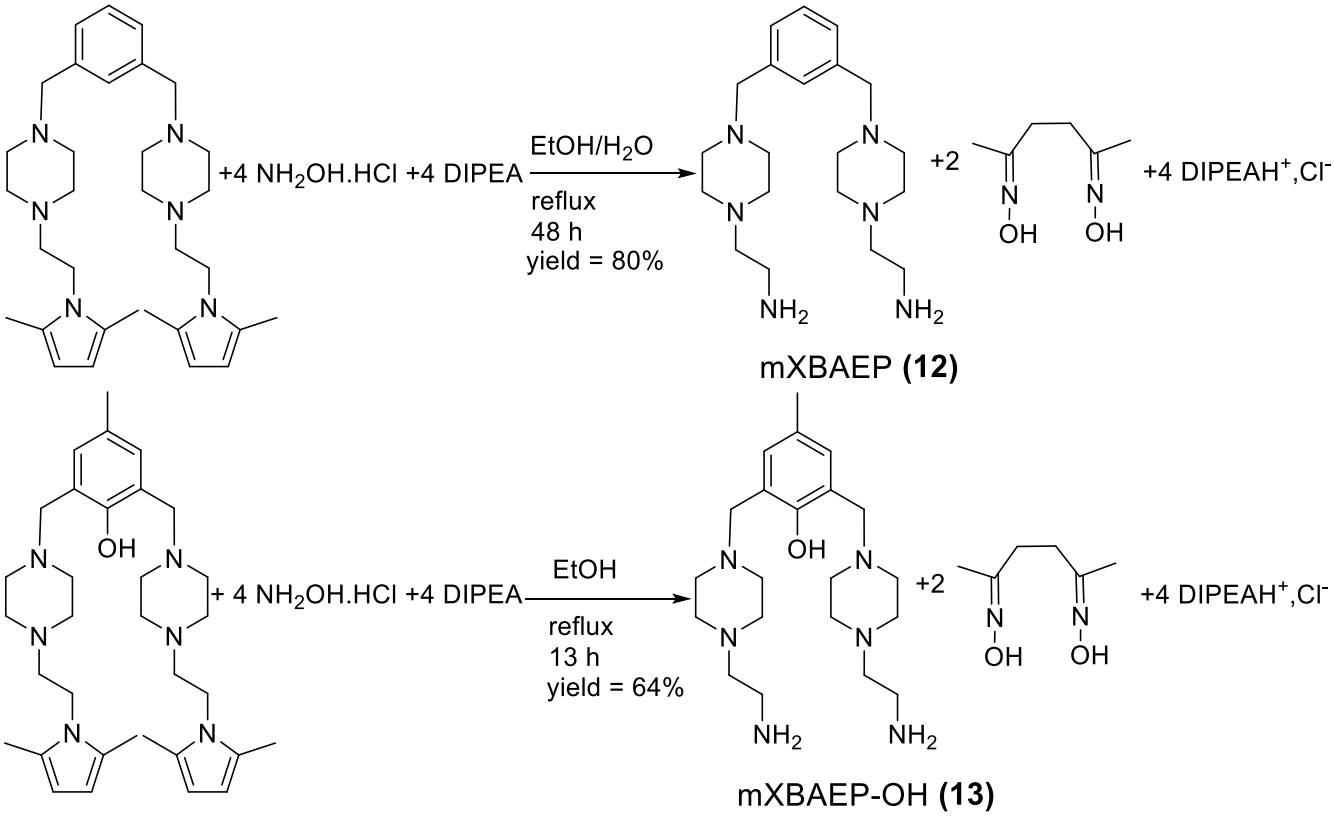

Scheme 13: *Deprotection of the primary amine groups with synthesis of the molecules mXBAEP **(12)** and mXBAEP-OH **(13)**.*

This last synthetic strategy *via* selective protection of the primary amine of aminoethylpiperazine turned out to be successful for obtaining the key precursors of the two trinucleating ligands. These two diamines are versatile molecules which have two piperazine units capable of hosting two metal centers and they can be further functionalized by adding many different functional groups on the primary amine sides. For the synthesis of the trinucleating ligands here presented the two diamines were functionalized by adding two different pyridine groups by reductive amination.

4. Synthesis of trinucleating ligands

The two trinucleating ligands BPBPyr and BPBPyr-OH were synthetized by grafting two pyridine unities to the diamines, in order to obtain a third coordinating position in a symmetric ligand. The ligand BPBPyr **(14)** was obtained through a reductive amination between mXBAEP and two equivalents of pyridine-2-carboxyaldehyde, using sodium borohydride as reducing agent (Scheme 14).

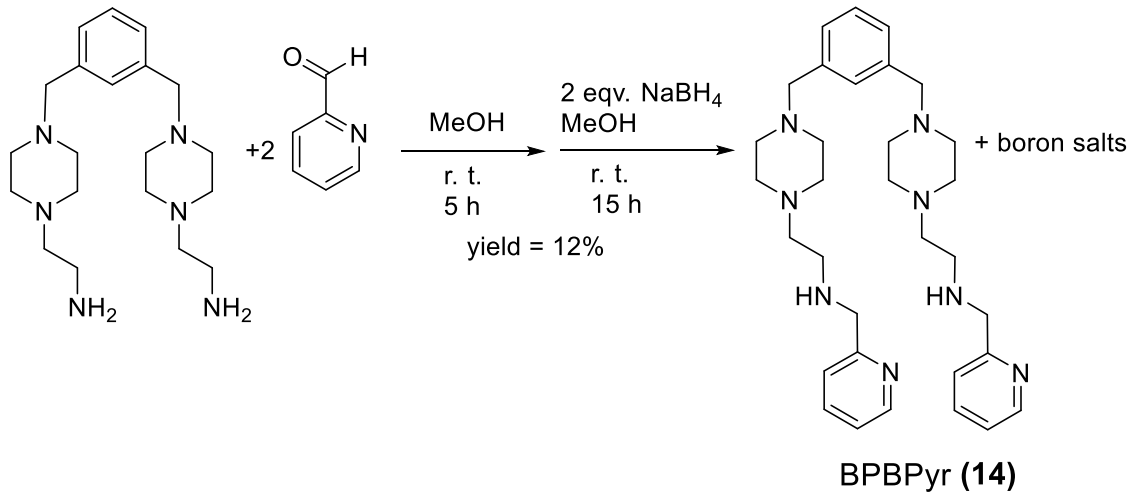

Scheme 14: *Synthesis of the ligand BPBPyr* ***(14)****.*

The reaction was performed firstly by adding two equivalents of the aldehyde to the diamine and then reducing with an excess of sodium borohydride. The ligand BPBPyr was obtained in poor yields, due to two principal reasons. Firstly, the reaction seemed incomplete, since during the chromatographic purification an important quantity of product of reduction of pyridine-2-carboxyaldehyde was recuperated. Secondly, the ligand has the tendency to stay on the column, so a part of it could be lost during the purification.

The ligand BPBPyr-OH **(15)** was obtained in a similar way, through reductive amination between mXBAEP-OH and two equivalents of 6-methoxy-2-pyridinecarboxyaldehyde, using sodium borohydride as reducing agent (Scheme 15). The difficult point of this last step of synthesis of the ligand was the fact that the quantity of diamine mXBAEP-OH can be overestimated if some impurities remain in the product; consequently the quantity of added aldehyde could not respect the real stoichiometry of the reaction, increasing the formation of byproducts.

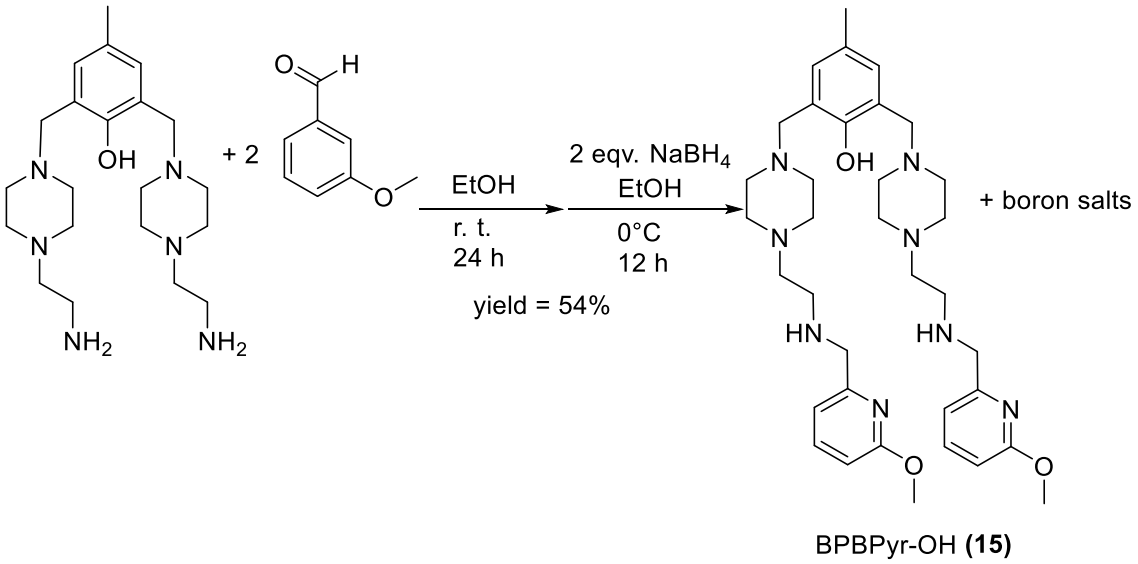

Scheme 15: *Synthesis of the ligand BPBPyr-OH* ***(15)****.*

c. Conclusions

Two new trinucleating ligands have been obtained with the aim of synthesizing new trinuclear copper complexes inspired by the active site of multicopper oxidases. Their synthesis, summarised in Scheme 16, was made difficult due to selectivity problems. Isolation of pure products was sometimes challenging due to their polarity and basicity (water solubility, difficult elution in chromatography). The two diamines mXBAEP and mXBAEP-OH were particularly tough to obtain pure; several synthetic strategies were tested and the their synthesis was finally unblocked by selective protection of primary amine by formation of 2,5-dimethylpyrrole derivatives. These deprotected diamines were here functionalized by grafting pyridine entities as coordinating groups for the third copper center. Moreover, their versatility as organic building blocks which can be functionalized with many different coordinating groups opens the way to a new class of ligands for copper or other metals.

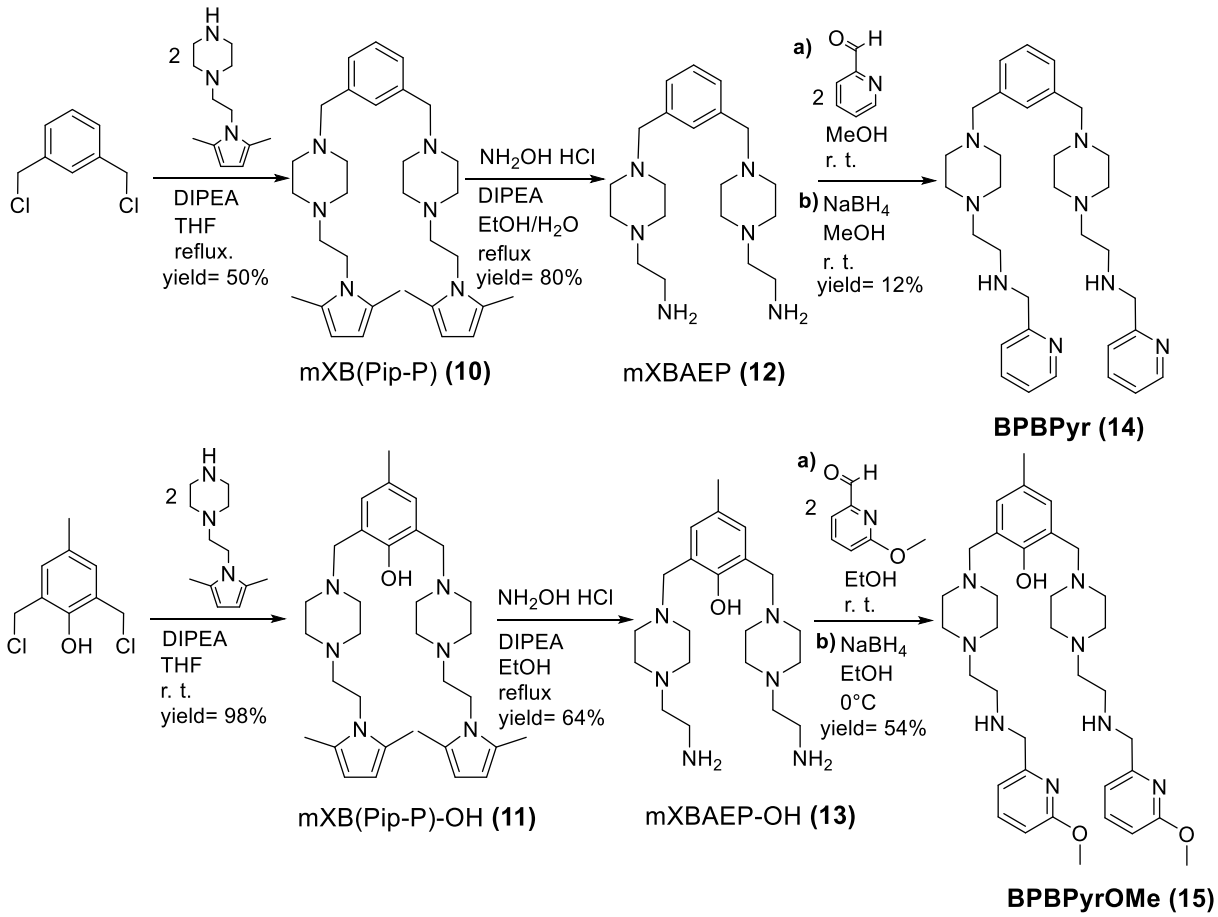

Scheme 16: *Synthetic routes for the trinucleating ligands BPBPyr (top) and BPBPyrOMe (bottom).*

d. Experimental section

Synthesis of 1,3-bis(piperazin-1-ylmethyl)benzene (mXBP) (8)

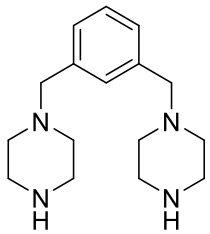

The synthesis was performed by adapting a literature protocol[29].

0.491 g of homopiperazine (MW= 86.14 g mol^{-1}, 5.71 mmol) and 0.908 g of homopiperazine dihydrochloride (MW= 159.06 g mol^{-1}, 5.71 mmol) were suspended in 20 mL of ethanol and stirred at 65°C for 30 minutes, until a clear solution was obtained. 0.500 g of dichloro-m-xylene (MW= 175.05 g mol^{-1}, 2.85 mmol) were then dissolved in 5 mL of ethanol and added dropwise to the reaction mixture, which was stirred at 65°C for three hours, with the formation of a white precipitate.

The reaction mixture was then cooled at room temperature and the precipitate filtered off. Further 70 mL of ethanol were added to the reaction mixture, then gaseous HCl was bubbled, causing precipitation of the product as its hydrochloride. This was recuperated as a white powder by vacuum filtration and washing with toluene. The free base was obtained by treating the hydrochloride with a concentrated aqueous solution of KOH and extracting the free base with dichloromethane.

m = 0.839 g (hydrochloride)

MW (tetrahydrochloride) = 420.21 g mol^{-1}

Yield = 70%

^{1}H-NMR (free base, δ, ppm, $CDCl_3$, 400 MHz): 7.22 (m, 4H), 3.49 (s, 4H), 2.86 (t, J=, 8H), 2.41 (bs, 8H)

^{13}C-NMR (free base, δ, ppm, $CDCl_3$, 100 MHz): 138.07 (Q), 130.26 (CH), 128.16 (CH), 128.14 (CH), 63.78 (CH_2), 54.65 (CH_2), 46.22 (CH_2)

(+) ESI-MS (free base, m/z): 275 $(M + H^+)^+$, 138 $(M + 2H^+)^{2+}$

Synthesis of 1-(2-(2,5-dimethyl-1H-pyrrol-1-yl)ethyl)piperazine (Pip-P) (9)

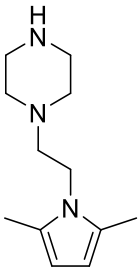

The reaction was performed following a literature experimental protocol[28].

5 mL of aminoethyl piperazine (MW= 129.20 g mol^{-1}, d= 0.985 g mL^{-1}, 38 mmol) were dissolved in 30 mL of toluene with around 10 mg of PTSA and 4.6 mL of 2,5-hexandione (MW= 114.14 g mol^{-1}, d= 0.976 g mL^{-1}, 39 mmol). The mixture was then refluxed for 3 hours using a Dean-Stark apparatus, in order to distil away the water formed during the reaction. After 3 hours the reaction mixture was cooled to room temperature and washed with 2 x 10 mL of aqueous NaOH (pH = 12). The product was then extracted from the organic phase with 4 x 30 mL of saturated solution of $NaHCO_3$ and this aqueous phase was acidified with 20 mL of solution of HCl 12 N. The acidified aqueous phase was washed with 2 x 10 mL of CH_2Cl_2 and then basified at pH = 12 with solid NaOH. The basified aqueous phase was extracted with 4 x 50 mL of CH_2Cl_2 and the collected organic phase was dried over Na_2SO_4 and then evaporated, affording the pure product, which appears as a yellow/orange oil and tends to darken if exposed to light.

m = 4.92 g

MW = 207.32 g mol^{-1}

Yield = 62%

^{1}H-NMR (δ, ppm, $CDCl_3$, 400 MHz): 5.78 (s, 2H), 3.92 (t, J= 7.7 Hz, 2H), 2.96 (t, J= 4.9 Hz, 4H), 2.54 (m, 6H), 2.26 (s, 6H)

^{13}C-NMR (δ, ppm, $CDCl_3$, 100 MHz): 127.43 (Q), 105.29 (CH), 58.91 (CH_2), 54.43 (CH_2), 45.76 (CH_2), 41.26 (CH_2), 12.47 (CH_3)

(+) ESI-MS (m/z): 208 $(M + H^+)^+$

Synthesis of 1,3-bis-((4-(2-(2,5-dimethyl-1H-pyrrol-1-yl)ethyl)piperazin-1-yl)methyl)benzene (mXB(Pip-P)) (10)

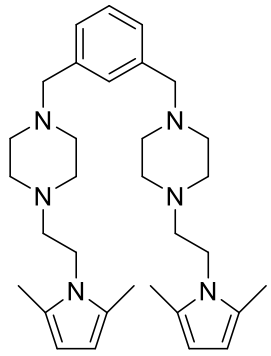

0.850 g of **9** (MW = 207.32 g mol^{-1}, 4.13 mmol) were dissolved in 25 mL of THF with 2.4 mL of DIPEA (MW= 129.25 g mol^{-1}, 0.742 g mL^{-1}, 13.7 mmol) and 0.240 g of dichloro-m-xylene (MW= 175.05 g mol^{-1}, 1.37 mmol). The mixture was refluxed under argon, protected from light, for 48 hours. The formation of some white precipitate in an orange solution was observed. The solvent was then evaporated and an orange oil with some white precipitate was afforded. This was suspended in 30 mL of ethyl acetate and washed with 4 x 10 mL of a saturated solution of NH_4Cl. The obtained clear organic phase was then dried over Na_2SO_4 and the solvent evaporated. The obtained orange oil was purified by column chromatography on alumina (eluent mixture 8:2 hexane : ethyl acetate, Rf = 0.3). The purified product appeared as a pale yellow oil, which tended to darken if exposed to light.

m = 0.358 g

MW = 516.78 g mol^{-1}

Yield = 50%

^{1}H-NMR (δ, ppm, $CDCl_3$, 400 MHz): 7.31 (m, 4H), 5.77 (s, 4H), 3.92 (t, J= 7.9 Hz, 4H), 3.57 (s, 4H), 2.59 (m, 20H), 2.24 (s, 12H)

^{13}C-NMR (δ, ppm, $CDCl_3$, 100 MHz): 138.00 (Q), 129.93 (CH), 128.10 (CH), 127.95 (CH), 127.43 (Q), 105.24 (CH), 62.94 (CH_2), 58.46 (CH_2), 53.75 (CH_2), 52.99 (CH_2), 41.32 (CH_2), 12.52 (CH_3)

(+) ESI-MS (m/z): 517 ($M + H^+$), 259 $(M +2H^+)^{2+}$

Synthesis of 2,6-bis((4-(2-(2,5-dimethyl-1H-pyrrol-1-yl)ethyl)piperazin-1-yl)methyl)-4-methylphenol (mXB(Pip-P)-OH) (11)

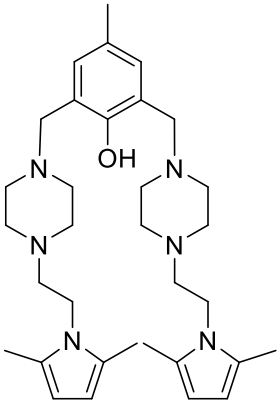

3.46 g of **9** (MW = 207.32 g mol^{-1}, 16.7 mmol) were dissolved in 400 mL of THF with 13.7 mL of DIPEA (MW= 129.25 g mol^{-1}, d= 0.742 g mL^{-1}, 78.5 mmol) and stirred at room temperature and a yellow solution was observed. 1.61 g of **2** (MW= 204.01 g mol^{-1}, 7.85 mmol) were dissolved in 70 mL of THF and then added dropwise to the other solution, which became orange with some white precipitate. The reaction was stirred at room temperature for 20 hours, then the solvent was evaporated, and an orange oil was afforded. This was dissolved in 30 mL of CH_2Cl_2 and washed with 3 x 15 mL of a saturated solution of NH_4Cl and 5 x 15 mL of water. The organic phase was recuperated, dried over Na_2SO_4 and evaporated, leaving an orange solid.

m = 4.26 g

MW = 546.80 g mol^{-1}

Yield = 98%

^{1}H-NMR (δ, ppm, CD_3OD, 400 MHz): 6.91 (s, 2H), 5.66 (s, 4H), 3.95 (t, J= 7.7 Hz, 4H), 3.64 (s, 4H), 2.57 (m, 20H), 2.24 (s, 3H), 2.22 (bs, 12H)

(+) ESI-MS (m/z): 547 ($M + H^+$)

Synthesis of 2,2'-((1,3-phenylenebis(methylene))-bis(piperazine-4,1-diyl)bis(ethan-1-amine) (mXBAEP) (12)

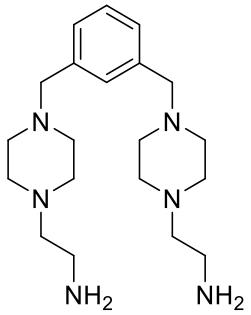

0.358 g of **10** (MW = 516.78 g mol^{-1}, 0.689 mmol) were dissolved in 7 mL of a mixture 2.5:1 ethanol : water with 0.708 g of NH_2OH HCl (MW= 69.49 g mol^{-1}, 10.4 mmol) and 0.720 mL of DIPEA (MW= 129.25 g mol^{-1}, d= 0.742 g mL^{-1}, 4.16 mmol). The mixture was refluxed under argon for 48 hours. The solvent was then evaporated and a pale yellow oil was afforded. This was dissolved in the minimum amount of methanol and precipitated by adding dropwise some diethyl ether. The solvent was separated from a tiny white precipitate, which formed a white foam after drying. The foam was then dissolved in the minimum amount of ethanol and treated with gaseous ammonia, in order to obtain the free base of the molecule. The formation of some white precipitate of NH_4Cl was observed and it was filtered away. The solution was then evaporated and the pure product was obtained as a transparent oil.

m = 0.198 g

MW = 360.55 g mol^{-1}

Yield = 80%

^{1}H-NMR (δ, ppm, CD_3OD, 400 MHz): 7.82 (s, 1H), 7.70 (dd, J= 7.7 Hz, 2H), 7.56 (t, J= 7.6 Hz, 1H), 4.34 (s, 4H), 3.27 (t, J= 4.8 Hz, 8H), 3.12 (t, J= 5.5 Hz, 4H), 2.86 (bs, 8H), 2.77 (t, J= 5.5 Hz, 4H)

^{13}C-NMR (δ, ppm, CD_3OD, 100 MHz): 133.90 (Q), 133.19 (CH), 131.27 (CH), 129.37 (CH), 59.83 (CH_2), 53.32 (CH_2), 51.62 (CH_2), 49.63 (CH_2), 36.12 (CH_2)

(+)-ESI-MS (m/z): 361 ($M + H^+$), 181 $(M +2H^+)^{2+}$

Synthesis of 2,6-bis((4-(2-aminoethyl)piperazin-1-yl)methyl)-4-methylphenol (mXBAEP-OH) (13)

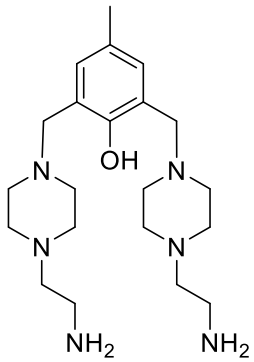

4.26 g of **11** (MW = 546.80 g mol^{-1}, 4.85 mmol) were dissolved in 80 mL of ethanol with 4.55 mL of DIPEA (MW= 129.25 g mol^{-1}, d= 0.742 g mL^{-1}, 29.12 mmol) and 8.1 g of NH_2OH HCl (MW= 69.49 g mol^{-1}, 72.80 mmol) and refluxed for 13 hours. After cooling the reaction to room temperature, a white precipitate was filtered off and the orange filtrate was evaporated. The obtained crude product was then dissolved in 20 mL of methanol and addition of 150 mL of acetonitrile caused the separation of an orange oil. The separated oil was dried and then dissolved in 20 mL of methanol and precipitated with 100 mL of diethyl ether. The precipitate was separated from the solution and it was further washed by dissolving it in 20 mL of methanol and precipitating with 100 mL of acetonitrile, obtaining the purified product as its hydrochloride. The free base was obtained by dissolving the hydrochloride in the minimum amount of CH_2Cl_2, by adding a few mL of saturated solution of sodium carbonate and recuperating the organic phase after stirring for several minutes at room temperature. The organic phase was then evaporated, giving the pure product as an orange oil.

m = 1.95 g

MW = 390.58 g mol^{-1}

Yield = 64%

^{1}H-NMR (δ, ppm, CD_3OD, 400 MHz): 7.22 (s, 2H), 4.19 (s, 4H), 3.13 (m, 12H), 2.77 (m, 12H), 2.31 (s, 3H).

(+)-ESI-MS (m/z): 391 ($M + H^+$)

Synthesis of 2,2'-((1,3-phenylenebis(methylene))bis(piperazine-4,1-diyl))bis(N-(pyridin-2-ylmethyl)ethan-1-amine) (BPBPyr) (14)

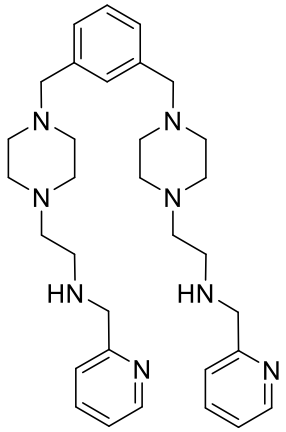

0.198 g of **12** (MW = 360.55 g mol^{-1}, 0.561 mmol) were dissolved in 1 mL of methanol and stirred at room temperature. 0.126 g of pyridine-2-carboxyaldehyde (MW= 107.11 g mol^{-1}, 1.18 mmol), previously filtered on alumina, were dissolved in 2.5 mL of methanol and added to the reaction mixture, which turned from colourless to intense yellow. The reaction mixture was stirred at room temperature for 5 hours, then 69 mg of $NaBH_4$ (MW= 37.83 g mol^{-1}, 1.65 mmol) were slowly added. The formation of effervescence was observed and the solution became paler. After further 15 hours stirring at room temperature the solvent was evaporated and a yellow oil with some white precipitate was obtained. This was suspended in 5 mL of CH_2Cl_2 and washed with 2 mL of saturated solution of NH_4Cl. The aqueous phase was then basified to pH = 10 with solid NaOH and extracted with 4 x 1.5 mL of CH_2Cl_2. All the organic phases were then combined, dried over Na_2SO_4 and evaporated. The obtained yellow oil was then purified by column chromatography on silica. The impurities (Rf= 0.4 and Rf= 0.2) were eliminated by elution with diethyl ether, while the pure product stayed on the top of the column and it could be recuperated by eluting with methanol. The purified product appeared as a yellow oil.

m = 0.0349 g

MW = 542.78 g mol^{-1}

Yield = 12%

^{1}H-NMR (δ, ppm, $CDCl_3$, 400 MHz): 8.54 (d, J= 3.8 Hz, 2H), 7.62 (t, J= 7.4 Hz, 2H), 7.29 (d, J= 7.7 Hz, 2H), 7.20 (m, 4H), 7.14 (t, J= 5.6 Hz, 2H), 3.91 (s, 4H), 3.48 (s, 4H), 2.73 (t, J= 6.8 Hz, 4H), 2.52 (t, 6.1 Hz, 4H), 2.45 (bs, 16H)

^{13}C-NMR (δ, ppm, $CDCl_3$, 100 MHz): 159.87 (Q), 149.25 (CH), 137.99 (Q), 136.43 (CH), 130.04 (CH), 128.01 (CH), 127.95 (CH), 122.24 (CH), 121.90 (CH), 65.83 (CH_2), 62.98 (CH_2), 57.88 (CH_2), 53.21 (CH_2), 53.04 (CH_2), 45.99 (CH_2)

(+)-ESI-MS (m/z): 543 ($M + H^+$),

Synthesis of 2,6-bis((4-(2-(((6-methoxypyridin-2-yl)methyl)amino)ethyl)piperazin-1-yl)methyl)-4-methylphenol (BPBPyr-OH) (15)

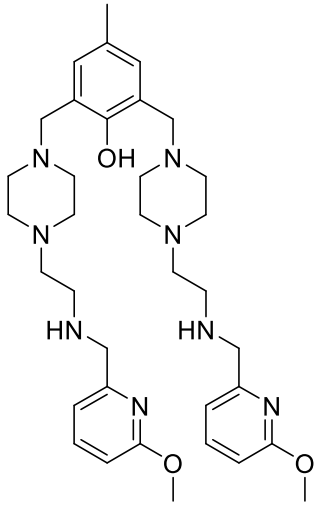

0.110 g of **13** (0.28 mmol) were dissolved in 30 mL of ethanol and an orange solution was observed. 68 μL of 6-methoxy-2-pyridinecarboxyaldehyde (MW= 137.14 g mol^{-1}, d= 1.140 g mol^{-1}, 0.56 mmol) were then added under stirring at room temperature and the formation of some precipitate was observed. The reaction mixture was stirred at room temperature for 24 hours, then 0.016 g of $NaBH_4$ (MW= 37.83 g mol^{-1}, 0.42 mmol) were added to the reaction mixture, previously cooled with an ice bath and diluted with further 6 mL of ethanol. During the addition of the reducing agent it was possible to observe the formation of some effervescence and changes in the colour of the reaction mixture, which turned from orange to yellow. The reaction was left warming to room temperature and stirred overnight, then the solvent was evaporated. The crude product was suspended in 6 mL of CH_2Cl_2, ten drops of saturated solution of Na_2CO_3 were added and the mixture was left stirring for 2 hours. The organic phase was then dried over Na_2SO_4 and evaporated. The ligand was afforded as a dark yellow oil.

m = 0.095 g

MW = 632.85 g mol^{-1}

Yield = 54%

^{1}H-NMR (δ, ppm, CD_2Cl_2, 400 MHz): 7.62 (t, J= 7.8 Hz, 2H), 7.35 (d, J= 6.5, 2H), 6.88 (s, 2H), 6.75 (d, J= , 2H), 4.19 (s, 6H) 3.96 (s, 4H), 3.60 (s, 4H), 2.78 (t, J= 5.6 Hz, 4H), 2.50 (m, 20H), 2.25 (s, 3H)

^{13}C-NMR (δ, ppm, CD_3OD, 100 MHz): 163.63 (Q), 157.83 (Q), 150.58 (Q), 139.79 (CH), 129.10 (Q), 127.64 (Q), 127.45 (Q), 116.42 (CH), 106.55 (CH), 59.46 (CH_2), 57.54 (CH_2), 53.75 (CH_3), 53.58 (CH_2), 53.32 (CH_2), 52.52 (CH_2), 46.64 (CH_2), 21.81 (CH_3).

(+)-ESI-MS (m/z): 633 ($M + H^+$)

e. Bibliography

(1) Fenton, D.; Okawa, H. *J. Chem. Soc. Dalton Trans.* **1993**, 1349–1357.
(2) Karlin, K. D.; Gan, Q.; Farooq, A.; Liu, S.; Zubieta, J. *Inorg. Chim. Acta* **1989**, *165*, 37–39.
(3) Frey, S.; Sun, H.; Murthy, N.; Karlin, K. *Inorg. Chim. Acta* **1996**, *242*, 329–338.
(4) Brown, E. C.; Johnson, B.; Palavicini, S.; Kucera, B. E.; Casella, L.; Tolman, W. B. *Dalton Trans.* **2007**, 3035–3042.
(5) Lionetti, D.; Day, M. W.; Agapie, T. *Chem. Sci.* **2013**, *4*, 785–790.
(6) Guillet, G. L.; Gordon, J. B.; Di Francesco, G. N.; Calkins, M. W.; Cizmar, E.; Abboud, K. A.; Meisel, M. W.; Garcia-Serres, R.; Murray, L. J. *Inorg. Chem.* **2015**, *54*, 2691–2704.
(7) Suh, M.; Han, M.; Lee, J.; Min, K.; Hyeon, C. *J. Am. Chem. Soc.* **1998**, *120*, 3819–3820.
(8) Karlin, K. D.; Gan, Q.; Farook, A.; Liu, S.; Zubieta, J. *Inorg. Chem.* **1990**, *29*, 2549–2551.
(9) Ohi, H.; Tachi, Y.; Itoh, S. *Inorg. Chem.* **2004**, *43*, 4561–4563.
(10) Ohi, H.; Tachi, Y.; Itoh, S. *Inorg. Chem.* **2006**, *45*, 10825–10835.
(11) Ghiladi, R. A.; Rheingold, A. L.; Siegler, M. A.; Karlin, K. D. *Inorg. Chim. Acta* **2012**, *389*, 131–137.
(12) Tsui, E. Y.; Kanady, J. S.; Day, M. W.; Agapie, T. *Chem. Commun.* **2011**, *47*, 4189–4191.
(13) Tsui, E. Y.; Day, M. W.; Agapie, T. *Angew. Chem. Int. Ed.* **2011**, *50*, 1668–1672.
(14) Di Francesco, G. N.; Gaillard, A.; Ghiviriga, I.; Abboud, K. A.; Murray, L. J. *Inorg. Chem.* **2014**, *53*, 4647–4654.
(15) Murray, L. J.; Weare, W. W.; Shearer, J.; Mitchell, A. D.; Abboud, K. A. *J. Am. Chem. Soc.* **2014**, *136*, 13502–13505.
(16) Adams, H.; Bailey, N.; Dwyer, M.; Fenton, D.; Hellier, P.; Hempstead, P.; Latour, J. *J. Chem. Soc.-Dalton Trans.* **1993**, 1207–1216.
(17) Gonzalez-Alvarez, A.; Alfonso, I.; Cano, J.; Diaz, P.; Gotor, V.; Gotor-Fernandez, V.; Garcia-Espana, E.; Garcia-Granda, S.; Jimenez, H. R.; Lloret, F. *Angew. Chem. Int. Ed.* **2009**, *48*, 6055–6058.
(18) Inoue, M.; Ikeda, C.; Kawata, Y.; Venkatraman, S.; Furukawa, K.; Osuka, A. *Angew. Chem. Int. Ed.* **2007**, *46*, 2306–2309.
(19) Tse, E. C. M.; Schilter, D.; Gray, D. L.; Rauchfuss, T. B.; Gewirth, A. A. *Inorg. Chem.* **2014**, *53*, 8505–8516.
(20) Santagostini, L.; Gullotti, M.; Pagliarin, R.; Bianchi, E.; Casella, L.; Monzani, E. *Tetrahedron-Asymmetry* **1999**, *10*, 281–295.
(21) Monzani, E.; Casella, L.; Zoppellaro, G.; Gullotti, M.; Pagliarin, R.; Bonomo, R. P.; Tabbi, G.; Nardin, C.; Randaccio, L. *Inorg. Chim. Acta* **1998**, *282*, 180–192.
(22) Chen, P. P.-Y.; Yang, R. B.-G.; Lee, J. C.-M.; Chan, S. I. *Proc. Natl. Acad. Sci. U. S. A.* **2007**, *104*, 14570–14575.
(23) Nagababu, P.; Maji, S.; Kumar, M. P.; Chen, P. P.-Y.; Yu, S. S.-F.; Chan, S. I. *Adv. Synth. Catal.* **2012**, *354*, 3275–3282.
(24) Ross, M. O.; Rosenzweig, A. C. *JBIC J. Biol. Inorg. Chem.* **2017**, *22*, 307–319.
(25) Bento, I.; Martins, L. O.; Lopes, G. G.; Carrondo, M. A.; Lindley, P. F. *Dalton Trans.* **2005**, 3507–3513.
(26) Messerschmidt, A.; Ladenstein, R.; Huber, R. *J. Mol. Biol.* **1992**, *224*, 179–205.
(27) Messerschmidt, A.; Luecke, H.; Huber, R. *J. Mol. Biol.* **1993**, *230*, 997–1014.
(28) Hayashi, S.; Hirao, A.; Imai, A.; Nakamura, H.; Murata, Y.; Ohashi, K.; Nakata, E. *J. Med. Chem.* **2009**, *52*, 610–625.
(29) Cymerman Craig, J.; Young, R. J. *Org. Synth.* **1962**, *42*, 19–21.

Chapter 4: Nitrene transfer catalysis with a binuclear copper complex

This chapter focuses on experiments of nitrene transfer catalysis performed with the binuclear copper complex $[Cu_2(mXBMP\text{-}O)(CH_3COO)_2]ClO_4.(CH_3CN).(MeOH)$, described in Chapter 2. This complex was chosen between the three binuclear complexes described in Chapter 2 because it was the only one whose structure and purity were completely stated. An introduction about nitrene transfer will be presented, with a focus on aziridination catalysis with copper complexes. Catalysis studies with the complex mentioned above will be then presented. Results of catalytic tests performed with both bis-Cu(II) and bis-Cu(I) forms of the complex will be presented first, with an analysis of the different conditions used to perform the reactions. The catalytic activity will be then analyzed from the mechanistic point of view, with studies on the approach of the nitrene with the complex and the mechanism of transfer on substrates.

a. Introduction

1. Early development of nitrene transfer catalysts, in particular for aziridination

As mentioned in the introduction, the discovery that nitrene transfer to an organic substrate can be initiated through decomposition of an organic azide by a metal salt was published in 1967 by Kwart and Kahn[1,2]. These authors indeed observed that treatment of benzenesulfonylazide ($PhSO_2N_3$) by copper metal or $CuCl_2$ in the presence of DMSO forms the sulfoximine product $(CH_3)_2S(O)(NSO_2Ph)$[1]. Similarly, when the reaction is done in the presence of cyclohexene several aminated products are formed: aziridine, enamine, allylic amine[2]. Another landmark was due to Sharpless and coll. who reported a few years later that the trioxoimido osmium complexes $OsO_3(NR)$ (R= *tert*-Butyl, Adamantyl) react with various olefins to give the vicinal aminoalcohols[3]. A significant progress in the development of efficient catalytic systems of nitrene transfer was made in 1975 with the introduction of a new class of reagents, the iminoiodinanes of general formula PhI=NTs (p-methylbenzenesulfonylaminophenyliodinane), which were shown to transfer tosylnitrene to easily oxidizable substrates such as sulfides and phosphines[4]. Elaborating on this finding, in the early 1980s, Breslow reported the intramolecular amination of a prefunctionalized substrate upon treatment by an iron or manganese porphyrin[5] and the intermolecular amination of cyclohexane by reaction with PhI=NTs in the presence of the same catalysts[6]. At the same time, the group of Mansuy reported the preparation of a nitrene derivative of an

iron porphyrin[7–9] and the development of aziridination[10] and amination[11,12] systems. Notwithstanding these early seminal studies, the real development of metal-catalyzed nitrene transfer reactions was due to the group of Evans in the beginning of the 1990s who reported efficient and enantioselective olefin aziridination catalyzed by Cu^{I} and Cu^{II} salts.[13,14] Soon thereafter, Jacobsen and coll. developed enantioselective copper catalysts for aziridination by using chiral diimine ligands[15–18].

Dirhodium tetracarboxylates are another class of frequently used nitrene transfer catalysts,[19,20] however, they are less reactive for aziridination than for aliphatic amination. Indeed, to reach an efficient aziridination, comparable to that of copper catalysts, the nitrene donor PhI=NTs must be replaced by the more electrophilic PhI=NNs (p-nitrobenzenesulfonylaminophenyliodinane) where the donating p-methyl group has been replaced by a p-nitro group.[21]

A new generation of active ruthenium(VI) porphyrin catalysts has been developed by Che [22,23]. These catalysts are active for aziridination as well as amination reactions. More recently, non heme Fe catalysts for aziridination[24] have appeared as for amination, but their understanding and their efficiency must still be improved.

2. *Brief survey of copper aziridination catalysts*

As mentioned above the development of efficient copper-nitrene transfer catalysts was initiated by the group of Evans in the beginning of the 1990s and these have been the most studied catalysts especially for aziridination. Evans group used various Cu^{I} and Cu^{II} salts leading to aziridination of styrene in yields ranging from 56 % (with coordinating anions such as CuBr) up to > 90 % (with $Cu(ClO_4)$, Cu(OTf), $Cu(acac)_2$, $Cu(OTf)_2$)[13,14]. Comparable yields were obtained for Cu^{I} and Cu^{II} salts, in spite of necessarily different mechanisms (see below). Soon thereafter, using diimine ligands, Jacobsen developed enantioselective aziridination processes and provided important clues to their mechanism[15,17,18]. Another major contribution is due to the group of Pérez who, over the last two decades, introduced and developed series of Cu^{I} tetrapyrazolylborates and studied their mechanism both experimentally and theoretically[25,26] (Figure 1). More recently, Stavropoulos used a tris-[(tetramethylguanidino)-phenyl]-amine ligand to prepare an extremely efficient mononuclear Cu^{I} catalyst and study in depth its mechanism[27] (Figure 1).

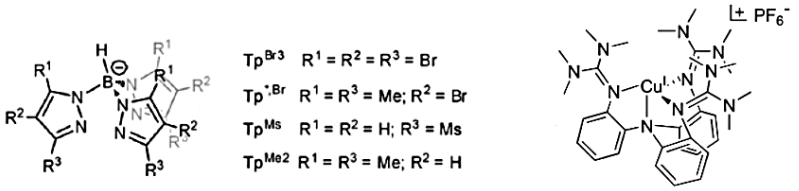

Pérez 2013 **Stavropoulos 2014**

Figure 1: *Systems used by Pérez and Stavropoulos for performing nitrene transfer catalysis with Cu(I) complexes.*

3. Mechanistic aspects of aziridination reaction catalyzed by copper complexes

a. Cu(I)

From the beginning aziridination mechanisms have been discussed in relation with those for cyclopropanation, especially in the case of Cu^{I} catalysts, owing to the fact that some of them are able to catalyze both reactions.[25] The major issues to be resolved in the study of this kind of reaction are:

- The occurrence of a concerted as opposed to a sequential mechanism allowing the formation of an intermediate radical species.
- The possibility of a redox mechanism as opposed to a catalysis by a Lewis acid since the aziridination can be catalyzed also by non-redox metals such as zinc[14,28].
- The mechanistic difference between Cu^{I} and Cu^{II} catalysts.

The first experimental clue for the intervention of a Cu^{III}-nitrene intermediate in a redox mechanism was offered by the group of Jacobsen. In fact, they observed identical enantioselectivity in styrene aziridination whether the nitrene precursor is an iodinane PhI=NTs or an azide TsN_3 under photochemical activation[17]. Indeed, if the reaction occurred through a Lewis acid activation of the reagent distinct reactivities should be observed and the identical reactivity cannot be explained otherwise than due to the existence of the same intermediate which they formulated Cu^{III}=NTs[17]. The occurrence of such an intermediate was further substantiated by DFT calculations[29].

In the investigations of nitrene transfer mechanism the distinction between concerted and stepwise mechanisms is generally based on the use of stereoselective substrates such as *cis*-stilbene and *cis*-β-methylstyrene (Figure 2, left, bottom). Indeed, in a concerted mechanism the product will retain the stereochemistry of the substrate whereas in a stepwise

mechanism with the formation of a radical intermediate the product of the reaction will be the thermodynamically more stable *trans* isomer. For an estimation of the lifetime of the intermediate radical the use of more sophisticated substrates called radical clocks is required (Figure 2, left, middle).

There is no general mechanism for copper catalysts and both concerted and stepwise mechanisms have been documented depending on the systems. The most thorough study from the mechanistic point of view is due to the group of Pérez who analyzed in parallel the mechanisms of Cu^{I} and Ag^{I} catalysts obtained from the same ligands by combining catalytic tests on stereoselective substrates and substrates competitions (Figure 2, top) to explore the electronic effects through Hammett-like correlations and DFT analyses of the reaction profiles[26].

It is assumed that the copper-nitrene intermediate can exist in a singlet form "Cu=NR" or a triplet form "$Cu^{\bullet}$-$^{\bullet}$NR" and the two are responsible respectively for the concerted and the stepwise process (Figure 2, right). However, the DFT analysis reveals that the situation is less clear-cut since singlet and triplet reactive surfaces can intersect. A stepwise process appears to be the most generally found experimentally through stereoselective experiments. It can be substantiated also by the failure of Hammett-like correlations based exclusively on polarity effects to account for the competition experiments; inclusion of a radical delocalization parameters through a "dual-correlation"[30] is thus necessary and is the signature of this mechanism.

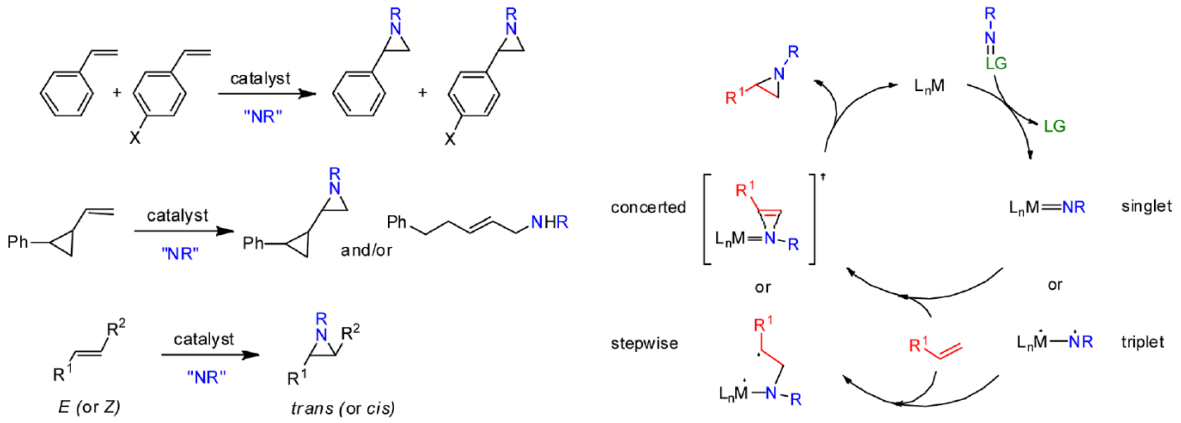

Figure 2: *Mechanistic analysis of copper catalysed nitrene tranfer to olefins. Left panel: competition experiments for styrene aziridination (top), radical clock substrate reactions (middle) and stereoselective substrate reactions (bottom). Right panel: singlet and triplet nitrene species and associated mechanisms. LG = leaving group, (ArI for an iodinanes, N_2 for organic azides).*

Therefore the mechanism of action of Cu^{I} catalysts, which is more or less agreed upon, involves three main stages:

1. In the initial stage, the iodinane (or the organic azide) coordinates to the Cu^{I} ion to form the adduct Cu^{I}-NR(LG) (LG= PhI in the case of iodinane, LG= N_2 in the case of organic azide);
2. The formed adduct then rearranges to the Cu^{III}=NR nitrene by elimination of the leaving group (LG), in a reaction which is akin to a two-electron oxidative addition;
3. The remaining part of the mechanism depends on the electronic structure of the active Cu^{III}=NR nitrene species, or in other words whether its electronic structure corresponds to the singlet or the triplet form described above (Scheme 1, right).

b. Cu(II)

By contrast, the mechanism of Cu^{II} catalysts is less clear. If it were similar to that of the Cu^{I} catalyst it would involve the generation of a Cu^{IV}-nitrene species, which is difficult to envisage. In such a case, a Lewis acid mechanism can be considered, which appears more viable in the case of Cu^{II} than for Cu^{I} owing to the increased acidity of the oxidized form. In this mechanism, the active species would be the adduct between the nitrene precursor and the catalyst Cu^{II}←N(Ts)(IPh), then the nitrene transfer to the substrate would occur without prior liberation of PhI. This possibility has been studied more in-depth in the case of the reactions with the oxo analog iodosobenzene. The oxygen transfer capacity of these adducts

was demonstrated on porphyrin systems[31] more than fifteen years ago and more recently on a non-heme equivalent[32]. Moreover, an adduct to an iron complex has been structurally characterized and the oxo transfer to a substrate evidenced[33].

Nevertheless, such a process has been discounted by Comba and co-workers in the case of Cu^{II} catalysts with bispidine ligands, as done by Jacobsen and co-workers with Cu^{I} diimine catalysts[17], by observing that the bulkiness of the aromatic part of the iodinane (Ph vs bulky Ar) has no effect on the enantioselectivity of the nitrene transfer[34]. By contrast, a correlation of the activity of the Cu^{II} catalyst with the Cu^{I}/Cu^{II} redox potential has led to the proposal that the iodinane PhI=NTs at some stage of the mechanism reduces the Cu^{II} catalyst to Cu^{I} [35]:

$$Cu^{2+} + PhI{=}NTs \longrightarrow Cu^{+} + PhI^{\bullet+}$$

The possibility of this kind of electron transfer is counterintuitive owing to the fact that iodinanes are generally oxidative reagents. Comba's group described also the catalytic behavior of a Cu(II) complex with a slightly different bispidine ligand and he proposed that in this case the nitrene donor would not oxidize the metal center, by forming a reactive intermediate with a diradical on nitrogen[34]. By writing the resonance formula of this intermediate it is possible to envisage that this species is actually a Cu^{III}=•NTs (Scheme 1).

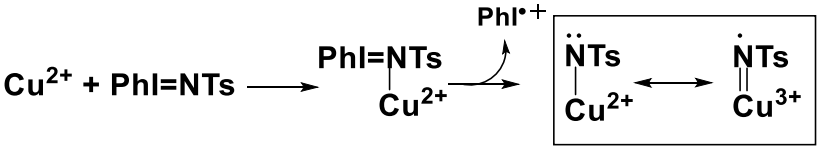

Scheme 1: *Resonance formula of nitrene intermediate proposed by Comba and co-workers[34].*

The existence of this kind of intermediate has been proposed also by Norrby's group[29]. In this kind of mechanism the electronic redistribution would occur within the iodinane adduct. Indeed, the generation of a very high-valent and strongly oxidant Cu^{IV} nitrene species by taking two electrons from the copper ion would be energetically very demanding. In these conditions, one-electron oxidation of iodobenzene rather than copper may be more accessible. In other words the two-electron oxidative rearrangement would be effected at the expense of the copper ion (one electron) and iodobenzene (one electron). This proposal makes more sense than the reduction of Cu(II) by the iodinane because it hypothesizes that

oxidizing Cu^{III} to Cu^{IV} is more energetically demanding than oxidizing PhI to $PhI^{+\bullet}$, which is reasonable.

In the following chapter the complex $[Cu_2(mXBMP\text{-}O)(CH_3COO)_2]ClO_4.(CH_3CN).(MeOH)$ synthesized and characterized in Chapter 2 will be used as catalyst for aziridination reaction. First of all the results of catalytic reactions on styrene with the bis-Cu(II) and the *in situ* generated bis-Cu(I) species will be presented. Then mechanistic studies aimed at investigating the nature of the intermediate species and the nitrene transfer mechanism for the two catalytic species will be described.

b. Catalysis of nitrene transfer with the complex $[Cu_2(mXBMP-O)(CH_3COO)_2]ClO_4.(CH_3CN).(MeOH)$

The complex $[Cu_2(mXBMP-O)(CH_3COO)_2]ClO_4.(CH_3CN).(MeOH)$ described in Chapter 2 have been chosen to perform some tests of nitrene transfer catalysis. Since catalytic activity with both Cu(II) and Cu(I) complexes is reported in literature, the catalytic tests have been carried out with both the bis-Cu(II) complex and its reduced bis-Cu(I) analog.

1. Generation of the bis-Cu(I) complex

The bis-Cu(I) species was generated in situ by reduction of the bis-Cu(II) complex with hydroxylamine hydrochloride. Since the presence of an excess of reducing agent can be detrimental to the catalytic activity, a preliminary titration of the complex with the reducing agent was performed, in order to define the correct ratio between the bis-Cu(II) complex and hydroxylamine. As it is possible to observe in Figure 3, the bis-Cu(II) complex underwent complete reduction with the addition of two equivalents of hydroxylamine hydrochloride. The bis-Cu(I) complex is then generated for all the experiments starting from a solution of bis-Cu(II) complex reduced with two equivalents of hydroxylamine hydrochloride.

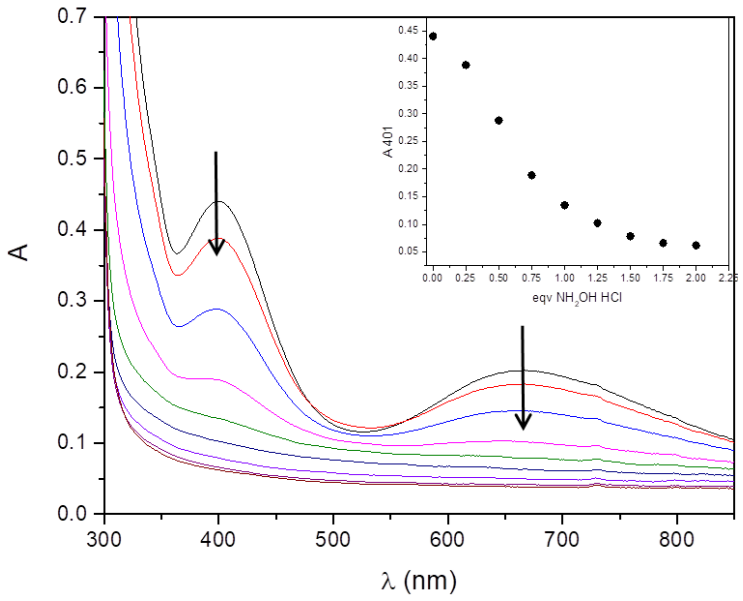

Figure 3: *Titration of the complex $[Cu_2(mXBMP-O)(CH_3COO)_2]ClO_4.(CH_3CN).(MeOH)$ with hydroxylamine hydrochloride from 0 to 2 equivalents of reducing agent. Inset: variation of the absorbance at 401 nm from 0 to 2 equivalents of reducing agent.*

2. *Aziridination catalysis tests*

In order to test the ability of the complex as nitrene transfer catalyst, aziridination catalysis was performed using styrene as substrate. The nitrene donor chosen for the reaction was PhINTs, of the family of iodinanes based on hypervalent iodine, a quite oxidizing reagent capable of generating a tosyl nitrene when activated (Figure 4).

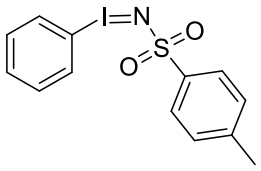

Figure 4: *Structure of PhINTs.*

The catalysis tests were performed in different conditions but following a common experimental protocol. The copper complex was dissolved in the suitable quantity of dry acetonitrile and this solution mixed with an excess of substrate, transferred on solid PhINTs, and left reacting at room temperature under argon. PhINTs is only slightly soluble in acetonitrile, so at the beginning it was suspended in the reaction mixture and solubilised during the reaction. The reaction was quenched by removing the copper complex by filtration on silica gel and evaporation of the solvent and the excess of unreacted substrate.

During the reaction the nitrene unit is transferred on the substrate, giving rise to the aziridine and tosylamine as byproduct of degradation (Figure 5, top). Moreover, in all performed experiments another product containing two tosyl moieties was observed. It was identified as the molecule N,N'-methylenebis(4-methylbenzenesulfonamide) (MBTA), already described by Stavropoulos and co-workers[27] (Figure 5, top). The origin of this product is still unknown, and in the different experiments it was observed in different ratios between 5% and 18%. The quantification of the nitrene transfer was done by ^{1}H-NMR analysis of the crude reaction mixture obtained after elimination of the metal complex. It is based on peaks of the aromatic residue of the tosyl group, which appear as two doublets forming an AX pattern. The three products have well separated peaks in this region which can be easily integrated, allowing a reliable quantification of the compounds. As it is possible to observe in the ^{1}H-NMR spectra illustrated in Figure 5, bottom, the aziridine has a couple of peaks at 7.84 ppm, tosylamine has two peaks at 7.75 ppm and MBTA has two peaks at 7.63 ppm.

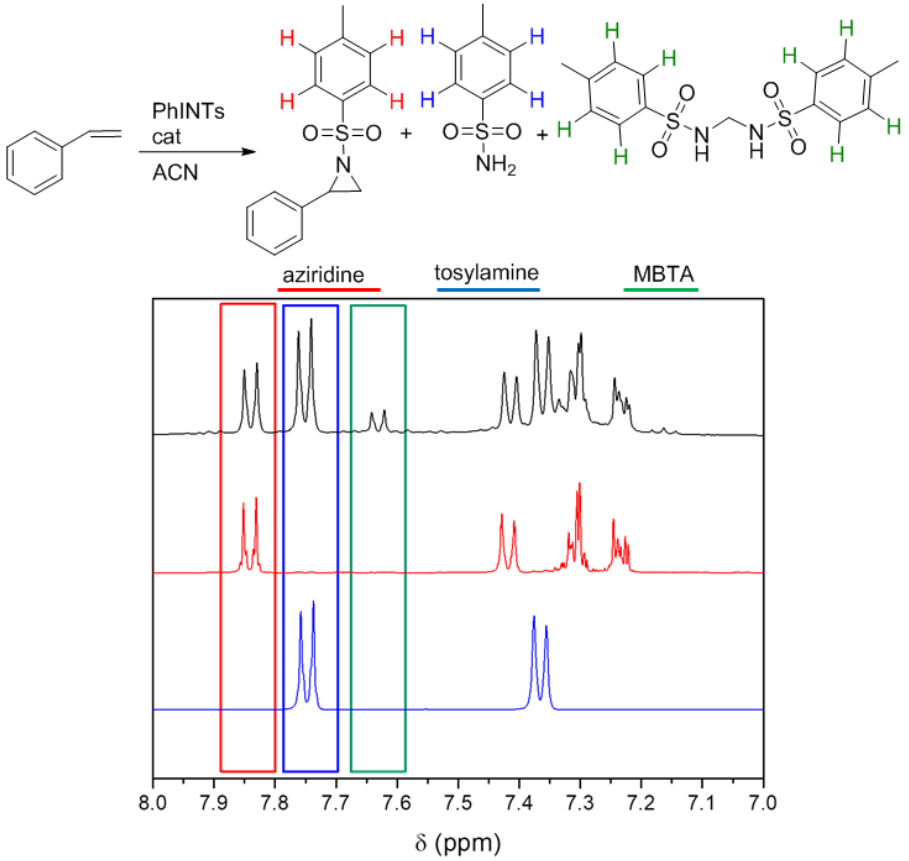

Figure 5: *Reaction of nitrene transfer on styrene with its main products (top) and their ^{1}H-NMR spectra (bottom). Blue line= spectrum of pure tosylamine, red line= spectrum of pure aziridine, black line= spectrum of crude product of catalysis with MBTA peaks highlighted in green (spectra recorded in CD_3CN).*

When doing the quantifications by integration of NMR spectra care must be taken because PhINTs can spontaneously undergo degradation to tosylamine in presence of moisture and light and a variable quantity of tosylamine is always present at the end of its synthesis or is formed during storage. Therefore the quantity of tosylamine measured by NMR analysis of the product of catalysis is overestimated and the percentage of the purity of PhINTs must be taken into account to estimate the yields of the different products. This is generally assessed by combining prior NMR analysis of PhINTs before use and catalytic test by using thioanisole as substrate and a very reactive diiron complex as catalyst. In this reaction total conversion of PhINTs is realized and the detected tosylamine is the impurity originally present. The overall uncertainty on the measured conversion and aziridine yield is estimated from previous systematic studies to 3%.

The catalysis tests have been performed using different reaction conditions, by using both the bis-Cu(II) and the bis-Cu(I) complexes. The first couple of experiments with bis-Cu(II) and

bis-Cu(I) complexes (Entries 1-2 Table 1) were performed in dry acetonitrile, with a concentration of complex of 1.3 10^{-3} M. The reduced form of the complex in experiment 2 had been generated from the same solution by adding two equivalents of solid hydroxylamine hydrochloride. Styrene and PhINTs were added in a ratio complex/PhINTs/styrene of 0.05/1/10, following the experimental protocol described above.

In experiment 1 with bis-Cu(II) complex no significant changes of the appearance of the reaction mixture were observed during the reaction. The green colour observed at the beginning did not change during the reaction; PhINTs was dissolved over the course of the reaction.

In experiment 2 with bis-Cu(I) complex the solution with the complex and styrene, colourless at the beginning, became green when it was poured on solid PhINTs. The two reactions were quenched after fifteen hours by separation of the copper complex on silica gel and the crude products were analysed by ^{1}H-NMR (solvent CD_3CN). As it is possible to read in the Table 1 (Entries 1-2) the two reactions gave substantial conversion, with a slightly better reactivity with the bis-Cu(I) complex. It is also interesting to observe that when using the bis-Cu(II) complex a non-negligible amount of MBTA is produced.

Since the bis-Cu(II) complex appeared quite long to dissolve in pure acetonitrile, a new couple of experiments with bis-Cu(II) and bis-Cu(I) complexes was performed with the addition of 1% of anhydrous DMF in the reaction mixture (Table 1, entries 3-4). Moreover, the reduction of the complex in experiment 4 was made by addition of a DMF solution of hydroxylamine hydrochloride. In fact, as stated before, the presence of an excess of reducing agent is detrimental to the reactivity and the addition of a solution instead of a solid enables a better control of the quantity added to the reaction mixture. The two reactions were performed by following the protocol described before but they were stirred at room temperature for twenty hours instead of fifteen hours.

It is interesting that in the case of bis-Cu(II) complex (Table 1, Entry 3) an improvement of both the conversion and the yield of aziridination is observed. As a consequence, in this couple of experiments the bis-Cu(II) complex has a better catalysis performance compared to the bis-Cu(I) species.

In order to test more the performance of the catalysts, some experiments with different ratios of nitrene donor and substrate were performed. Also in these cases the reducing agent for the generation of the bis-Cu(I) species had been added in DMF solution but unlike experiments 3-4 no further DMF was added in the mixture. For both the bis-Cu(II) and the bis-Cu(I) complexes two experiments with ratios Cx/PhINTs/styrene 0.025/1/10 and 0.05/1/10 as usual were carried out. The concentration of complex was of 6.2 10^{-4} M in the four cases and the reactions were left stirring for 24 hours.

Entries 5-8 of the Table 1 show that halving the amount of catalyst causes no significant change of the conversion and only a slight decrease of the aziridine yield in the case of the bis-Cu(II) complex. In addition, formation of unidentified byproducts is also observed (Entry 7). A better reactivity of the bis-Cu(II) complex is also observed in these cases.

Entry	Complex	[cx] (M)	Ratio cx/PhINTs/styrene	Time (h)	Conversion (%)	Yield aziridine (%)	Yield MBTA (%)
1	bis-Cu(II)	1.3E-03	0.05/1/10	15	58	40	18
2	bis-Cu(I)	1.3E-03	0.05/1/10	15	63	58	5
3	bis-Cu(II)	1.0E-03	0.05/1/10	20	78	70	8
4	bis-Cu(I)	1.0E-03	0.05/1/10	20	59	45	14
5	bis-Cu(II)	6.2E-04	0.025/1/10	24	73	64	9
6	bis-Cu(II)	6.2E-04	0.05/1/10	24	80	64	16
7	bis-Cu(I)	6.2E-04	0.025/1/10	24	54	46	8
8	bis-Cu(I)	6.2E-04	0.05/1/10	24	58	45	13

Table 1: *Experimental conditions of reaction in the different tests of nitrene transfer catalysis and yields of the reactions. The percentage are calculated by integration of 1H-NMR peaks and the uncertainty on these values is estimated about 3%.*

To sum up, the experiments shown that the complex is able to catalyse the nitrene transfer reaction in both the oxidised and reduced forms. With the exception of the first two experiments, in the other reactivity tests (in presence of DMF) better conversions were observed with the bis-Cu(II) species. Looking at the various experimental conditions used in the experiments, the time of reaction seems to have a small influence on the conversion rates. A lower amount of catalyst has no significant effect on the reactivity with bis-Cu(I) complex and only on aziridine yield in the case of bis-Cu(II) complex. The by-product MBTA was observed in all the performed reactions but its distribution using catalytic conditions for the moment does not allow a rationalization of the causes of its formation.

In order to better understand the reactivity of the two species, their reaction mechanisms were investigated, focusing both on studies of the interaction of the nitrene with the catalyst and on the mechanism of nitrene transfer from the active species to the substrate.

3. Study of the reaction mechanism

The complex shows a catalytic activity with both the bis-Cu(II) and bis-Cu(I) species. More detailed studies have been performed in order to better understand the catalytic mechanism. The mechanism has been studied from two points of view. On one hand the interaction of the nitrene with the copper complex has been investigated through low temperature experiments, trying to trap some active intermediate species. On the other hand, the mechanism of nitrene transfer from the active species to the substrates has been studied by competitive catalytic reactions between substituted styrenes and the use of a stereochemically sensitive substrate.

a. Study of the interaction of nitrene precursor with the complexes

1. UV-vis monitoring of the catalytic reactions

First of all the reaction of catalysis was monitored by UV-vis spectroscopy, in the hope of observing some spectral changes during the reaction. The conditions used for both the experiments with bis-Cu(II) and bis-Cu(I) complexes were the standard conditions used for the catalytic reactions studied before, with a catalyst/PhINTs/styrene ratio of 0.05/1/10.

The experiment was firstly performed by dissolving the bis-Cu(II) complex in acetonitrile, in order to have a concentration of 0.5 mM. After recording a spectrum of the complex alone (Figure 6 left, dashed black line), the suitable quantity of styrene was added, and a second spectrum collected. It is possible to notice an increase of the background of the spectrum due to the slow dissolution of styrene in the reaction mixture (Figure 6 left, dashed red line). The solution was then transferred to another UV-vis cuvette which contained the suitable quantity of PhINTs, starting the recording of spectra every five minutes for one hour (Figure 6 left, continuous lines). As stated already, this nitrene donor is not soluble in acetonitrile so in order to avoid too noisy spectra the solution was not stirred continuously.

During the monitoring with the bis-Cu(II) complex it was possible to observe that the peak at 401 nm becomes less apparent while the maximum of d-d transitions slightly moves to

higher energies, passing from 670 nm to 650 nm. The evolution seems to rapidly reach a stationary state. Since the peak at 401 nm is attributed to a charge transfer from the bridging phenolate to the copper centers, its disappearance may indicate the loss of phenoxido bridge. Since a shoulder persists in this region it is also possible that this absorption is obscured by a more intense at higher energy. So at this point it is difficult to give a firm conclusion.

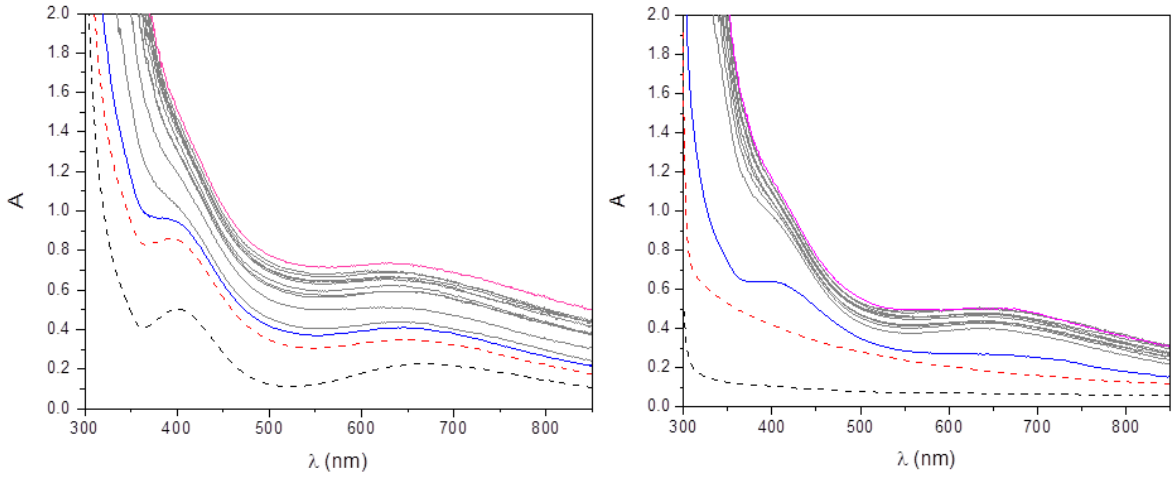

Figure 6: *Monitoring of the catalysis reaction with bis-Cu(II) (left) and bis-Cu(I) (right). Black dashed lines: complexes alone, [complex]= 4.89 10^{-4} M. Red dashed lines: complexes mixed with styrene, [styrene]= 9.8 10^{-2} M. Continuous lines: spectra recorded after the addition of 9.1 mg of PhINTs (2.45 10^{-2} mmol); each spectrum was collected after 5 minutes of reaction. Blue continuous lines: spectra collected and the beginning of the monitoring. Pink continuous lines: spectra collected at the end of the monitoring.*

The same experiment was repeated with the bis-Cu(I) species. This was generated *in situ* by reduction of the bis-Cu(II) species with two equivalents of hydroxylamine hydrochloride dissolved in DMF. The addition of the reducing agent gave rise to the complete bleaching of the solution of complex (Figure 6 right, dashed black line). The suitable quantity of styrene was added to the solution, which was then transferred to the UV-vis cuvette containing PhINTs, and the reaction was monitored for one hour by recording a spectrum every five minutes (Figure 6 right, continuous lines).

The observed situation was not very different from the one of the previous case; when the solution with the reduced complex and styrene was added to solid PhINTs, it immediately turned from colourless to green, with the appearance of the bands at 410 nm and 650 nm, consistent with the oxidation of copper centers. Also the following spectral evolution of the solution seems similar to the previous study, with only a difference in the intensity of the

spectra, which are less intense in this second case. This can be due to experimental reasons, because as described before, PhINTs is not soluble in the reaction mixture, so its presence as suspension can affect the UV-vis spectrum. Another reason can be the fact that in the second case not all the Cu(I) was oxidized when PhINTs was added, resulting in less intense absorptions. These first two experiments revealed important similarities in the catalytic behavior of the bis-Cu(II) and bis-Cu(I) complexes, but at this stage it is not possible to state if the two complexes have similar reaction mechanism.

In order to better investigate the reaction pathways of the two species, low temperature experiments without substrate were performed. The goal of these experiments was the observation of the initial interaction between the complex and the nitrene donor. The experiments were in general performed in absence of substrate and using a stoichiometric quantity of nitrene donor. This requires that the reaction is performed in a homogenous phase which precludes the use of the poorly soluble PhINTs. For this reason, the nitrene donor used in these experiments was ArINTs (Figure 7) which has a moderate solubility in acetonitrile even at low temperature.

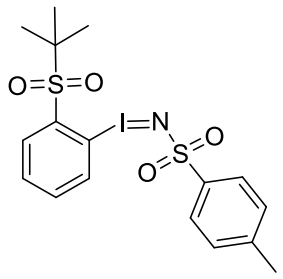

Figure 7: *Structure of ArINTs.*

2. UV-vis study of the interaction of bis-Cu(II) complex with nitrene precursor

The experiment was firstly performed with the bis-Cu(II) complex, by adding one equivalent of nitrene donor dissolved in acetonitrile to a solution 3 10^{-4} M of the complex. The reaction was monitored by UV-vis for 30 minutes, by recording a spectrum every 20 s. The same procedure was repeated at three different temperatures: -30°C, -15°C and room temperature.

As it is possible to notice in Figure 8, in the three cases the addition of ArINTs did not have dramatic effects on the UV-vis spectra of the system. It is possible that the system reacts too fast even at low temperature and has returned to its original state. Alternatively, 1 eqv. of

ArINTs may not be enough to ensure binding and an excess is needed. The system has not yet been further investigated.

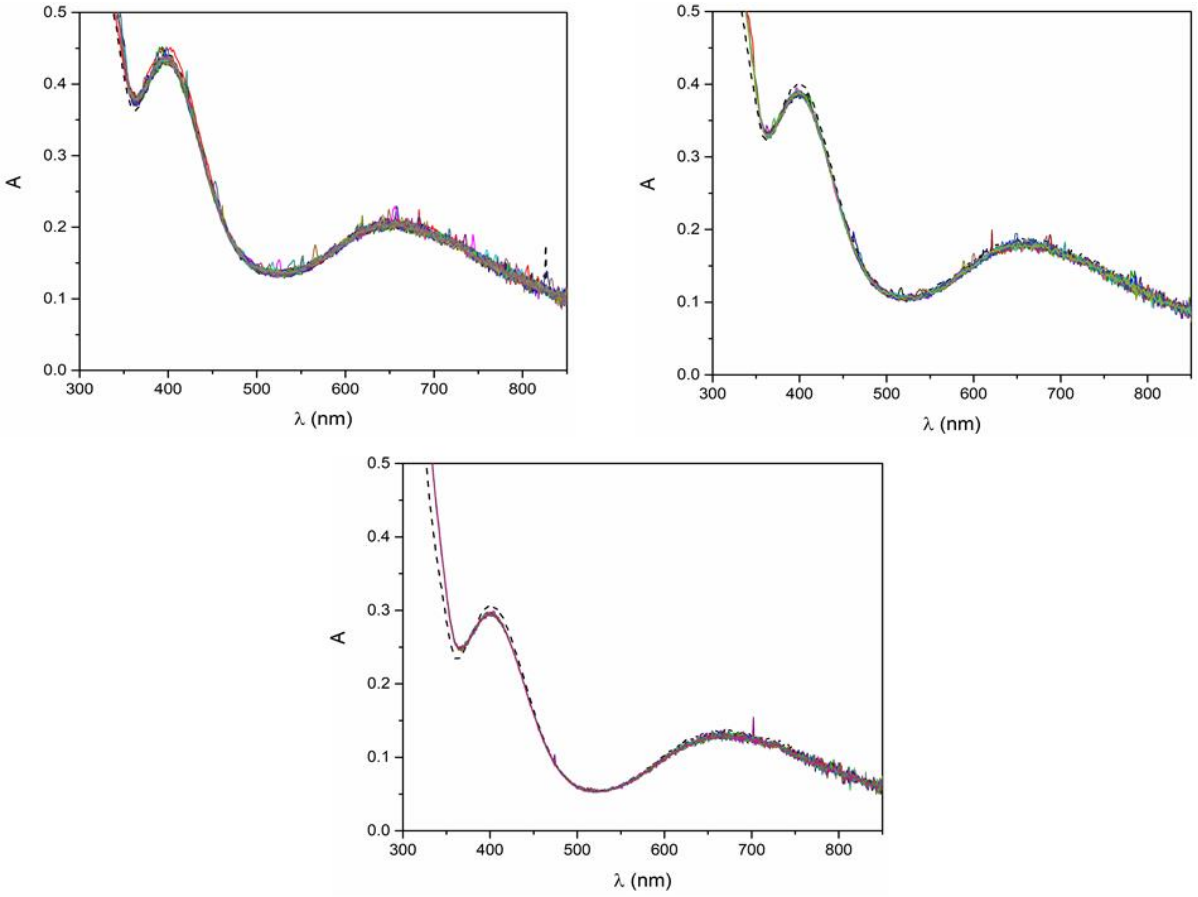

Figure 8: *UV-vis monitoring of stoichiometric reaction between bis-Cu(II) and ArINTs. Top, left: T= -30°C. Top, right: -15°C. Bottom: room temperature. Dashed black lines: spectra of the starting bis-Cu(II) complex, [complex]= 3.4 10^{-4} M. Continuous lines: spectra recorded after the addition of ArINTs; each spectrum was collected every 20 s for 30 minutes.*

3. Spectroscopic study of the interaction between bis-Cu(I) complex and nitrene precursor

- UV-vis spectroscopy

The experiment was then repeated with the bis-Cu(I) complex. As for the catalysis reactions described above, the reduced form was generated by reducing a 3 10^{-4} M solution of the oxidized complex in acetonitrile with two equivalents of hydroxylamine hydrochloride dissolved in dry dimethylformamide. Once the complex was completely reduced, this was put reacting with one equivalent of ArINTs dissolved in acetonitrile and the reaction was followed for 20 minutes, by recording a spectrum every 15 s. As in the experiment with the bis-Cu(II) complex, the reaction was monitored at -30°C, -15°C and room temperature.

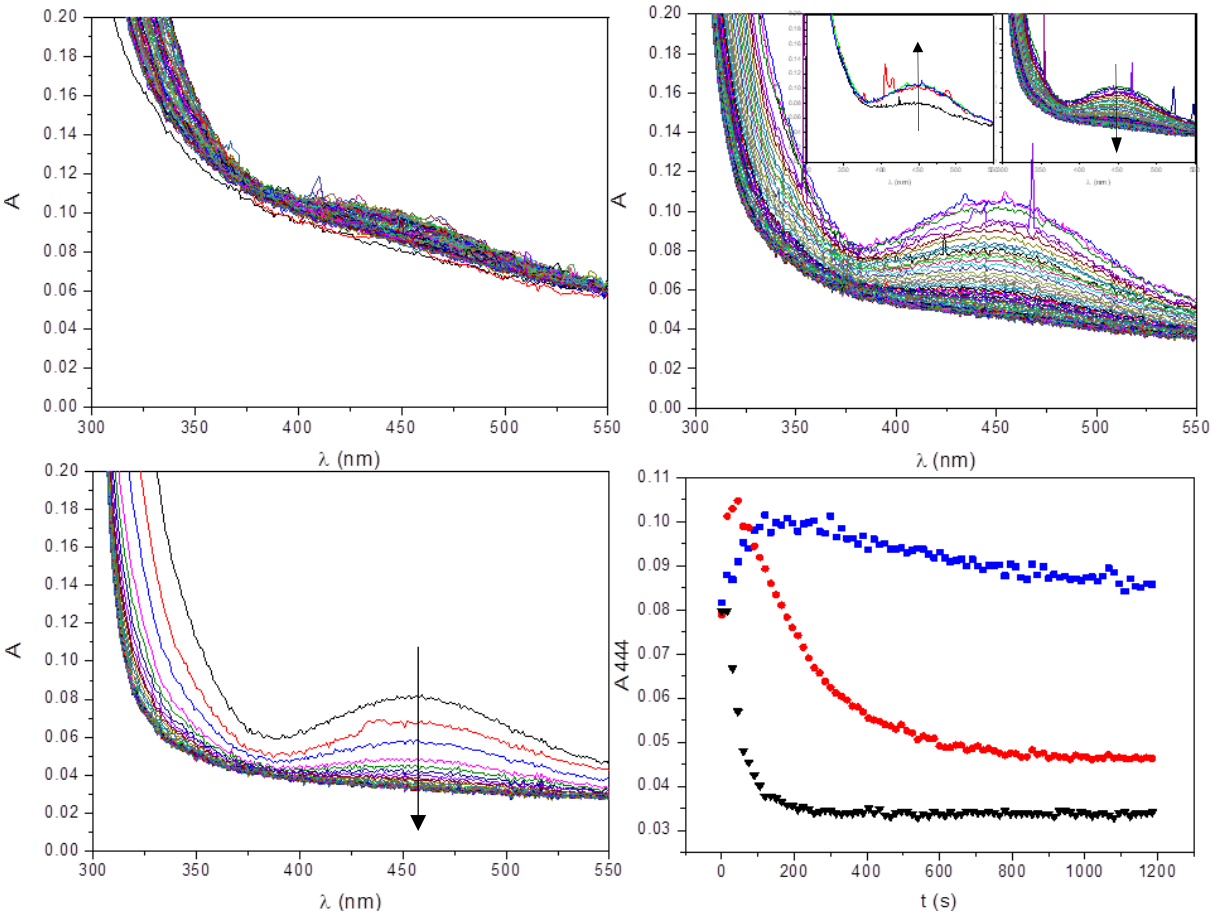

Figure 9: *UV-vis monitoring of the reaction of the bis-Cu(I) ([complex]= 3.42 10^{-4} M) with a stoichiometric quantity of ArINTs (each spectra was collected every 15 s for twenty minutes in the three experiments). Top, left: T= -30°C. Top, right: -15°C (inset: detail of the increasing and decreasing phases). Bottom, left: room temperature. Bottom, right: variation of the absorbance at 444 nm (Blue squares: T= -30°C. Red circles: T= -15°C. Black triangles: room temperature).*

In the three cases it is possible to observe the apparition of a peak at 444 nm which disappears during the monitoring (Figure 9). At the end of the monitoring the solution in the cuvette appeared colourless which indicates that the species has been reduced back to the bis-Cu(I) state. The formation and the disappearance of the peak at 444 nm were strongly temperature dependent (Figure 9, bottom right). Whereas at room temperature only its disappearance is detected, at -15°C it reaches the maximum at around 45 s before decreasing with a half-life of 200 s. At -30°C the peak increases over the first 100 s and stays for the next 200 s before slowly losing intensity.

Since the absorption peak at 444 nm is in the region of the charge transfer transitions phenoxido → Cu(II), it is likely that the addition of the nitrene donor provoked an oxidation of the complex which then underwent reduction. In order to have some insights about the

involved species, an EPR monitoring of the reaction made at -30°C had been performed. Samples were collected after 150 s, 300 s and 1200 s of reaction (see below).

In order to investigate the further fate of the reaction, a second equivalent or ArINTs was added at the end of the reaction at -30°C, and the evolution was monitored by recording spectra every 15 seconds (Figure 10, left). It is possible to observe also in this case the formation of a peak at 444 nm but here it accumulated during time instead of decomposing (Figure 10, right). This made the species of particular interest because it allowed further studies for its identification. The product obtained after twenty minutes was analysed by EPR spectroscopy and by mass spectroscopy, in order to have a better idea of the products obtained during the reaction.

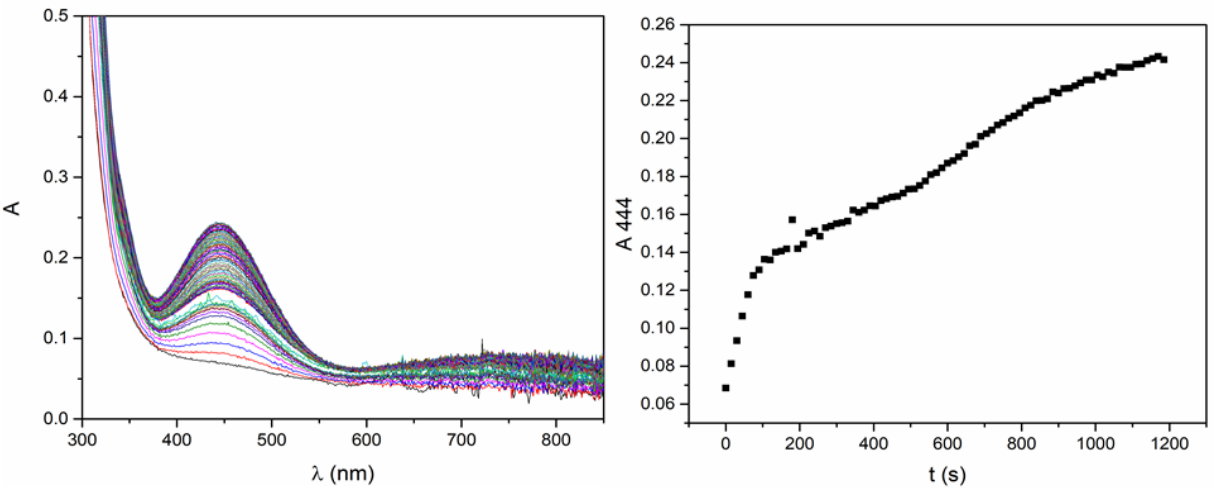

Figure 10: *UV-vis monitoring of the reaction after the addition of a second equivalent of ArINTs at -30°C ([complex]= 3.42 10^{-4} M). Left: spectra collected every 15 s for twenty minutes. Right: variation of the absorbance at 444 nm during the experience.*

The spectra obtained after the addition of the second equivalent of nitrene donor is quite similar even if more intense than the transient spectrum observed after addition of 1 eqv. of ArINTs. This suggests that the same species are generated but after the addition of one equivalent of ArINTs they are not stable for a long time whereas they accumulate when a second equivalent of ArINTs is added. The spectra recorded after the addition of 1 eqv. of ArINTs account for both the formation and the decomposition of this species. In particular, spectra recorded at -30°C show that the two reactions reach a stationary state before 300 s and then the reaction of decomposition overcomes on the formation of the active species.

- EPR spectroscopy

In order to get more insights about the species generated during the reaction of the catalyst with the nitrene donor, samples for EPR analysis were collected during the UV-vis monitoring at -30°C, frozen in liquid nitrogen and analysed by EPR. Samples for the study of the reactivity with the first equivalent of ArINTs were collected before the addition of the nitrene donor, after 150 s of reaction, after 300 s and after 1200 s, at the end of the UV-vis monitoring. As it is possible to observe in Figure 11, the spectrum recorded before the addition of ArINTs (light blue) is not well defined and large, indicating some traces of Cu(II) present after the reduction, not detected by UV-vis spectroscopy. After the addition of ArINTs it is possible to observe an interesting evolution. Spectra recorded after 150 s (green spectrum) and 300 s of reaction (red spectrum) are superimposable and show the presence of at least to components with slightly different hyperfine constants. The two components of the spectra are stable for 300 s, but the component with smaller $g_{\parallel}$ has completely disappeared at the end of the monitoring, while the other with higher $g_{\parallel}$ is still present, even if it has lost intensity (blue spectrum).

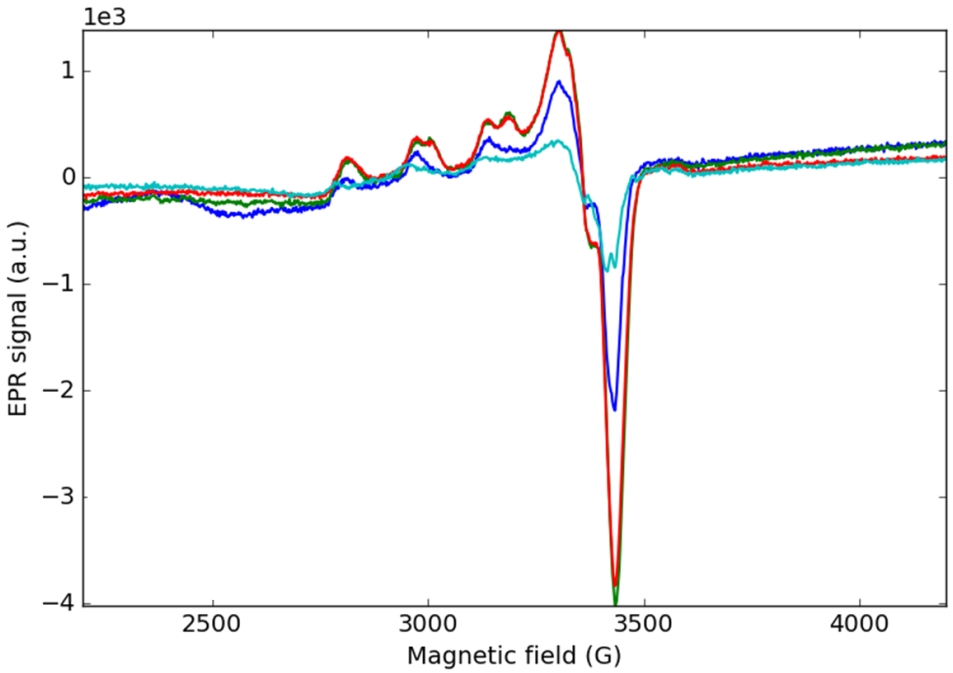

Figure 11: *EPR spectra recorded during the monitoring of the reaction between bis-Cu(I) complex and 1 eqv. of ArINTs (T= 10 K, P= 33 dB, solvent= acetonitrile/0.2% DMF). Light blue= bis-Cu(I) species before the addition of ArINTs, green= after 150 s of reaction, red= after 300 s of reaction, blue= after 1200 s of reaction.*

This behaviour suggests the formation of two paramagnetic copper centers in roughly equal amounts, one reacting faster than the other. In order to verify this hypothesis the spectra of these two species were simulated and their contribution to the experimental spectrum evaluated. The individual spectra of the two species were simulated, then the spectrum after 300 s of reaction was simulated by assuming that the two species are present at the same concentration in the sample. As observed in Figure 12, the simulated spectrum (light blue) matches with the experimental spectrum recorded after 300 s of reaction at -30°C, what consequently validates the simulation of the individual components. This suggests that after the addition of ArINTs Cu(I) is oxidised, with the formation of two Cu(II) species, which react at different rates. Since the starting complex is binuclear, the two different species can be the two copper centers that interact in a different way with the nitrene.

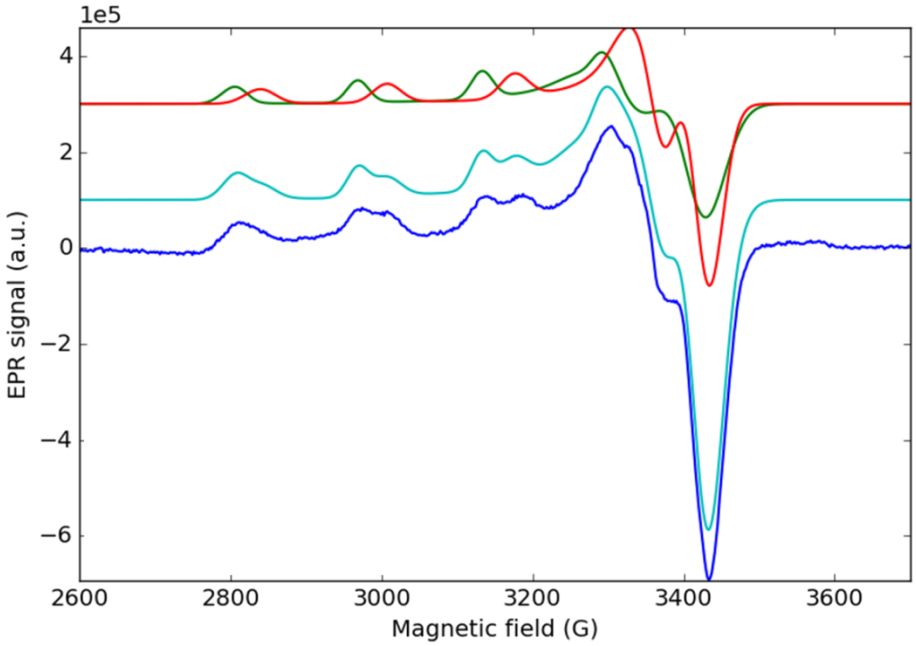

Figure 12: *Simulation of EPR spectra of the reaction of bis-Cu(I) complex with 1 eqv. of ArINTs after 300 s. Green, red= simulated spectra of the two species, light blue= simulated spectrum with the contribution of the two species, blue= experimental spectrum of the sample collected after 300 s of reaction (T= 10 K, P= 33 dB, solvent= acetonitrile/0.2% DMF).*

EPR analysis was performed also after the addition of the second equivalent of ArINTs to the reaction mixture. Since the UV-vis analysis shown the accumulation of a species over all the monitoring, a single sample was collected after 1200 s, at the end of the monitoring, and analysed in the same conditions as the other samples. The obtained spectrum (Figure 13, blue line) appears more complex than the ones previously recorded. It suggests the presence

of several components with close g values and it is difficult to state the presence of the same species observed after the addition of 1 eqv. of ArINTs (Figure 13, green line). Also in this case it is possible to affirm that the addition of ArINTs causes an oxidation of the complex. In this case the formed species seem stable for the time of the monitoring and they are not consumed. The formation of stable species at -30°C enabled their analysis by mass spectroscopy.

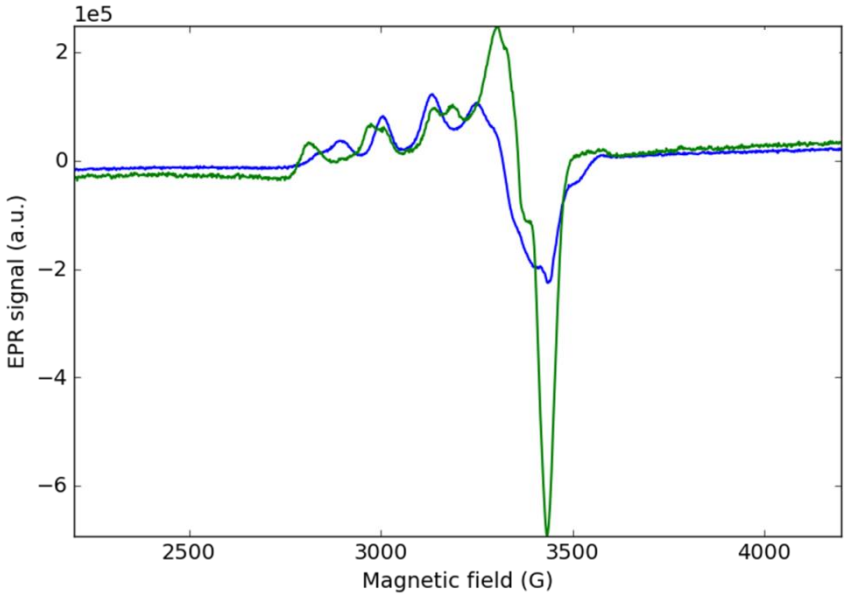

Figure 13: *EPR spectra recorded after 300 s of reaction between the complex bis-Cu(I) and 1 eqv. of ArINTs (green line) and after 1200 s of reaction after the addition of a second equivalent of ArINTs (blue line). (T= 10 K, P= 33 dB, solvent= acetonitrile/0.2% DMF)*

Samples of the reaction mixture obtained after the addition of a second equivalent of ArINTs at -30°C were analysed by electrospray ionization mass spectrometry in different experiments. They shown a complex situation, in which it is possible to find some hints about the different species formed during the reaction. Firstly, in all the observed species the entity Cu_2(mXBMP-O) is present and it indicates that the complex unit is always present in the active species. Several peaks were observed that revealed the presence of a "NTs" group in the corresponding species. Figure 14 shows a full spectrum of the solution (top) and zooms on the experimental (center) and theoretical (bottom) isotopic patterns of the peaks observed at m/z = +727 and +879, respectively.

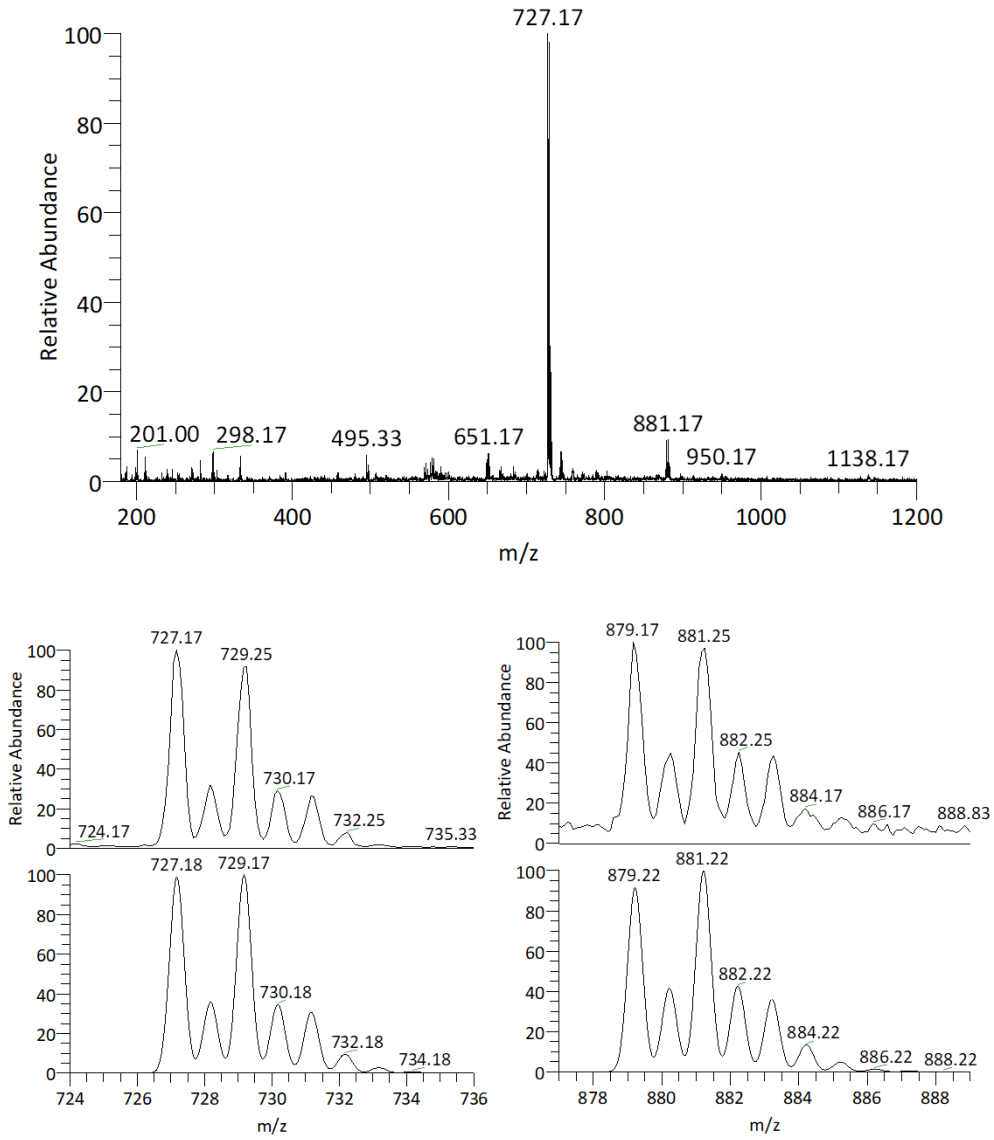

Figure 14: *ESI-MS analysis of the product obtained after the addition of 2 eqv. of ArINTs. Top: full spectrum. Center: experimental isotopic patterns of m/z= +727 and m/z= +879. Bottom: theoretical isotopic patterns.*

The almost perfect match of the isotopic patterns lends credence to the assignments which are reported in Figure 15. The "727 species" comprises an acetate anion and an acetonitrile in addition to a tosylamidate $TsN(H)^{2-(-)}$ and the formula of this monocation is consistent with a dicopper(II) species. The possibility that this species comprises a Cu^{III}=NTs entity and a protonated ligand is unlikely. Several potential structures are illustrated in FIgure 15 (top); they vary in the arrangements of the various ligands: (i) a tosylamidate bridge as in the Cu^{II}-(μ-NTs)-Cu^{II} unit with terminal acetate and acetonitrile, the resulting neutral molecule being protonated; (ii) a bridging acetate, with terminal NHTs and acetonitrile, the resulting molecule being a monocation; (iii) and (iv) a bridging (or chelating) tosylacetamidate with a

bridging (or chelating) acetate (see below). The "879 species" has lost the acetate and contains two tosylamidates and two acetonitrile molecules. Again, the formula corresponds to a dicopper(II) species, and possible structures are represented on Figure 15 bottom.

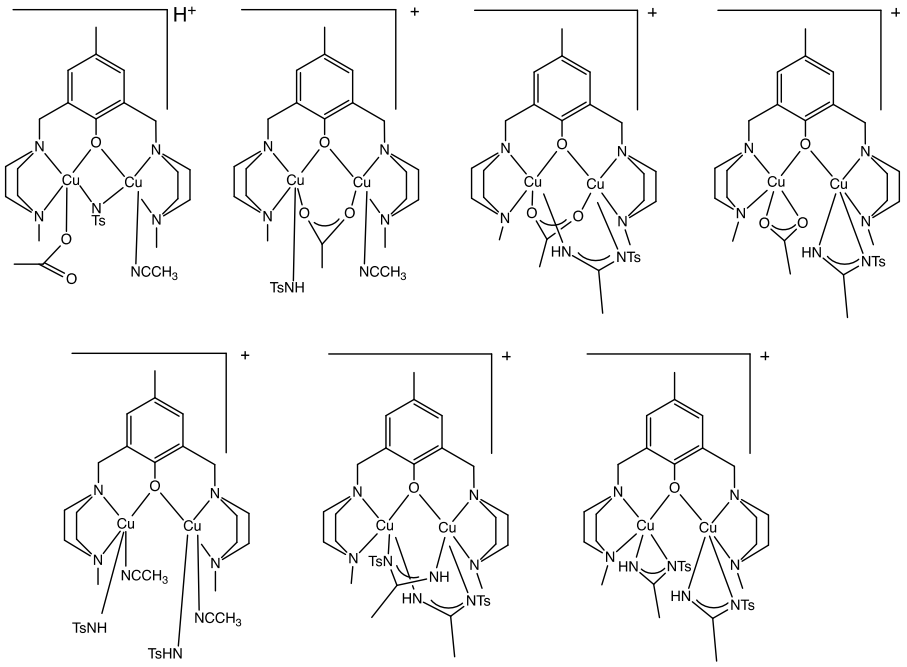

Figure 15: *Schematic representations of the "727 species" (top) and "879 species" (bottom).*

It must be noted that the detection of acetonitrile ligands in these species is uncommon because in most cases solvent molecules are eliminated in the conditions of ESI-MS recording. A possible explanation can be found in the recent observation by Warren and colleagues[36] that acetonitrile can react reversibly with a nitrene in the copper coordination sphere to give an amidinate (Figure 16):

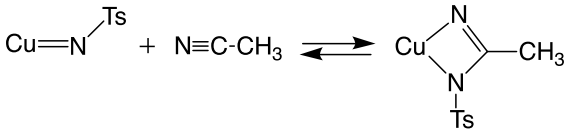

Figure 16: *Formation of the amidinate proposed by Warren and co-workers.*

The presence of a chelating or bridging tosylamidinate in both species thus appears a possible alternative which is depicted in Figure 15. Its occurrence twice in the "879 species" would be surprising nevertheless. It is thus difficult to reach a firm conclusion on this point at the moment. By contrast it can be safely assumed that in both species the nitrene group "NTs" has been transformed in an amidinate "NHTs" probably through $H^{\bullet}$ abstraction. Several potential $H^{\bullet}$ donors can be envisaged: the ligand itself through benzylic or methyl

groups or the acetonitrile solvent. The MS analyses did not provide any evidence for tosylamination of the ligand. By contrast, several fragments could be assigned to monocopper complexes and evidenced the loss of a complexing branch, a process that can be initiated by benzylic oxidation. Whether they are true species in solution or result from a fragmentation process is not clear at the moment. Finally, $H^{\bullet}$ abstraction from acetonitrile must be considered also.

b. Study of nitrene transfer on substrates

1. Use of stereosensitive substrates

As described in the introduction of this chapter, the metal-nitrene intermediate can exist in the singlet form “Cu=NR” and in the triplet form "$Cu^{\bullet}$-$^{\bullet}NR$". The two intermediates give rise respectively to a concerted nitrene transfer on styrene or a stepwise mechanism, with the formation of a radical intermediate. In order to have an idea about the involved mechanism, catalytic tests with stereoselective substrates can be performed. In these studies catalytic aziridination of cis-stilbene with both bis-Cu(II) and bis-Cu(I) was performed. If the mechanism is concerted only the *cis*-aziridine can be formed, while a stepwise mechanism gives rise to a radical intermediate, with the loss of the stereochemical information and the formation of a mixture of *cis* and *trans* isomers (Scheme 2).

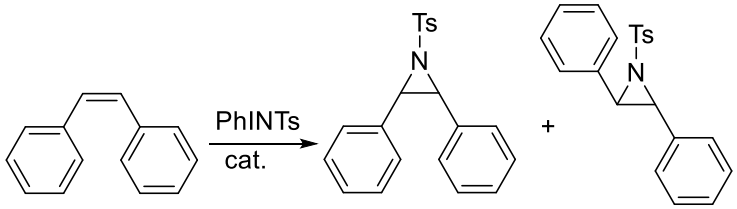

Scheme 2: *Possible products of aziridination of cis-stilbene.*

The catalytic tests were performed by using a ratio complex/PhINTs/*cis*-stilbene of 0.05/1/10 and by applying the experimental procedure already described for the catalytic tests of aziridination of styrene (the applied protocol for the bis-Cu(II) complex corresponds to Experiment 6, for bis-Cu(I) complex to the Experiment 8 of the aziridination of styrene tests). The ratio between the *cis* and *trans*-aziridine was estimated by ^{1}H-NMR of the crude products. As it is possible to observe in Table 2, with both bis-Cu(II) and bis-Cu(I) catalysts a mixture of the two stereoisomers was produced, indicating the occurence of a stepwise mechanism. However, the cis/trans ratio of the product differs significantly: ~ 3/1 for the bis-

Cu(II) and for the bis-Cu(I) only ~ 1/1. This ratio depends on the lifetime of the radical intermediate, or in other words on the competition between the closure of the aziridine ring and the configuration inversion. This difference can thus be taken as suggestive that the two catalyst operate on distinct mechanisms. However, it must be kept in mind that different steric hindrance to the inversion configuration for the two catalysts can affect this ratio also.

Entry	Complex	% *cis*-aziridine	% *trans*-aziridine
1	bis-Cu(II)	77	23
2	bis-Cu(I)	54	46

Table 2: *Ratio of cis/trans products of aziridination of cis-stilbene. See text and experimental section for reaction conditions.*

2. Competition experiments

In order to get more insights on the mechanism of nitrene transfer, substrate competition tests were performed. In this kind of experiments it is assumed that, in the same reaction, substrate that reacts faster gives rise to a higher amount of product of aziridination. By putting equimolar quantities of different p-substituted styrenes with styrene it is possible to evaluate the ratio between their products of aziridination and build the Hammett plots. In these plots the logarithm of ratio between the kinetic constants of the formation of p-substituted aziridine (k_R) and aziridine derived from styrene (k_H) is plotted vs. one or more parameters. They mainly take into account the polarity effects due to the presence of different p-substituents and effects of radical delocalization. In a concerted mechanism the presence of different p-substituent on styrenes strongly influences the conversion to aziridine. Styrenes with electron-withdrawing substituents are less prone to react with nitrene; as a result, a competition test with styrene results in a low ratio between the p-substituted aziridine and the aziridine derived from styrene. By performing competition reaction in presence of different p-substituted styrenes an important variation in the ratio should be observed passing from electron-withdrawing substituent to electron-donor substituents and the Hammett plot should show a linear dependence of these ratios by a single parameter of polarization effect. As described in the introduction of the chapter, examples of pure concerted mechanism are rare in literature and in the majority of the systems a mixture of concerted and stepwise mechanisms. As a result, for Hammett

correlation the single parameter of polarization effect is no more sufficient and a second radical delocalization parameter is introduced.

Competition experiments were performed for both the bis-Cu(II) and bis-Cu(I) complexes. The applied experimental protocol was the same used for the reactions with cis-stilbene but in this case the catalyst/PhINTs/substrate ratio took into account the presence of an equimolar quantity of two substrates, so the applied ratio for all the competition reaction was 0.05/1/5/5 catalyst/PhINTs/styrene/p-substituted styrene. The ratio between the different aziridines was evaluated by ^{1}H-NMR. In this case the quantification of the products was made in the aliphatic region of the spectra (Figure 17). Protons in this region are more affected by the presence of p-substituents and their peaks are better separated than the aromatic peaks previously used for the quantification of the yield of aziridination.

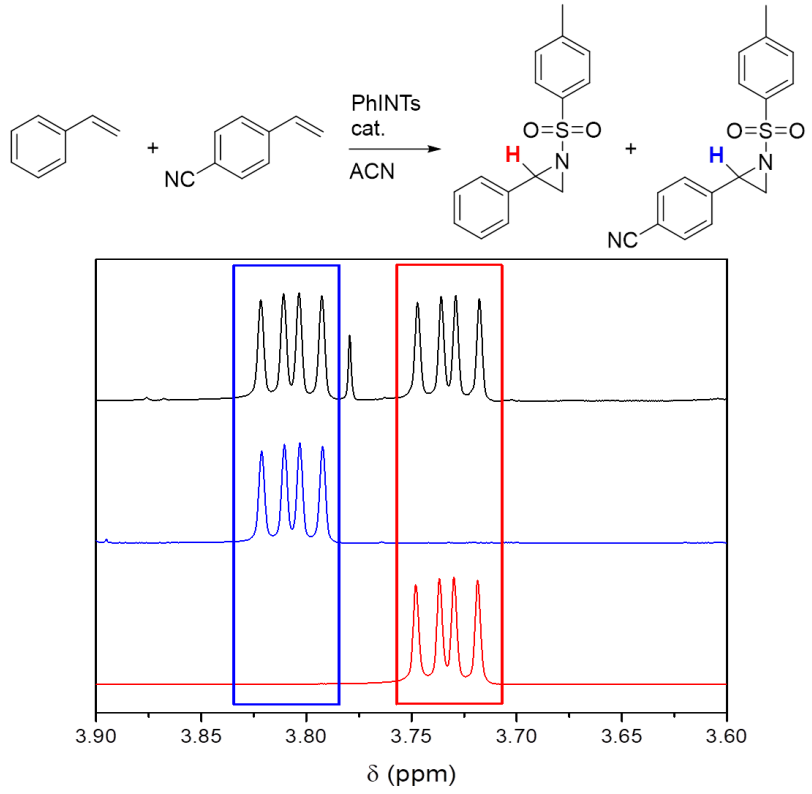

Figure 17: *Example of competition reaction (top) and ^{1}H-NMR peaks used for the quantifications (bottom). Red line= aziridine X= H, blue line= aziridine X= CN, black line= example of product of competition reaction. Solvent: CD_3CN*

Bis-Cu(II) complex		
Entry	**X**	**Ratio X/H aziridine**
1	NO_2	2.22
2	CN	1.12
3	CF_3	1.02
4	Cl	1.45
5	Me	1.35
6	OMe	1.78

Table 3: *Results of the competition reactions with the bis-Cu(II) complex. See text and experimental section for reaction conditions.*

Bis-Cu(I) complex		
Entry	**X**	**Ratio X/H aziridine**
1	NO_2	1.46
2	CN	1.08
3	CF_3	1.03
4	Cl	1.38
5	Me	1.51
6	OMe	1.67

Table 4: *Result of the competition reaction with the bis-Cu(I) complex. See text and experimental section for reaction conditions.*

Tables 3 and 4 list the results of the competition experiments in the form of the ratios of the yields of the aziridines of the substituted styrenes *vs*. that of styrene itself and Figure 18 presents the plot of these data as the logarithm of this ratio (which is assimilated to that of the corresponding rate constants $\log(k_X/k_H)$ against the parameter σ^+ which accounts for the polarity effect of the p-substituents of the styrenes. No linear correlation is apparent and none can be obtained by including a second parameter accounting for a radical delocalization (σ_{jj}, dual correlation). At this stage three observations can be made: i) the bis-Cu(II) and bis-Cu(I) catalysts seem to behave in the same way, ii) the overall electronic influence of the substituents is weak, iii) all the substituted styrenes are more reactive than styrene itself. The significance of these preliminary observations will be assessed in the following paragraph.

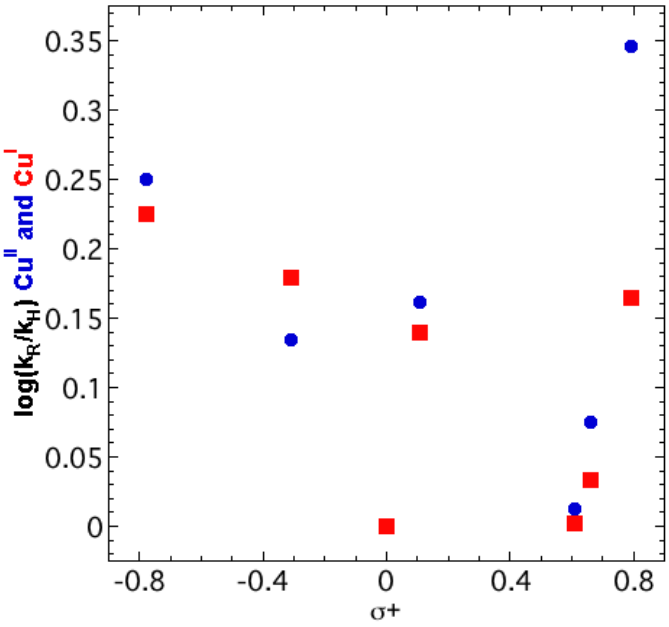

Figure 18: *Hammett plots of log(k_R/k_H) vs. parameter σ^+. Blue circles= bis-Cu(II) complex, red squares= bis-Cu(I) complex.*

c. Discussion of results

In this section we will try to explain the various observations that we made with both bis-Cu(II) and bis-Cu(I) systems. We will consider successively: i) the interaction of the nitrene donor with the copper species, and ii) the nitrene transfer to the substrates.

1. Literature on copper-nitrene complexes

The observation of efficient nitrene transfers catalyzed by copper salts and complexes (especially Cu(I) species) has motivated several groups to try and isolate Cu-nitrene intermediates active in nitrene transfer reactions. A major effort was due to the group of Warren who reacted several organic azides R-N_3 with Cu^I-β-diketiminates[37–39]. They were able to isolate a series of dicopper-nitrene complexes of general formula $(LCu)_2$(μ-NR) with L= substituted β-diketiminate, R= aryl or adamantyl. They shown by variable temperature ^{1}H-NMR experiments that this species is in equilibrium with a mononuclear Cu^{III}=NR species which is the true active species (Figure 19)[37].

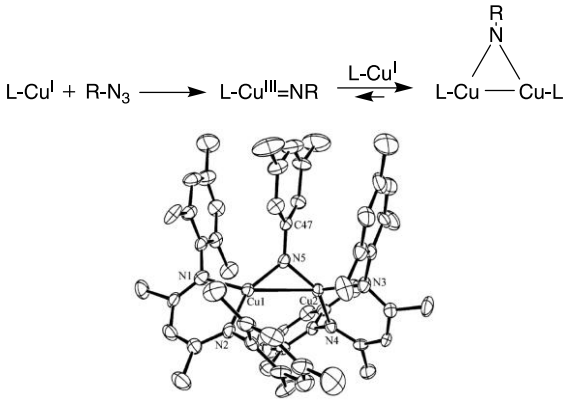

Figure 19: *Formation of Cu-nitrene species (top) and representation of the X-ray structure of a bis-copper phenylnitrene (bottom)*[37]*.*

These mononuclear Cu(III)-nitrene species are very elusive and the group of Ray succeeded in stabilization one of it by binding to an acidic metal Sc^{3+} (Figure 20, top)[40]. Alternatively and elegantly they used an azide embedded in a tris-nitrogen macrocycle: reaction of a Cu(I) salt with this reagent afforded a copper-nitrene stabilized by binding to four nitrogen within the macrocyclic. Extensive studies led to propose a Cu(II)-$^{\bullet}$NAr electronic structure (Figure 20, bottom)[41].

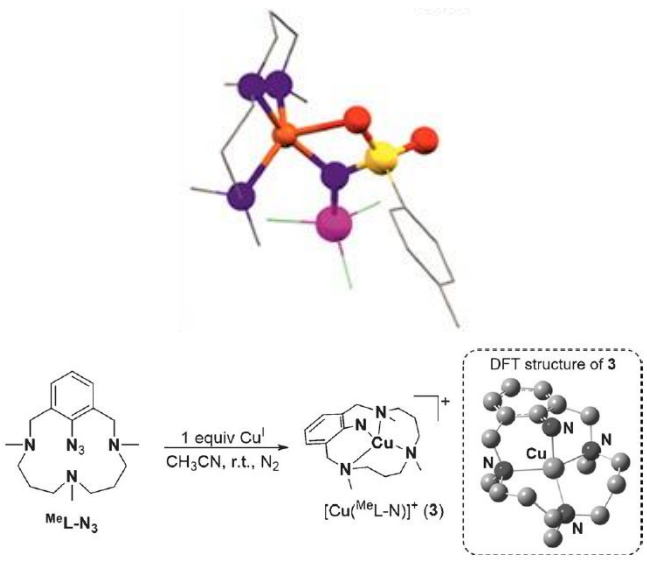

Figure 20: *Representation of the X-ray structure of a Sc^{3+} adduct of a copper nitrene (top)*[40] *and of the DFT optimized structure of a copper nitrene embedded in a macrocycle (bottom)*[41]*.*

The last examples of structurally characterized copper-nitrenes are due to Bertrand and colleagues who reported a series of mononuclear and binuclear complexes using strongly encumbered phosphonitrenes (Figure 21)[42]. Anchoring the nitrene to a phosphorus atom stabilizes it and the steric bulk on the phosphorus further limits potential intermolecular

interactions. Of course this derivations are likely to be detrimental to the reactivity in nitrene transfer reactions.

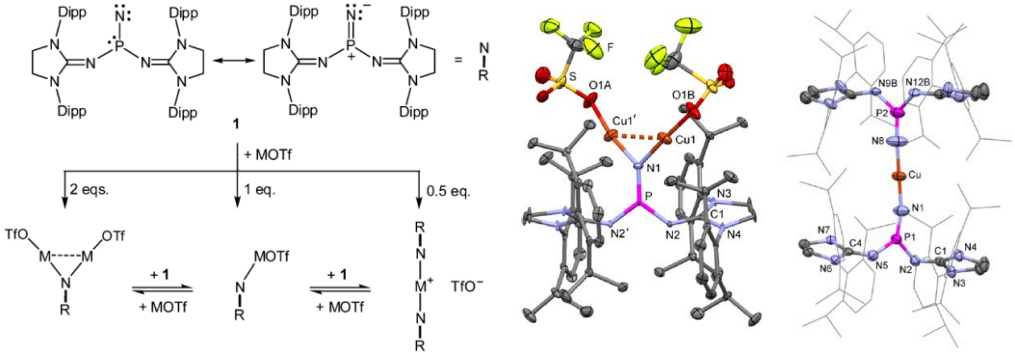

Figure 21: *Representation of the X-ray structure of copper phosphonitrenes*[42].

2. *Interaction copper-nitrene*

a. Interaction of bis-Cu(I) complex with nitrene precursor

The UV-vis spectroscopic monitoring of the reaction revealed a complex phenomenon involving successively the growing and the decrease of the 444 nm absorption after the addition of 1 eqv. of ArINTs and its regeneration after addition of a second equivalent of nitrene donor. According to the literature, possible explanations of this behavior are illustrated in Scheme 4. In path (a) the copper(III)-nitrene is trapped by a copper(I) starting species as was observed by Warren and co-workers[37–39] and Bertrand and coll.[42] and the resulting species is an amido-bridged dicopper(II) complex. In path (b) copper(III)-nitrene is trapped by H atom abstraction from a ligand or solvent molecule and ends up as a tosylamido Cu(II) compound.

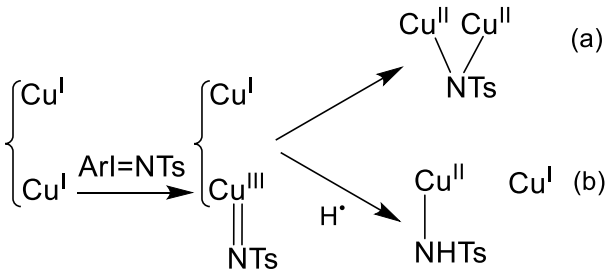

Scheme 3: *Formation and degradation of a copper-nitrene species.*

Neither of these processes is consistent with our experimental observations:

- the EPR spectrum of the first intermediate reveals the presence of Cu(II) species;
- the disappearance of this species is associated to a bleaching of the solution suggesting the formation of a Cu(I) species; this is supported by the disappearing of the EPR spectrum

To account for the above observations we propose the following scheme (Scheme 5):

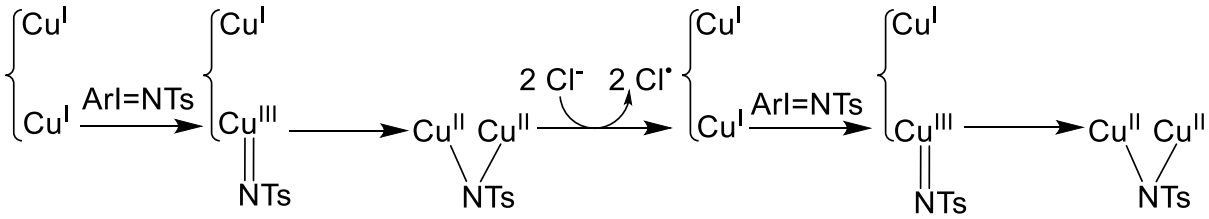

Scheme 4: *Main species involved in an alternative mechanism of formation and consumption of copper-nitrene species.*

This can be explained by taking into account the presence of chloride anions coming from the hydroxylamine hydrochloride used for the *in situ* generation of the bis-Cu(I) complex. These are quite easily oxidized, so the active species generated after addition of the first equivalent of ArINTs can react with chlorides, with the generation of radical species which fast decompose and the regeneration of the bis-Cu(I) complex. The addition of the second equivalent of ArINTs regenerates the active species that this time cannot react anymore with chlorides and it accumulates over time. According to this mechanism the first process that is detected by UV-vis at low temperature is the decomposition of the very reactive Cu(III)=NTs species by hydrogen abstraction. That the final (regenerated) species is a phenoxido-Cu(II)-tosylamido compound is consistent with the spectroscopic observations:

- presence of a phenoxido → Cu(II) charge transfer transition and d-d absorption
- typical Cu(II) EPR spectrum
- ESI-mass spectrum dominated by a peak assigned to $[Cu_2(mXBMP\text{-}O)(CH_3COO)(NHTs)(CH_3CN)]^+$ or $\{ [Cu_2(mXBMP\text{-}O)(CH_3COO)(NTs)(CH_3CN)] H\}^+$

Interestingly, this species is able to oxidize chloride anions, so it can be envisioned that it may transfer a “NTs” group through an electron transfer mechanism. This possibility will have to be checked on very oxidizable substrates, such as p-methoxythioanisole.

b. Interaction of bis-Cu(II) complex with nitrene precursor

As mentioned in the introduction of this chapter, the interaction of Cu(II) complexes with nitrene precursors is less well understood. UV-vis monitoring of the stoichiometric interaction between the bis-Cu(II) complex and ArINTs shown so small changes that a redox reaction can be excluded. Moreover, even the binding of the iodinane to the copper is not warranted. By contrast, the UV-vis spectra recorded during the catalytic reaction evidence a shift of the d-d transitions from 670 nm to 650 nm, which is consistent with the binding of the iodinane. Therefore 1 eqv. of iodinane may not be sufficient to displace the acetate anions which coordinate the copper centers. Alternatively, it can not be totally excluded that the bulkiness of the aryl substituent $tBuSO_2$ hinder the binding of the iodinane.

3. Interaction with the substrate

As already mentioned in the introduction of the chapter, Hammett correlations are commonly used to investigate aziridination mechanisms through competition experiments. An overall trend associating an increase of the reactivity to the most electron-donating substituents is generally observed in agreement with the nitrene species being electrophilic. When this electronic influence is less pronounced, inclusion of a term accounting for radical delocalization is necessary to build a linear dual-correlation[30], as found for some copper catalysts[26,27,43]. However, with our competition data no linear correlation can be obtained with the classical polarity parameter or through the dual correlation including both polarity and delocalization effects. As depicted in Figure 22, our data both for bis-Cu(II) and bis-Cu(I) clearly show two distinct behaviors: a moderate decrease of the reactivity when the substituents become less electron-donating, what is expected, and a strong increase when the electron withdrawing effect increases from p-CF_3 to p-CN to p-NO_2. An approximately linear correlation can be found in the "donating domain", whereas that of the "withdrawing domain" is excellent. This overall behavior suggests a change of mechanism with the electronic influence of the substituents.

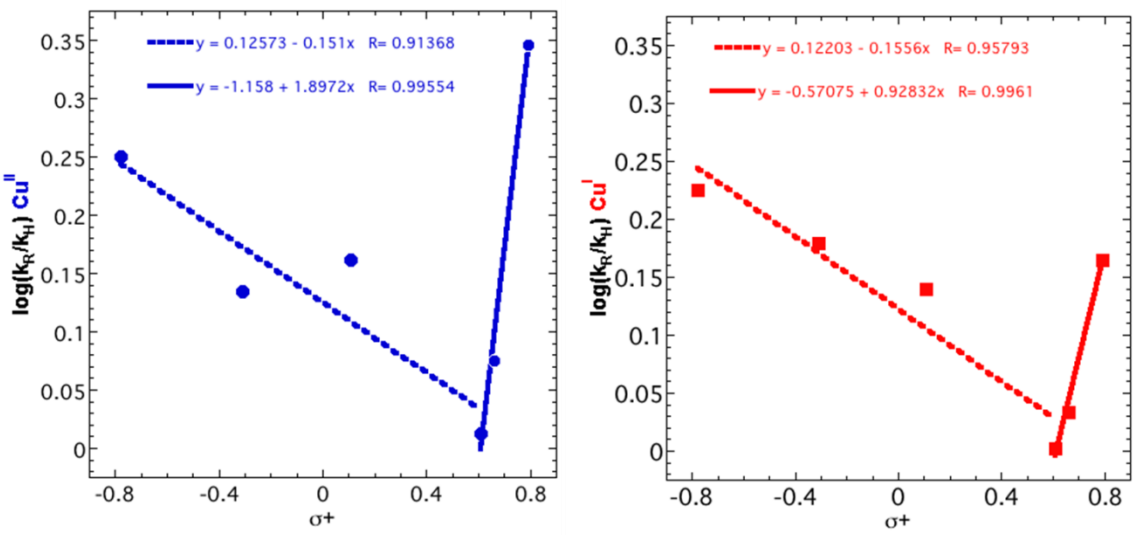

Figure 22: *Hammett plots of competition catalytic tests for bis-Cu(II) (left) and bis-Cu(I) complexes. The linear correlations have been made by separating the substrates in "withdrawing domain" and "donating domain".*

This is reminiscent of the so-called "curved Hammett plots"[44,45] such as that depicted in Figure 23[46]. Indeed, separated correlations based on polarity effect are observed for substrates having either electron-withdrawing or electron-donating substituents, as depicted in Figure 23. This kind of peculiar behavior can be attributed to several potential effects: i) a change in the mechanism when going from electron donors to electron attractors, ii) a change in the rate determining step with change in the nature of the substrate and iii) a change in the nature of the transition state. At the moment we lack data to discriminate between these three hypotheses.

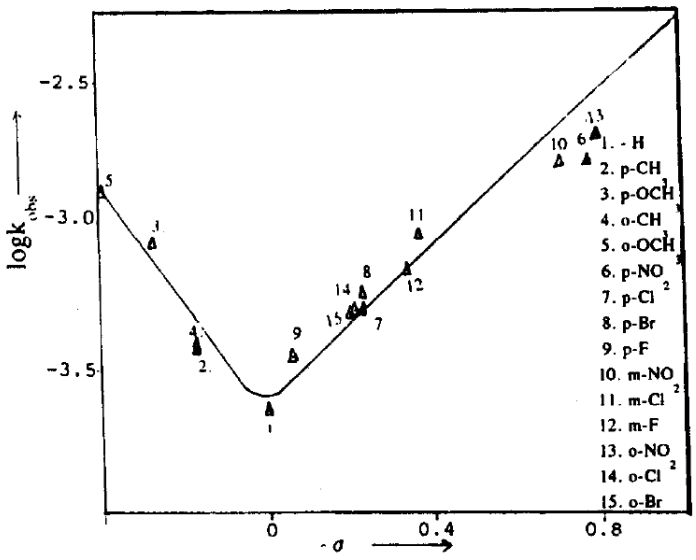

Figure 23: *An example of curved Hammett plot*[46]*.*

4. Mechanistic interpretation

The above results have revealed two peculiar features worth discussing more in depth: (i) the change in the aziridination mechanism when going from electron donating to electron withdrawing styrene substituents, and (ii) the occurrence of a nucleophilic mechanism with the latter. Whereas examples of such behaviours can be found in the literature, to the best of our knowledge, none is associated to aziridination.

When addressing the first aspect, it appears that the electrophilic aziridination becomes in competition with a yet unidentified process when its efficiency decreases. We have already presented in Scheme 3 that the putative nitrene species formed initialy " Cu^{I}_Cu^{III}=NTs " can deactivate through an internal electron transfer leading to " Cu^{II}-(NTs)-Cu^{II} ", the species detected in mass spectrometry at *m/z* 727. In the latter species, the NTs group is bound to two Cu^{II} and has thus lost its strongly oxidizing/electrophilic character; by contrast, it can be viewed as an amide, a doubly deprotonated tosylamine, and has thus acquired a strongly nucleophilic character. The reversal between the two mechanisms would therefore be due to a competition between the electrophilic aziridination and the internal electron transfer, as illustrated in Scheme 5.

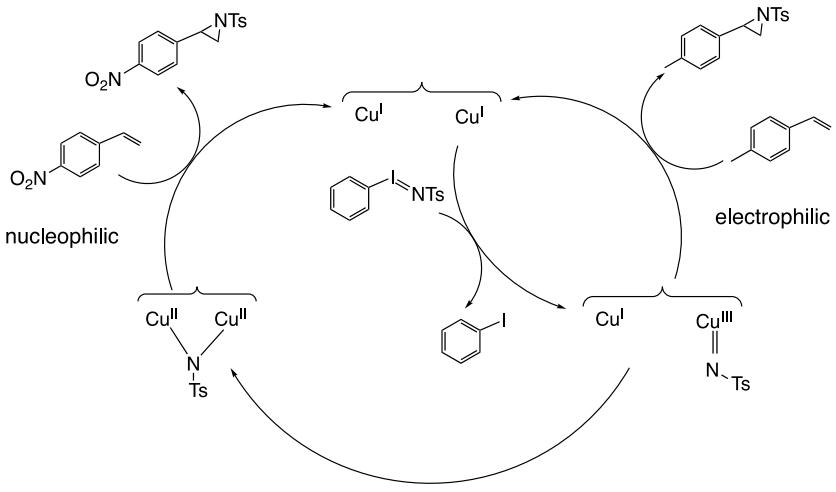

Scheme 5. *Overall mechanistic scheme illustrating the competition between electrophilic aziridination (top right) and internal reduction (middle) leading to nucleophilic aziridination (top left).*

The occurrence of a nucleophilic aziridination in the present case is illustrated in the following Scheme. Attack of the amide nitrogen doublet on styrene C_β would lead to a zwitterionic intermediate with a styrene C_α carbanion bound to an ammonium. Attack of the carbanion onto the nitrogen would form the aziridine ring with release of the two copper ions as Cu^I.

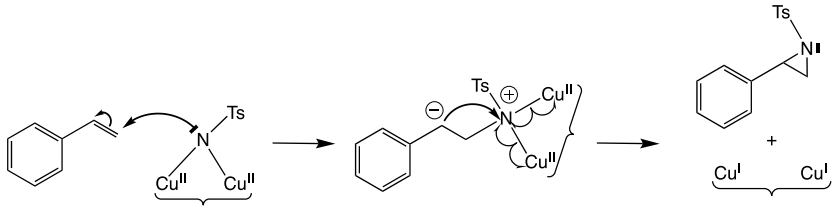

Scheme 6. *Mechanism of nucleophilic aziridination*

The latter mechanistic proposals provide attractive explanations for all observations. However, their full validation will require further experiments to investigate more in depth the electrophilic and nucleophilic reactions involved.

d. Conclusions

This chapter described the catalytic activity performed with the binuclear complex $[Cu_2(mXBMP\text{-}O)(CH_3COO)_2]ClO_4.(CH_3CN).(MeOH)$, both in its bis-Cu(II) and bis-Cu(I) forms. To our knowledge, no binuclear copper systems performing aziridination catalysis are reported in literature. Catalytic tests performed in several different conditions show good yields in aziridine with general little formation of byproducts. Other experimental conditions will be tested (time of reaction, percentage of catalyst, testing of different reducing agents for the generation of bis-Cu(I) species) in order to optimize the catalytic performance.

The catalytic activity was studied from the mechanistic point of view, giving interesting hints about the behaviour of the two complexes. Study of the interaction of the bis-Cu(I) complex with the nitrene precursor led to unprecedented observations: starting by an oxidative insertion of the nitrene with the formation of a " Cu^{III}=NTs " active species (not directly observed), and further reaction through an internal electron transfer, forming the species " Cu^{II}-(NTs)-Cu^{II} " (observed by different spectroscopic techniques). The occurrence of these

two species would be at the origin of the two opposite NTs transfer mechanisms. In the case of the bis-Cu(II) complex, the behaviour is more difficult to establish because UV-vis spectroscopy did not reveal clear changes during its interaction with the nitrene donor. This let suppose either a non-redox mechanism of aziridination or the fact that in the experimental conditions used for the studies (stoichiometric quantity of iodinane instead of excess used in catalytic tests) the quantity of nitrene donor was not sufficient to form the copper-nitrene adduct. Further studies are planned to better discriminate between the envisaged possibilities.

The observation of a change in mechanism when the styrene substituents become electron-withdrawing is striking. To our knowledge this is unprecedented in aziridination. As striking as the change itself is the observation that, in the "withdrawing domain", the reactivity increases with the electron-withdrawing character of the substituent. In other words, the aziridination should occur through a nucleophilic process. The oddity of both observations requires that more experiments be performed to ascertain these observations, in particular to validate the individual correlations. Also, the spectroscopic monitoring of the catalysis was performed with styrene and it appears now required to perform it with both types of substrates to potentially discriminate different mechanisms.

e. Experimental section

^{1}H-NMR spectra of the product of catalytic tests were recorded on a Bruker 400 MHz spectrometer, by putting D1= 10.00 s and P1= 70° for having quantitative spectra.
Acetonitrile used in all the experiments was distilled under argon on CaH_2 and stored in glovebox. Anhydrous N,N-dimethylformamide (DMF) was purchased by Sigma Aldrich. The reagents PhINTs and ArINTs were synthetized by following literature protocols[4,47].

Titration of the complex $[Cu_2(mXBMP\text{-}O)(CH_3COO)_2]ClO_4.(CH_3CN).(MeOH)$ with hydroxylamine hydrochloride

0.9 mg of $[Cu_2(mXBMP\text{-}O)(CH_3COO)_2]ClO_4.(CH_3CN).(MeOH)$ (MW= 749.19 g mol^{-1} 1.20 10^{-3} mmol) were dissolved in 2.5 mL of acetonitrile and put in a UV-vis cuvette, and a spectrum of the starting complex was recorded. A mother solution of hydroxylamine hydrochloride was prepared by dissolving 29.3 mg in 10 mL of methanol (MW= 69.49 g mol^{-1} concentration of the final solution: 0.042 M). The solution of complex was then titrated by adding 0.25

equivalent of hydroxylamine hydrochloride from 0 to 2 equivalents. UV-vis spectra were recorded after every addition of reducing agent.

Experiments of nitrene transfer catalysis

The catalytic tests were performed by following a general experimental protocol, in which the quantity of reagents and reaction time were varied for the different experiments.

General experimental protocol: an acetonitrile solution of complex bis-Cu(II) (MW=749.19 g mol^{-1}) was mixed under argon with the suitable amount of styrene (MW= 104.15 g mol^{-1}) and acetonitrile, stirred at room temperature and then added on solid PhINTs (MW= 373 g mol^{-1}). The mixture was left stirring at room temperature under argon, observing the progressive dissolution of the nitrene donor. At the end of the reaction the mixture was filtered on silica gel in order to eliminate the copper complex, and crude product eluted with acetonitrile. The obtained crude product was then dried under vacuum and analysed by ^{1}H-NMR for the quantification of the products (solvent: CD_3CN). The PhINTs used for the reactions contained 20% of tosylamine impurity. For the catalytic tests performed with the bis-Cu(I) complex, this was generated *in situ* before the reaction by reducing a mother solution of bis-Cu(II) complex in dry acetonitrile with hydroxylamine hydrochloride (MW= 69.49 g mol^{-1}).

- *Experiment 1:* $m_{bis\text{-}Cu(II)}$= 3 mg (4 10^{-3} mmol), V_{CH3CN}= 3.008 mL, $V_{styrene}$= 92 μL (0.8 mmol); (V_{tot}= 3.1 mL, [cx]= 1.3 10^{-3} M). This mixture was added on 29.1 mg of solid PhINTs (8 10^{-2} mmol). Time of reaction= 15 hours.
- *Experiment 2:* the bis-Cu(I) complex was generated by adding 2.6 mg of solid hydroxylamine hydrochloride (3.7 10^{-2} mmol) to 14 mg of bis-Cu(II) complex dissolved in 14 mL of dry acetonitrile. Quantities used for the catalytic test: $V_{bis\text{-}Cu(I)}$= 3 mL (4 10^{-3} mmol), V_{CH3CN}= 8 μL, $V_{styrene}$= 92 μL (0.8 mmol); (V_{tot}= 3.1 mL, [cx]= 1.3 10^{-3} M). This mixture was added on 29.1 mg of solid PhINTs (8 10^{-2} mmol). Time of reaction= 15 hours.
- *Experiment 3:* $m_{bis\text{-}Cu(II)}$= 2.1 mg (2.8 10^{-3} mmol), $V_{CH3CN+1\%DMF}$= 2.776 mL, $V_{styrene}$= 64 μL (0.56 mmol); (V_{tot}= 2.84 mL, [cx]= 1.0 10^{-3} M). This mixture was added on 22.0 mg of solid PhINTs (5.6 10^{-2} mmol). Time of reaction= 20 hours.

- *Experiment 4:* the bis-Cu(I) complex was generated by adding 6.2 μL of a dry DMF solution of hydroxylamine hydrochloride 2.6 M ($1.6\ 10^{-2}$ mmol) to 6.0 mg of bis-Cu(II) complex dissolved in 7 mL of dry acetonitrile with 1% of dry DMF. Quantities used for the catalytic test: $V_{bis\text{-}Cu(I)}$= 2.5 mL ($2.8\ 10^{-3}$ mmol), V_{CH3CN}= 0.276 mL, $V_{styrene}$= 64 μL (0.56 mmol); (V_{tot}= 2.84 mL, [cx]= $1.0\ 10^{-3}$ M). This mixture was added on 22.0 mg of solid PhINTs ($5.6\ 10^{-2}$ mmol). Time of reaction= 20 hours.
- *Experiment 5:* $m_{bis\text{-}Cu(II)}$= 1.4 mg ($2.0\ 10^{-3}$ mmol), V_{CH3CN}= 3.008 mL, $V_{styrene}$= 92 μL (0.8 mmol); (V_{tot}= 3.1 mL, [cx]= $6.2\ 10^{-4}$ M). This mixture was added on 29.1 mg of solid PhINTs ($8.0\ 10^{-2}$ mmol). Time of reaction= 24 hours.
- *Experiment 6:* 1.4 mg ($2.0\ 10^{-3}$ mmol), V_{CH3CN}= 3.054 mL, $V_{styrene}$= 46 μL (0.4 mmol); (V_{tot}= 3.1 mL, [cx]= $6.2\ 10^{-4}$ M). This mixture was added on 16.0 mg of solid PhINTs ($4.0\ 10^{-2}$ mmol). Time of reaction= 24 hours.
- *Experiment 7:* the bis-Cu(I) complex was generated by adding 3 μL of a DMF solution of hydroxylamine hydrochloride 3.1 M (10^{-2} mmol) to 3.8 mg of bis-Cu(II) complex ($5\ 10^{-3}$ mmol) dissolved in 8 mL of dry acetonitrile. Quantities used for the catalytic test: $V_{bis\text{-}Cu(I)}$= 3 mL ($2.0\ 10^{-3}$ mmol), V_{CH3CN}= 8 μL, $V_{styrene}$= 92 μL (0.8 mmol); (V_{tot}= 3.1 mL, [cx]= $6.2\ 10^{-4}$ M). This mixture was added on 29.1 mg of solid PhINTs ($8.0\ 10^{-2}$ mmol). Time of reaction= 24 hours.
- *Experiment 8:* the bis-Cu(I) complex was generated by adding 3 μL of a DMF solution of hydroxylamine hydrochloride 3.1 M (10^{-2} mmol) to 3.8 mg of bis-Cu(II) complex ($5\ 10^{-3}$ mmol) dissolved in 8 mL of dry acetonitrile. Quantities used for the catalytic test: $V_{bis\text{-}Cu(I)}$= 3 mL ($2.0\ 10^{-3}$ mmol), V_{CH3CN}= 54 μL, $V_{styrene}$= 46 μL (0.4 mmol); (V_{tot}= 3.1 mL, [cx]= $6.2\ 10^{-4}$ M). This mixture was added on 16.0 mg of solid PhINTs ($4.0\ 10^{-2}$ mmol). Time of reaction= 24 hours.

UV-vis monitoring of the catalytic reaction of aziridination

0.9 mg of $[Cu_2(mXBMP\text{-}O)(CH_3COO)_2]ClO_4.(CH_3CN).(MeOH)$ (MW= 749.19 g mol^{-1}, $1.2\ 10^{-3}$ mmol) were dissolved in 2.5 mL of dry acetonitrile ([cx]= $4.89\ 10^{-4}$ M) and put in a UV-vis cuvette. A spectrum of the starting complex was recorded, then 28 μL of styrene (MW= 104.15 g mol^{-1}, 0.245 mmol) were added to the solution and a second spectrum recorded. The solution was then poured into a second UV-vis cuvette which contained 9.1 mg of PhINTs (MW= 373 g mol^{-1}, $2.45\ 10^{-2}$ mmol) and the monitoring of the reaction was started; a

spectrum every five minutes was recorded and the evolution of the reaction was followed for one hour. Since PhINTs is suspended in the reaction medium, the mixture was not continuously stirred in order to have less noisy spectra.

The same procedure was followed with the bis-Cu(I) species. This was generated in situ by reduction of 0.9 mg of bis-Cu(II) complex (1.2 10^{-3} mmol) with 6 μL of a 0.4 M solution of hydroxylamine hydrochloride in DMF.

Low temperature experiments of stoichiometric reactivity between bis-Cu(II) complex and ArINTs

A mother solution of bis-Cu(II) complex was prepared by dissolving 3.1 mg of bis-Cu(II) complex in 12.5 mL of dry acetonitrile (MW=749.19 g mol^{-1}, [cx]= 3.4 10^{-4} M). 2.5 mL of this solution were put in a UV-vis cuvette and a spectrum was recorded. After that, 0.147 mL of a 5.76 10^{-3} M solution of ArINTs (MW= 493.37 g mol^{-1}) in dry acetonitrile were added and the reaction was stirred for 30 minutes, while recording a spectrum every 20 s. The same procedure was repeated at -30°C, -15°C and room temperature.

Low temperature experiments of stoichiometric reactivity between bis-Cu(I) complex and ArINTs

A mother solution of bis-Cu(II) complex was prepared by dissolving 2.6 mg of the complex in 10 mL of dry acetonitrile (MW=749.19 g mol^{-1},[cx]= 3.42 10^{-4} M). 2.5 mL of this solution (which contained 8.54 10^{-7} mol of the complex) were put in a UV-vis cuvette, and a UV-vis spectrum was recorded. This solution was then reduced by adding 5.3 μL of a DMF solution of hydroxylamine hydrochloride 0.32 M and a second spectrum was collected. After that, 0.160 mL of an acetonitrile solution of ArINTs 5.35 10^{-3} M (493.37 g mol^{-1}, 8.54 10^{-7} mol) was added to the complex and the reaction was monitored for 20 minutes, by recording a UV-vis spectrum every 15 s.

The same procedure was repeated at -30°C, -15°C and room temperature. In the experiment performed at -30°C, samples for EPR studies were collected after 150 s, 300 s and 1200 s. Moreover, in this case further 0.160 mL of ArINTs were added at the end of the twenty minutes and a further monitoring by UV-vis spectroscopy was performed using the same conditions. Again after twenty minutes, the product was analyzed by mass spectroscopy and a sample was collected for EPR analysis.

Catalytic aziridination tests on cis-stilbene

Experimental protocol followed with the bis-Cu(II) complex: 1.5 mg of complex (MW= 749.19 g mol^{-1}, 2.0 10^{-3} mmol, [cx]= 6.60 10^{-4} M) were dissolved in 3.032 mL of dry acetonitrile with 68 μL of *cis*-stilbene (d= 1.001 g mL^{-1}, MW= 180 g mol^{-1}, 0.38 mmol) and stirred at room temperature. The obtained mixture was then poured on 16 mg solid of PhINTs (MW= 373 g mol^{-1}, 4.2 10^{-2} mmol) and the reaction mixture stirred at room temperature for 24 hours. The reaction mixture was then filtered on silica gel, in order to eliminate the copper complex and the crude product eluted with acetonitrile. The eluted crude product was then dried under vacuum and analyzed by ^{1}H-NMR (solvent: $CDCl_3$).

Experimental protocol followed with the bis-Cu(I) complex: the bis-Cu(I) complex was generated *in situ* by dissolving 11.7 mg of bis-Cu(II) complex in 23.5 mL of dry acetonitrile ([cx]= 6.64 10^{-4} M) and by reducing it with 21.6 μL of a hydroxylamine hydrochloride solution 1.45 M in DMF. 3 mL of the solution of the reduced complex (corresponding to 2.0 10^{-3} mmol) were used for the reaction by using the same quantity of other reagents and the same conditions used for the catalytic test with the bis-Cu(II) complex.

Competition reaction experiments

Experimental protocol followed with the bis-Cu(II) complex: for every catalytic test 1.5 mL of complex were dissolved in 3 mL of dry acetonitrile (MW= 749.19 g mol^{-1}, 2.0 10^{-3} mmol), with 21.9 μL of styrene (d= 0.909 g mL-1, MW= 104, 0.19 mmol), the equimolar quantity of p-substituted styrene and a variable quantity of acetonitrile (quantities detailed below), in order to have the same final volume for all the reactions ([cx]= 6.60 10^{-4} M). This reaction mixture was then poured on 16 mg of solid PhINTs (MW= 373 g mol^{-1}, 4.2 10^{-2} mmol) and left reacting for 24 hours. The complex was then eliminated by filtration on silica gel and the crude product eluted with acetonitrile. The ratio between the different aziridines was evaluated by ^{1}H-NMR (solvent: CD_3CN).

- Experiment 1: p-nitrostyrene= 24.5 μL (d= 1.163 g mL^{-1}, MW= 149 g mol^{-1}, 0.19 mmol) + 53.6 μL of acetonitrile.
- Experiment 2: p-cianostyrene= 24.7 μL (d= 1 g mL^{-1}, MW= 129 g mol^{-1}, 0.19 mmol) + 53.4 μL of acetonitrile.

- Experiment 3: p-trifluorostyrene= 28.3 μL (d= 1.16 g mL^{-1}, MW= 172 g mol^{-1}, 0.19 mmol) + 49.8 μL of acetonitrile.
- Experiment 4: p-chlorostyrene= 26.5 μL (d= 1.155 g mL^{-1}, MW= 138 g mol^{-1}, 0.19 mmol) + 55 μL of acetonitrile.
- Experiment 5: p-methylstyrene= 25 μL (d= 0.895 g mL^{-1}, MW= 118 g mol^{-1}, 0.19 mmol) + 53 μL of acetonitrile.
- Experiment 6: p-methoxystyrene= 25 μL (d= 1.009 g mL^{-1}, MW= 134 g mol^{-1}, 0.19 mmol) + 53 μL of acetonitrile.

Experimental protocol followed with the bis-Cu(I) complex: the bis-Cu(I) complex was generated as already described in the experimental protocol of the aziridination tests of *cis*-stilbene and the competition reactions were performed by following the same protocol used with the bis-Cu(II) complex.

f. Bibliography

(1) Kwart, H.; Kahn, A. A. *J. Am. Chem. Soc.* **1967**, *89*, 1950–1951.
(2) Kwart, H.; Kahn, A. A. *J. Am. Chem. Soc.* **1967**, *89*, 1951–1953.
(3) Sharpless, K. B.; Patrick, D. W.; Truesdale, L. K.; Biller, S. A. *J. Am. Chem. Soc.* **1975**, *97*, 2305–2307.
(4) Yamada, Y.; Yamamoto, T.; Okawara, M. *Chem. Lett.* **1975**, 361–362.
(5) Breslow, R.; Gellman, S. H. *J. Am. Chem. Soc.* **1983**, *105*, 6728–6729.
(6) Breslow, R.; Gellman, S. H. *J. Chem. Soc. Chem. Commun.* **1982**, No. 24, 1400–1401.
(7) Mahy, J. P.; Battioni, P.; Mansuy, D.; Fisher, J.; Weiss, R.; Mispelter, J.; Morgenstern-Badarau, I.; Gans, P. *J. Am. Chem. Soc.* **1984**, *106*, 1699–1706.
(8) Mahy, J. P.; Battioni, P.; Mansuy, D. *J. Am. Chem. Soc.* **1986**, *108*, 1079–1080.
(9) Mahy, J. P.; Battioni, P.; Bedi, G.; Mansuy, D.; Fischer, J.; Weiss, R.; Morgenstern-Badarau, I. *Inorg. Chem.* **1988**, *27*, 353–359.
(10) Mahy, J. P.; Bedi, G.; Battioni, P.; Mansuy, D. *J. Chem. Soc. Perkin Trans. 2* **1988**, 1517–1524.
(11) Mahy, J. P.; Bedi, G.; Battioni, P.; Mansuy, D. *Tetrahedron Lett.* **1988**, *29*, 1927–1930.
(12) Mahy, J. P.; Bedi, G.; Battioni, P.; Mansuy, D. *New J. Chem.* **1989**, *13*, 651–657.
(13) Evans, D. A.; Faul, M. M.; Bilodeau, M. T. *J. Org. Chem.* **1991**, *56*, 6744.
(14) Evans, D. A.; Faul, M. M.; Bilodeau, M. T. *J. Am. Chem. Soc.* **1994**, *116*, 2742–2753.
(15) Li, Z.; Conser, K. R.; Jacobsen, E. N. *J. Am. Chem. Soc.* **1993**, *115*, 5326.
(16) Zhang, W.; Lee, N. H.; Jacobsen, E. N. *J. Am. Chem. Soc.* **1994**, *116*, 425–426.
(17) Li, Z.; Quan, R. W.; Jacobsen, E. N. *J. Am. Chem. Soc.* **1995**, *117*, 5889.
(18) Quan, R. W.; Li, Z.; Jacobsen, E. N. *J. Am. Chem. Soc.* **1996**, *118*, 8156–8157.
(19) Müller, P.; Fruit, C. *Chem. Rev.* **2003**, *103*, 2905–2919.
(20) Roizen, J.; Harvey, M.; Du Bois, J. *Acc. Chem. Res.* **2012**, *45*, 911–922.
(21) Müller, P.; Baud, C.; Jacquier, Y. *Tetrahedron* **1996**, *52*, 1543–1548.
(22) Au, S. M.; Huang, J. S.; Yu, W. Y.; Fung, W. H.; Che, C. M. *J. Am. Chem. Soc.* **1999**, *121*, 9120–9132.
(23) Leung, S. K. Y.; Tsui, W. M.; Huang, J. S.; Che, C. M.; Liang, J. L.; Zhu, N. Y. *J. Am. Chem. Soc.* **2005**, *127*, 16629–16640.
(24) Fingerhut, A.; Serdyuk, O. V.; Tsogoeva, S. B. *Green Chem.* **2015**, *17*, 2042–2058.
(25) Pérez, P. J.; Brookart, M.; Templeton, J. *Organometallics* **1993**, *12*, 261–262.
(26) Maestre, L.; Sameera, W. M. C.; Mar Diaz-Requejo, M.; Maseras, F.; Pérez, P. J. *J. Am. Chem. Soc.* **2013**, *135*, 1338–1348.
(27) Bagchi, V.; Paraskevopoulou, P.; Das, P.; Chi, L.; Wang, Q.; Choudhury, A.; Mathieson, J. S.; Cronin, L.; Pardue, D. B.; Cundari, T. R.; Mitrikas, G.; Sanakis, Y.; Stavropoulos, P. *J. Am. Chem. Soc.* **2014**, *136*, 11362–11381.
(28) Ponduru, T. T.; Dias, H. V. R. *Dalton Trans* **2017**, -.
(29) Brandt, P.; Södergren, M. J.; Andersson, P. G.; Norrby, P.-O. *J. Am. Chem. Soc.* **2000**, *122*, 8013–8020.
(30) Jiang, X.-K. *Acc. Chem. Res.* **1997**, *30*, 283–289.
(31) Collman, J.; Chien, A.; Eberspacher, T.; Brauman, J. *J. Am. Chem. Soc.* **2000**, *122*, 11098–11100.
(32) Hong, S.; Wang, B.; Seo, M. S.; Lee, Y. M.; Kim, M. J.; Kim, H. R.; Ogura, T.; Garcia-Serres, R.; Clémancey, M.; Latour, J.-M.; Nam, W. *Angew. Chem. Int. Ed.* **2014**, *53*, 6388–6392.
(33) Lennartson, A.; McKenzie, C. J. *Angew. Chem. Int. Ed.* **2012**, *51*, 6767–6770.
(34) Comba, P.; Haaf, C.; Lienke, A.; Muruganantham, A.; Wadepohl, H. *Chem. Eur. J.* **2009**, *15*, 10880–10887.
(35) Comba, P.; Lang, C.; Lopez de Laorden, C.; Muruganantham, A.; Rajaraman, G.; Wadepohl, H.; Zajaczkowski, M. *Chem. Eur. J.* **2008**, *14*, 5313–5328.
(36) Bakhoda, A.; Jiang, Q.; Bertke, J. A.; Cundari, T. R.; Warren, T. H. *Angew. Chem.-Int. Ed.* **2017**, *56*, 6426–6430.

(37) Badiei, Y. M.; Krishnaswamy, A.; Melzer, M. M.; Warren, T. H. *J. Am. Chem. Soc.* **2006**, *128*, 15056–15057.
(38) Badiei, Y. M.; Dinescu, A.; Dai, X.; Palomino, R. M.; Heinemann, F. W.; Cundari, T. R.; Warren, T. H. *Angew. Chem. Int. Ed.* **2008**, *47*, 9961–9964.
(39) Aguila, M. J. B.; Badiei, Y. M.; Warren, T. H. *J. Am. Chem. Soc.* **2013**, *135*, 9399–9406.
(40) Kundu, S.; Miceli, E.; Farquhar, E.; Pfaff, F. F.; Kuhlmann, U.; Hildebrandt, P.; Braun, B.; Greco, C.; Ray, K. *J. Am. Chem. Soc.* **2012**, *134*, 14710–14713.
(41) Corona, T.; Ribas, L.; Rovira, M.; Farquhar, E. R.; Ribas, X.; Ray, K.; Company, A. *Angew. Chem. Int. Ed.* **2016**, *55*, 14005–14008.
(42) Dielmann, F.; Andrada, D. M.; Frenking, G.; Bertrand, G. *J. Am. Chem. Soc.* **2014**, *136*, 3800–3802.
(43) Diaz-Requejo, M.; Pérez, P. J.; Brookhart, M.; Templeton, J. *Organometallics* **1997**, *16*, 4399–4402.
(44) Drago, R. S.; Dadmun, A. P. *J. Am. Chem. Soc.* **1994**, *116*, 1792–1799.
(45) Aubart, M. A.; Bergman, R. G. *J. Am. Chem. Soc.* **1998**, *120*, 8755–8766.
(46) Sabapathy Mohan, R. T.; Gopalakrishnan, M.; Sekar, M. *Int. J. Rapid Publ. Crit.* **1994**, *50*, 10933–10944.
(47) Macikenas, D.; Skrzypczak, E.; Protasiewicz, J. *J. Am. Chem. Soc.* **1999**, *121*, 7164–7165.

Chapter 5: General conclusions

This thesis described the development of new bioinspired copper complexes for catalytic applications, both in the domain of electrocatalysis and functionalization of organic molecules. These have been developed with the aim of mimicking the active sites of copper enzymes, which are able to activate dioxygen, both for reducing it to water and performing oxygenation of substrates.

Binuclear complexes described in Chapter 2 have been designed as first models for developing trinuclear structures capable of efficiently catalysing dioxygen reduction. Flexible ligands were chosen in order to reduce the rearrangements of the complex when they undergo reduction or oxidation processes and consequently enhance fast electron transfers. Two bis-piperazinic ligands, mXBMP and mXBMP-OH were easily obtained and used for synthesizing three binuclear copper complexes. The structures of CxCl and Cx(pheno)Cl were not totally established while the one of $[Cu_2(mXBMP\text{-}O)(CH_3COO)_2]ClO_4.(CH_3CN).(MeOH)$ was completely identified through its crystal structure.

Electrochemical studies coupled with EPR experiments on the complexes CxCl and Cx(pheno)Cl revealed in the two cases the presence of a complex mixture of species in which a part of copper is reduced. Moreover, the two complexes do not come back to the original species after a cycle of reduction and reoxidation. These facts can be explained by observing the structure of the ligands used for these complexes. In fact their flexibility from one side enhances fast electron transfers but at the same time they do not give enough coordinating groups to the metal centers. Their coordination sphere is thus probably completed by chlorides or acetonitrile molecules which may favor their reduction. Chloride anions are oxidized at potentials near to the ones observed for the Cu(I)/Cu(II) couple in these complexes, so Cu(II) can oxidize them with the production of Cu(I).

The structure of the complex $[Cu_2(mXBMP\text{-}O)(CH_3COO)_2]ClO_4.(CH_3CN).(MeOH)$ results stabilized by the presence of two acetate anions which contribute with the phenolate unit of the ligand to the formation of a triply-bridged structure. The two Cu(II) centers are stabilized in a pentacoordinated geometry but the obtained rigid structure gives rise to slower electron transfers due to the important rearrangements when the complex undergoes reduction. As a result, the electrochemical behavior of the complex is dominated by broadened and irreversible cyclic voltammetry peaks. Moreover, the presence of oxygenated anions moves the oxidation potential of Cu(I) at more negative potentials.

Unproductive preliminary experiments of oxygen reduction combined with the observed problems of stability of the complexes made necessary the development of more sophisticated complexes. The adopted strategy described in Chapter 3 was the expansion of the binuclear architectures by adding a third copper center and forming [2 + 1] trinuclear structures. For obtaining these new complexes the formation of a further coordinating units on the ligands mXBMP and mXBMP-OH was necessary. The multistep synthesis of trinucleating ligands BPBPyr and BPBPyr-OH described in Chapter 3 was particularly challenging due to difficulties for obtaining the diamine precursors of the two final ligands. Several different strategies were tested and the synthesis of the desired products was finally achieved by an efficient protection strategy. The two obtained ligands and they can be used for synthesizing trinuclear complexes with copper or other metals.

Even if the binuclear complexes described in Chapter 2 seem not performing in dioxygen reduction, literature reports similar complexes capable of reacting with molecular oxygen for oxidation and oxygenation reactions. In the latter class of reactions, the oxygen atom transferred to substrates is often described as the very reactive “oxene” species resulting from the three-electron reduction of oxygen. Oxene is isolobal with the so-called “nitrene” species “R-N:”, often generated in organic chemistry for the synthesis of amines and the two species can have similar reactivity. Nitrene transfer catalysis have become of huge interest in the last years as a way of obtaining aminated products otherwise difficult to synthesize.

The complex $[Cu_2(mXBMP\text{-}O)(CH_3COO)_2]ClO_4.(CH_3CN).(MeOH)$ was used for nitrene transfer catalysis for the aziridination of styrene. Catalytic tests were performed with both bis-Cu(II) and bis-Cu(I) forms of the complex with promising results from the point of view of the conversion and yield of aziridination. The catalytic activity was also analyzed from the mechanistic point of view, with investigations both about the interaction of the metal complexes with the nitrene precursors and the mechanism of nitrene transfer to substrates. Through studies of the formation of metal-nitrene active species with bis-Cu(I) complex it is possible to hypothesize that the interaction between copper catalyst and iodinane generates a “ Cu^{III} = NTs ” species, whose product of further reaction “ Cu^{II}-(NTs)-Cu^{II} ” can be observed by several spectroscopic techniques. Further studies are in progress in order to verify this hypothesis, trying to trap the metal-nitrene intermediate. Moreover, chloride anions present in the reaction medium after reduction of bis-Cu(II) with hydroxylamine hydrochloride seem to have a detrimental effect on the “ Cu^{II}-(NTs)-Cu^{II} ” species. Other experiments with changes of the reducing agent and addition of an excess of chloride

anions in the reaction medium will give more insights about this interaction. Similar experiments of stoichiometric interaction between nitrene precursor and bis-Cu(II) complex failed to provide much information about their interaction. A non-redox mechanism of aziridine formation can be envisaged but this hypothesis has to be verified through other experiments.

The mechanism of formation of aziridine was studied by catalytic tests with stereosensitive substrates and competition experiments. These latter experiments revealed a complex phenomenon, never described for aziridination catalysis. Data obtained cannot be accounted for through classical Hammett plots, neither using correlation with electronic parameters nor dual correlations which take into account the effects of radical delocalization on the substrates. The observed behaviour is reminiscent of “curved Hammett correlations” and indicates a change in mechanism from electrophilic to nucleophilic. A mechanistic proposal has been advanced based on the occurrence of two distinct active species: the high-valent nitrene “ Cu^{III} = NTs ” species, and the amide “ Cu^{II}-(NTs)-Cu^{II} ” resulting from an internal electron transfer. Further experiments are planned to firmly establish this proposal.

English abstract

This manuscript presents the development of new copper complexes for catalytic purposes. The design of the complexes takes inspiration from the active sites of multicopper oxidases. Three binuclear copper complexes have been synthesized and characterized, with a focus on their electrochemical behaviour and their potential use as catalysts for oxygen reduction. Spectroscopic and electrochemical studies revealed the importance of the coordination environment on the stability of the complexes. Cu(II) centers coordinated by not strong enough ligands are spontaneously reduced in solution, giving rise to mixtures of different complexes. At the same time more rigid structures capable of stabilising the two copper centers give rise to slow electron transfers, an undesirable characteristic in electrocatalysts. For these reasons more complex ligands have been synthesized, with the aim of obtaining trinuclear copper complexes with good properties as catalysts for dioxygen reduction. One of the binuclear complexes have been tested as oxidation catalyst in nitrene transfer reactions. The complex shows good performance in aziridination catalysis, both in its bis-Cu(II) and bis-Cu(I) forms. The catalytic activity have been analysed also from the mechanistic point of view. Preliminary results suggest different mechanisms of interaction of the reduced and oxidized forms of the complex with the nitrene donors.

Résumé en français

Ce manuscrit présente le développement de nouveaux complexes de cuivre conçus comme catalyseurs. Ceux-là ont été développés en prenant inspiration des sites actifs des enzymes à cuivre comme les multicuivre oxydases. Trois complexes binucleaires de cuivre ont été synthétisés et caractérisés, avec un étude approfondi de leur comportement redox pour évaluer leur potentielle utilisation comme catalyseurs de réduction d'oxygène. Ces études, couplés avec des analyses spectroscopiques ont démontré l'influence de l'environnement de coordination sur la stabilité des complexes. En fait, quand les centres de Cu(II) sont coordonnés par de ligands pas assez forts, ils ont la tendance à se réduire spontanément en solution, produisant des mélanges de différentes espèces impossibles à purifier. Au même temps, quand le centre Cu(II) sont stabilisés dans des structures plus rigides le complexe montre des transferts d'électrons plus lents, une caractéristique peu désirable dans le développement de catalyseurs de réduction d'oxygène. Pour ces raisons des ligands plus sophistiqués ont été synthétisés avec le but d'obtenir des complexes trinucleaires de cuivre capables de catalyser efficacement la réaction de réduction d'oxygène. Un des complexes binucleaires developpes a été testé comme catalyseur de transfert de nitrene, en particulier dans la synthèse d'aziridines. Le complexe montre une bonne performance catalytique également sous les formes bis-Cu(II) et bis-Cu(I). L'activité catalytique a été analysé aussi du point de vue mécanistique et études préliminaires suggèrent la présence de différents mécanismes d'interaction entre le donneurs de nitrene et les deux formes du complexe.